ABSTRACT

Title of Dissertation:	MODELLING DECOMPOSITION AND NITROGEN RELEASE FROM SURAFCE COVER CROP RESIDUES IN NO-TILL SYSTEMS IN THE MID-ATLANTIC AND SOUTHEASTERN US
	Resham Thapa, Doctor of Philosophy, 2020
Dissertation directed by:	Associate Professor, Katherine L. Tully, Department of Plant Science and Landscape Architecture

In the mid-Atlantic and Southeastern US regions, cover crops (CCs) are planted during the winter fallow periods or between cash crops to provide living roots and to cover soil for extended time periods. Cover crops can provide a suite of agroecosystem services to cropping systems including soil and water conservation, weed suppression, and nitrogen (N) cycling. After CCs are terminated, the rate of residue decomposition determines both N availability and the longevity of residue cover in conservation tillage (reduced- and no-till) systems. Accurate predictions of plant-available N from decomposing CCs are needed to improve N fertilizer recommendations in order to reduce environmental losses of N while meeting cash crop N needs. The objective of this work is to improve our understanding of the factors controlling CC residue decomposition in conservation tillage systems at

varying temporal (diurnal to seasonal) and spatial (laboratory to regional) scales. At a diurnal scale, the moisture (θ_g)/water potential ($\psi_{residue}$) and temperature in the surface CC residue layers fluctuated more dramatically and dynamically than the underlying soils. Decomposition of surface CC residues also showed distinct diurnal patterns that were closely related to diurnal variations in residue θ_g or $\psi_{residue}$. In a controlled microcosm experiment, the effect of residue location on C and N mineralization during repeated dry-wet cycles were also primarily explained by differences in residue water dynamics than by differences in soil-residue contact between surface and incorporated residues. At a regional scale, the combination of residue quality and climatic variables explained the majority of the variations in residue decomposition rates, i.e. k-values. I found faster decomposition of surface CC residues in humid environments and in site-years with more frequent rain events. The k-values decreased with increasing biomass, C:N, residue holo-cellulose concentrations, and lignin:N, but increased with increasing residue carbohydrate concentrations. Mathematical equations were developed and integrated into the existing CERES-N sub-model to adjust k-values based on residue environment. Once such models are well-calibrated and well-validated, they will be used to make evidence-based management recommendations to farmers. Thus, this research helps to optimize provisioning of agroecosystem services in CC-based conservation tillage crop production systems.

MODELLING DECOMPOSITION AND NITROGEN RELEASE FROM SURAFCE COVER CROP RESIDUES IN NO-TILL SYSTEMS IN THE MID-ATLANTIC AND SOUTHEASTERN US

by

Resham Thapa

Dissertation submitted to the Faculty of the Graduate School of the
University of Maryland, College Park, in partial fulfillment
of the requirements for the degree of
Doctor of Philosophy
2020

Advisory Committee:
Professor Dr. Katherine L. Tully, Chair
Dr. Steven B. Mirsky
Dr. Miguel L. Cabrera
Dr. Harry H. Schomberg
Dr. John D. Lea-Cox
Dr. Stephanie Yarwood

Dedication

To the Thapa and Chhetri families.

Acknowledgements

I would like to thank my co-advisors, Dr. Katherine L. Tully and Dr. Steven B. Mirsky, and my committee members, Dr. Miguel L. Cabrera, Dr. Harry H. Schomberg, Dr. John D. Lea-Cox, and Dr. Stephanie Yarwood, for their endless guidance and assistance throughout my degree. I am also grateful to Dr. Chris Reberg-Horton, Dr. Julia Gaskin, Dr. Dennis Timlin, and Dr. David Fleisher for their valuable contributions to various parts of this dissertation. Special thanks to all the farmers who voluntarily participated in our on-farm research activities. I am thankful to all the personnel who were involved in this multi-state on-farm cover crop research, notably Brian W. Davis, Ethan Sweep, Alondra Thompson, Sarah A. Seehaver, Aurelie Poncet, Richard Hitchcock, Esleyther Henriquez Inoa, Aida Bagheri Hamaneh, and many others. I would also like to acknowledge my research team from the Sustainable Agricultural Systems Laboratory (USDA-ARS) and the Agroecology Lab (UMD) for their assistance during this project.

I sincerely acknowledge the funding support from the USDA Natural Resources Conservation Service (Conservation Innovation Grant # 8042-21660-004-36-R), the USDA National Institute of Food and Agriculture (Award # 2018- 68011-28372), and the Northeast Sustainable Agriculture Research and Education (SARE) graduate student grant (Award # GNE17-160-31064).

Special thanks to my parents, Hira Bahadur Thapa and Thum Kumari Thapa, family members, friends, and my beloved wife, Reema Chhetri Thapa, for their continuous love, support, and encouragement throughout my graduate career.

Table of Contents

List of Tables

List of Figures

Chapter 1: Introduction

Agricultural intensification increased crop yields and enabled us to feed more than 7 billion people worldwide (Erisman et al., 2008). However, unmanaged intensification in agricultural fields has resulted in severe environmental damage, land degradation, depletion of fresh water resources, climate change, biodiversity loss, and depletion of ecosystem services within agricultural systems (Foley et al., 2011; Tilman et al., 2002). For example, continuous tillage has negatively impacted the physical, chemical, and biological health of soil. Soil health degradation can compromise crop productivity, farm profitability, and long-term sustainability of our crop production systems. Overuse of synthetic fertilizers and pesticides has reduced air (volatilization losses and greenhouse gas emissions) and water (runoff and leaching losses) quality as well as generated pest management challenges as weeds have become herbicide-resistant. Given these destabilizing factors (i.e., climate change, water scarcity, declining soil and water quality, and pest management challenges) affecting global food and water security, procuring food, fiber, and energy needs for ever-increasing human population has become a *grand challenge* for modern agriculture.

Cover crops (CCs), in combination with conservation tillage, work synergistically to mitigate destabilizing factors threating modern agriculture. Conservation tillage has been increasingly adopted across the globe to protect soil from water and wind erosion, build soil health by enhancing soil organic carbon sequestration and improving aggregate stability, increase water infiltration and storage, reduce evapotranspiration, reduce fuel and labor costs (Grandy and

Robertson, 2007; Six et al., 2002; Zibliske and Bradford, 2007; Kern and Johnson, 1993). However, conservation tillage alone can result in extensive soil surface crusting that impedes water infiltration during rainfall events, leading to runoff losses (Merten et al., 2015; Shaver et al., 2002). The emergence of herbicide-resistant weeds has reduced the efficacy of currently-available chemistries in managing weeds, thereby threatening the future sustainability of conservation tillage in US cropping systems (Davis and Frisvold, 2017). Cover crops have been identified as tools to ameliorate these limitations while magnifying the positive benefits of conservation tillage (Tully and McAskill, 2019).

Cover crops are established during the winter fallow period or between cash crops to provide living roots and to cover soil for extended time-periods, thereby protecting soil from wind and/or water erosion (Dabney et al., 2001; Dabney, 1998; Jian et al. 2020). In recent years, CCs were heavily promoted as tools to improve water quality by reducing N losses from agroecosystems through N recycling and scavenging by selected CC species (Meisinger et al., 1991). In a meta-analysis using data from 28 studies, Thapa et al. (2018a) found that non-leguminous CCs, on average, reduce NO_3^- leaching losses by 56% compared to no CC controls. The capacity of CCs to retain soil N and reduce NO_3^- leaching is positively related to biomass levels (Finney et al., 2016; Thapa et al., 2018a). Besides these benefits, CCs assimilate more C (Poeplau and Don, 2015) and suppress weeds effectively during their growth (Osipitan et al., 2018). The adoption of CCs into existing cropping rotations also breaks disease and pest cycles. After they are terminated, CCs continue to provide additional ecosystem services depending on the longevity of CC residues

in cropping systems. For example, a highly persistent CC mulch layer can protect soil, conserve soil water, and suppress weeds more effectively but can increase N fertilizer needs due to its ability to immobilize soil N. On the other hand, a fast decomposing CCs releases N quickly and decreases N fertilizer needs of the succeeding cash crops (Poffenbarger et al., 2015). Therefore, depending on the management decisions (i.e., selection of CC species, planting and/or termination dates/methods), a trade-off exists in the ecosystem services provisioned by CCs.

Despite the potentially transformative benefits of CC-based conservation tillage crop production systems for ensuring global food and water security, adoption of CCs remain low in the US (<4% of US acreage; Zulauf and Brown, 2019). While CC are increasingly adopted over time, the rate of adoption has been slow. Among others, lack of site-specific information and management complexity is considered as barriers to CCs adoption. As CCs adoption ramps up across crop production systems in the US, demand for decision support tools that facilitate evidence-based management recommendations is also rising. One such decision support tool is the *Cover Crop N Availability Calculator* that farmers, agricultural professionals, and researchers can use to predict decomposition and N release from decomposing CC residues (Gaskin et al., 2019; Woodruff et al., 2018). Residue decomposition governs both N mineralization and the longevity of CC residues in conservation tillage systems. As the magnitude of ecosystem services provisioned by CCs depends on the quantity and quality of CC residues (Finney et al., 2016; Osipitan et al., 2019; Thapa et al., 2018b, 2020), availability of tools that can accurately predict decomposition

will assist in the optimization of ecosystem services in CC-based conservation tillage crop production systems.

Multiple factors control decomposition and N mineralization from CC residues. These factors include residue quantity and quality (C:N, residue C chemistry), tillage (surface-applied vs incorporated residues), climate (residue moisture and temperature), and the activity of decomposer communities (Cabrera et al., 2005; Poffenbarger et al., 2015; Vigil and Kissel, 1991; Wagger et al., 1998). Because of the complex interactions between these multiple controlling factors, predicting residue decomposition and N mineralization is highly challenging. To date, researchers have been successful in accurately predicting decomposition and N mineralization from incorporated CC residues (Quemada et al. 1997; Schomberg and Cabrera 2001; Woodruff et al. 2018). However, existing computer simulation models consistently overpredicted decomposition and N mineralization from residues left on the soil surface, as in the case of conservation tillage systems. With increased adoption of CC-based conservation tillage crop production systems in the US (Mirsky et al., 2012), a better tool is needed which can accurately predict decomposition and N mineralization from surface CC residues.

The next four chapters of this dissertation aimed at improving our understanding on the factors controlling CC residue decomposition in conservation tillage systems by conducting experiments at varying temporal (diurnal to seasonal) and spatial (laboratory to regional) scales. In a series of diurnal experiments, I investigated the effect of decomposition on residue water retention properties and

characterized diurnal variations in residue decomposition rates in response to changes in soil-residue-air environmental conditions (Chapter 2). Next, I conducted a controlled microcosm experiment to model the interactive effects of residue moisture and temperature on C and N mineralization from CC residues left on the soil surface (Chapter 3). In Chapter 4, I conducted another controlled microcosm experiment to determine the impact of residue management (residue type and location) on soil and residue microbiota and their potential ecosystem functions when subject to repeated dry-wet cycles (rain events). In Chapter 5, I determined the independent and combined effects of factors intrinsic to the field (latitude, soil, and climate) and extrinsic or management factors (CC residue quantity and quality) on the rate of decomposition of surface CC residues in no-till corn (*Zea mays* L.) systems in the mid-Atlantic and Southeastern US states. In the final chapter, I summarized the main findings from this dissertation.

Chapter 2: Cover crop residue moisture content controls diurnal variations in surface residue decomposition

Resham Thapa [a, b*], Katherine L. Tully [a], Miguel Cabrera [c], Carson Dann [c], Harry H. Schomberg [b], Dennis Timlin [d], Julia Gaskin [c], Chris Reberg-Horton [e], and Steven B. Mirsky [b]

[a] Department of Plant Science and Landscape Architecture, University of Maryland

[b] Sustainable Agricultural Systems Laboratory, USDA-ARS

[c] Department of Crop and Soil Sciences, University of Georgia

[d] Adaptive Cropping Systems Laboratory, USDA-ARS

[e] Department of Crop and Soil Sciences, North Carolina State University

Forms the basis of a manuscript submitted to Agricultural and Forest Meteorology

Highlights

- Cover crop residue water retention properties changes during decomposition.
- Cover crop residue lignin concentrations can be used as a proxy for water retention properties.
- Cover crop surface residues experience extreme diurnal fluctuations in moisture and temperature compared to underlying soils.
- Diurnal variations in decomposition tracked variations in cover crop residue moisture content.
- Cover crop decomposition in no-till systems is strongly moisture-limited.

Abstract

The effect of cover crop (CC) surface residues on water, carbon, and nitrogen cycling in no-till systems depends in part on the water retention properties of decomposing residues and the extent of decomposition. This study 1) examined the effect of decomposition on residue water retention properties; 2) characterized diurnal variations in residue decomposition rates in response to changes in soil-residue-air environmental conditions; and 3) examined the diurnal relationships between cover crop surface residue decomposition and residue environment (moisture and temperature). Maximum gravimetric water content (θ_g) and characteristic water release curves were determined for red clover (*Trifolium pratense* L.) and cereal rye (*Secale cereale* L.) residues collected at 0, 4, 10, and 16 weeks after termination for red clover, and at 2, 5, and 18 weeks for cereal rye. In addition, residue carbon dioxide (CO_2-C) flux, along with soil-residue-air environmental conditions, were measured diurnally for red clover at 4, 10, and 16 weeks after termination, and for cereal rye at 5 weeks after termination. Maximum residue θ_g decreased as decomposition progressed. Cover crop residue decomposition also influenced water release curves such that the water retained at any given water potential ($\psi_{residue}$) declined with increasing decomposition. These decomposition-associated changes in residue water retention properties were strongly related to residue lignin concentrations. Cover crop surface residue CO_2-C flux showed distinct diurnal patterns that were strongly related to $\psi_{residue}$ or residue θ_g. At a diurnal scale, residue CO_2-C flux increased during the nighttime from 18:00 to 06:00 h when residues gain moisture from the atmosphere and soil, and decreased during the

daytime from 06:00 to 18:00 h when residues lost moisture via evaporation. Increase in temperature decreased residue CO_2-C flux due to moisture limitations. Therefore, CC surface residue decomposition models must address both diurnal changes in $\psi_{residue}$and the changes in water retention properties as residues decompose.

Keywords: Cover crops, Residue water retention properties, Residue decomposition, Diurnal variations, No-till systems

Abbreviations: CC, cover crops; $\psi_{residue}$, residue water potential; ψ_{air}, air water potential θ_g, gravimetric water contents; RH, relative humidity; NIRS, near infra-red reflectance spectroscopy

Introduction

In the mid-Atlantic US states, cover crop (CC) based no-till grain production systems are widely promoted and incentivized to reduce nutrient and sediment loading into the Chesapeake Bay Watershed (Mirsky et al., 2012; NRC, 2011; Thapa et al., 2018a; Wallace et al., 2017). In these systems, CC residues are retained at the soil surface as a mulch and provide multiple ecosystem services, some of which include soil and moisture conservation, weed suppression, and nutrient cycling (Mirsky et al., 2012). The effect of surface residues on the underlying soil environment has been widely studied. Cover crop surface residues act as a physical barrier and protect soil from sealing and crusting by rainfall, conserve soil moisture during dry periods via reduced evaporation, decrease light transmittance, and moderate surface soil temperature fluctuations (Bristow 1988; Teasdale and Mohler, 1993). The extent to which CC surface residues affect soil physical environment

depends on the mass, thickness, and quality of the surface residue layer, which in turn drives decomposition (Dietrich et al., 2019; Poffenbarger et al., 2015). Therefore, understanding processes and drivers of surface residue decomposition is critical for developing effective residue management strategies in no-till systems.

It is well established from laboratory incubation studies that surface residue decomposition is strongly influenced by residue environmental conditions such as moisture (θ_g) and temperature (Quemada and Cabrera, 1997; Stott et al., 1986; See Chapter 3). The surface residue layer is directly exposed to solar radiation, wind, dew, and rainfall under field conditions. Hence, environmental conditions (θ_g and temperature) in the residue layer can change more dramatically and dynamically than in the underlying soil layers, which will likely result in temporal heterogeneity in the decomposition of surface residues. While soil θ_g and temperature is simple to measure and can be easily obtained from weather stations, continuous measurement or monitoring of θ_g and temperature in a CC surface residue layer is difficult. As a result, to our knowledge there are no field studies that measured diurnal variations in surface residue environmental conditions (θ_g and temperature) and their effect on decomposition in agricultural systems. Studies in temperate forest ecosystems have suggested that diurnal variations in the decomposition of forest floor litter samples tracked variations in air temperature (Jomura et al., 2012; Witkamp, 1969; Zimmermann et al., 2009). However, these studies were conducted in the cold and wet winter months (September - November) under dense forest canopies; findings from these studies in forest ecosystems may be of limited use in CC-based no-till

cropping systems in which decomposition of CC residues typically occurs during the hot and dry summer months. Therefore, it is critical to understand how θ_g and temperature in the CC residue layer change diurnally and how these changes drive decomposition.

Crop residues can store a significant amount of water depending on residue quantity and the frequency, intensity, and duration of rainfall or irrigation (Kozak et al., 2007; Savabi and Stott, 1994; Scopel et al., 2004). The maximum amount of water retained by undecomposed crop residues differs among crop species (Iqbal et al., 2013; Quemada and Cabrera, 2002; Savabi and Stott, 1994). Few studies have attempted to develop mathematical relationships to determine the water retention capability of crop residues based on residue characteristics (Iqbal et al., 2013; Quemada and Cabrera, 2002). Previous studies found that the maximum water retentive capacity of undecomposed crop residues is highly correlated to soluble carbohydrate concentrations (i.e. chemical characteristics; Quemada and Cabrera, 2002) or tissue density of the crop residues (i.e. physical characteristics; Iqbal et al., 2013). Since crop residues undergo physical and chemical transformations during decomposition, the maximum water retention capacity of the crop residues will most likely change over time. Moreover, the extent of decomposition may affect the evolution of residue θ_g during the evaporation period following rainfall or irrigation events and hence, may alter the residue θ_g and water potential ($\psi_{residue}$) relationships. Although it is evident that the absorption or desorption of θ_g from crop residues during wetting and drying periods is largely regulated by water retention properties, there is currently a knowledge gap on the decomposition associated

changes in CC residue water retention properties.

This study aimed to address existing knowledge gaps by (i) determining the effect of decomposition on the water retention properties of CC residues, (ii) characterizing diurnal variations in residue decomposition and soil-residue-air environmental conditions in no-till systems, and (iii) examining the diurnal relationships between residue decomposition and residue environment (moisture and temperature) in no-till systems.

Materials and Methods

Experimental site and management

This study was conducted in the Cover Crop Systems Project (CCSP), a long-term agricultural research (LTAR) site that is part of the USDA-ARS LTAR network, located at the Beltsville Agricultural Research Center (39°00'51.3"N, 76°56'29.0"W, Beltsville, MD, US). Soil at the experimental site was classified as Codorus (fine-loamy, mixed, active, mesic Fluvaquentic Dystrudepts) and Hatboro (fine-loamy, mixed, active, nonacid, mesic Fluvaquentic Endoaquepts) soil series with a silt loam texture (Soil Survey Staff, 2020). We selected two experimental plots from a conventionally-managed continuous no-till system in a corn (*Zea mays* L.)-soybean (*Glycine max* L.)-winter wheat (*Triticum aestivum* L.) rotation. Red clover (*Trifolium pratense* L.) was frost-seeded into winter wheat at the rate of 17 kg ha^{-1} on March 16, 2018 using a no-till drill. Cereal rye (*Secale cereale* L.) was drill-seeded at the rate of 134 kg ha^{-1} on October 24, 2018 following corn harvest. Red clover was terminated at the anthesis stage on May 8, 2019 using a mixture of 0.84 kg ha^{-1} glyphosate (N-

(phosphonomethyl) glycine)) 0.42 kg ha^{-1} dicamba (3,6-dichloro-2-methoxybenzoic acid), and 0.28 kg ha^{-1} 2,4-D (2,4-Dichlorophenoxyacetic acid). Similarly, cereal rye was terminated at the heading stage on May 9, 2019 using a mixture of 1.26 kg ha^{-1} glyphosate, 0.35 kg ha^{-1} glory (Metribuzin), and 1.49 kg ha^{-1} Dual II Magnum (S-metolachlor). Cover crop residues were left on the surface as a mulch following termination. Soybean was planted green into the preceding cereal rye CC using a no-till drill on May 8, 2019; corn was drilled into the red clover mulch on May 17, 2019.

Study periods and cover crop (CC) characterization

We performed a series of diurnal experiments to understand how surface residues at various stages of decomposition respond to changes in environmental conditions. Decomposition of red clover residues was measured at 4, 10, and 16 weeks after termination, which corresponded to corn growth stage of V1-V2, tasseling, and R6 stage, respectively. Similarly, cereal rye decomposition was measured at five weeks after termination, at the soybean V2 growth stage. During each study period, residue and soil θ_g, $\psi_{residue}$, residue, soil, and air temperatures, and air relative humidity (RH) were also measured (see below for more details). In addition to these diurnal study periods, CC residue samples were collected at week 0 (red clover), week 2 (cereal rye), and week 18 (cereal rye) and analyzed for maximum residue θ_g; water release curves were then generated.

Residue sub-samples from each sampling event were air-dried, finely ground, and sent to the Agriculture and Environmental Services Labs at the University of Georgia (Athens, GA) for quality analysis. Percent carbohydrate, cellulose,

hemicellulose, and lignin in the residue samples were determined via near infra-red reflectance spectroscopy (NIRS) using scanning monochromator (model 6500; FOSS NIRSystems, Silver Spring, MD). Total C and N concentrations in the CC residues were determined by dry combustion using a Leco TruMac CN Analyzer (LECO Corporation, St. Joseph, MI).

Determination of maximum residue water content and characteristic water release curves

To investigate the impact of residue decomposition on water retentive capacity, we determined the maximum residue θ_g at various stages of decomposition. The maximum residue θ_g was calculated following the procedure outlined by Quemada and Cabrera (2002). In brief, CC residues were cut into ≤0.5 cm pieces, immersed in distilled water overnight, and then drained to remove excess water. Triplicate samples of drained residue samples were weighed before and after oven-drying at 60 °C for 48 h. The maximum residue θ_g was finally expressed on an oven-dried weight basis.

We also investigated the impact of residue decomposition on characteristic water release curves for both red clover and cereal rye residues. Moisture release or water retention curves provide the relationship between $\psi_{residue}$ and residue θ_g. Residue collected from diurnal experiments was used to determine the water release curves of red clover (weeks 4, 10, and 16) and cereal rye residues (week 5). For other sampling events (red clover residues collected at week 0 and cereal rye residues collected at weeks 2 and 18), the water release curves were determined following the procedure described by Quemada and Cabrera (2002). The water-saturated pieces of

residue samples (handled as described above) were spread on trays and allowed to air-dry under ambient room conditions. At set points during the drying process, residue sub-samples were transferred to round sampling cups to measure $\psi_{residue}$ using a WP4C Dewpoint Potentiometer (METER Group, Inc., Pullman, WA). The residue cups were weighed immediately and then oven-dried at 60 °C for 2 d to determine residue θ_g.

Diurnal measurements of residue decomposition and soil-residue-air environmental conditions

Diurnal variations in red clover and cereal rye decomposition rates were determined by measuring residue CO_2-C flux at approximately 0:00, 6:00, 9:00, 12:00, 15:00, 18:00, and 21:00 hours. The CO_2-C flux from red clover residues was measured at 4 (June 3-5, 2019), 10 (July 18-20, 2019), and 16 (August 29-31, 2019) weeks after termination. Similarly, the CO_2-C flux from cereal rye residues was measured at five (Jun. 14-16, 2019) weeks after termination. No rain fell during any of these study periods. However, the experimental plots received variable amounts of rain on the day prior to the start of each study period (1.78, 11.9, 3.30, and 0.25 mm of rain on June 2, June 13, July 17, and August 28, respectively).

Residue CO_2-C flux was measured using a portable EGM-4 infrared gas analyzer system (PP Systems, Amesbury, MA) equipped with a flow-through closed SRC-2 Soil Respiration Chamber (PP Systems, Amesbury, MA). The chamber had a volume of 1171 cm^3 and a surface area of 78 cm^2. At the time of CO_2-C flux measurements, CC residues from an equivalent area (~78 cm^2) were cut and transferred to a beaker. The chamber tops were placed on beakers and sealed tightly

to measure CO_2-C flux from residues within 300 sec. This method was preferred because it allowed us to capture the actual decomposition rates of surface residues in no-till systems. Following CO_2-C flux measurements, CC residues were transferred into plastic zippered bags, sealed, and brought back to the laboratory to measure $\psi_{residue}$ and residue θ_g within 1-2 h. In addition, we collected surface soil samples (0-5 cm depth, 2-cm diameter probe) from the same place where the residue samples were taken for CO_2-C flux measurements. Measurements (residue and soil θ_g, $\psi_{residue}$, and residue CO_2-C flux) were replicated four times.

In the laboratory, residue samples were cut into ≤0.5 cm pieces and the $\psi_{residue}$ was measured using a WP4C Dewpoint Potentiometer. The residue cups were then weighed immediately and oven-dried at 60 °C for 2 d to determine residue θ_g. The $\psi_{residue}$ and residue θ_g were determined in triplicate sub-samples per replicate. Therefore, we had 12 values of $\psi_{residue}$ and residue θ_g for each measurement hour. To determine soil θ_g, surface soil samples were weighed before and after oven-drying at 104 °C for 2 d.

During each study period, air temperature and RH was monitored at 75 cm above the soil surface using a T9602-3-D-1 Humidity & Temperature Probe Sensor (Amphenol Advanced Sensors, Mansfield, TX) and recorded at 10 min intervals using a customized Arduino-based datalogger. A 107-Temperature Probe Sensor (Campbell Scientific, Inc., Logan, UT) was inserted inside the CC mulch layer to measure residue temperature. Soil temperature and volumetric moisture content (θ_g) were measured by installing a time-domain reflectometer TDR-310S probe sensor

(Acclima, Inc., Meridian, ID) at a 45° angle beneath the residue layer. Surface CC residue temperature, soil temperature, and soil θ_g were recorded at 10 min intervals using a CR1000 datalogger (Campbell Scientific, Inc., Logan, UT). Air water potential (ψ_{air}) was calculated from air temperature and RH data using the following equation:

$$\psi_{air} = \frac{R \cdot T}{V} \cdot \frac{ln(RH) \cdot 1\ MPa}{1{,}000{,}000\ Pa} \qquad \text{Eq. [1]}$$

where R is the universal gas constant (8.314 J K^{-1} mol^{-1}), T is the absolute air temperature (K), V is the partial molar volume of water (1.8×10^{-5} m^3 mol^{-1}), and RH is the air relative humidity expressed as a fraction (0-1).

Data analysis

Characteristic moisture release curves for each CC residue (red clover or cereal rye) at different stages of decomposition were fitted using the *nls* function in R. The basic form of the characteristic moisture release curve can be presented as follows:

$$\psi_{residue} = a \cdot (residue\ \theta_g)^{-b} \qquad \text{Eq. [2]}$$

where $\psi_{residue}$ is the residue water potential (MPa), θ_g is the gravimetric moisture content of the residue (g water g^{-1} dry residue), and 'a' and 'b' are empirical constants of the model. The 'a' represents the plateau of the moisture release curve (estimated maximum residue θ_g) and 'b' represents the shape of the moisture release curve (propensity of the residue to lose moisture as it dries, i.e. as $\psi_{residue}$

decreases). Simple linear regression was performed using *lm* function in R to examine if the maximum residue θ_g and the characteristic moisture release curves could be estimated based on residue chemical characteristics; the best fit parameters are presented in subsequent figures.

Linear and non-linear regression models were fitted to examine the relationship between residue CO_2-C flux and environmental variables for each study period independently. Data points where residue CO_2-C flux was equal to zero were excluded during analysis to avoid over-fitting of the model equations. Separate regression models were determined for each study period. To determine if residue type and the extent of decomposition affected the relationship between CC residue θ_g and CO_2-C flux, the slopes and intercepts of the linear models were compared using the *emmeans* package in R (Lenth, 2020).

Results

Residue chemistry changes during decomposition

As CC residue decomposition progressed, residue N concentrations increased, thus leading to lower C:N ratios over time (Table 2.1). The chemical characteristics of the CC surface residues also changed during decomposition. The percentage of carbohydrate in the red clover tissue decreased initially from week 0 to 4, while the proportion of cellulose and hemi-cellulose increased during the same period (Table 2.1). At later stages of decomposition, i.e. from week 4 to 16, carbohydrate and cellulose concentrations in the red clover tissue remained nearly constant. Hemi-cellulose concentrations in the remaining red clover residues slightly decreased from

week 4 to 16. In a similar manner, hemi-cellulose concentrations in the remaining cereal rye residues also decreased over time. Conversely, the lignin concentrations increased over time; the relative increase was greater for red clover than cereal rye. We found a quadratic relationship between lignin concentrations and time (red clover: $y = -0.04x^2 + 1.12x + 5.78$, $R^2 = 0.99$ and cereal rye: $y = -0.02x^2 + 0.71x + 6.03$, $R^2 = 1$).

Changes in residue water retention properties during decomposition were linked to changes in residue lignin concentrations

The maximum water retentive capacity of the CC residues decreased as decomposition progressed (Figure 2.1). The maximum θ_g of the red clover and cereal rye residues decreased by 53.1% (from week 0 to 16) and 15.7% (from week 2 to 18), respectively. Irrespective of the CC species and decomposition stage, the power function presented in equation [2] adequately fitted the relationship between $\psi_{residue}$ and residue θ_g (Figure 2.1; R^2 = 0.80 - 0.99). We observed differences among the moisture release curves of red clover residues sampled at weeks 0, 4, and 10 (Figure 2.1a). However, red clover residues sampled at weeks 10 and 16 showed no differences among the moisture release curves. As decomposition progressed, the water retained by red clover residues declined at high $\psi_{residue}$ (> -30.0 MPa). In other words, more water was retained by undecomposed (week 0) residues, followed by slightly-decomposed (week 4) residues, and then by moderately-to-highly decomposed red clover residues (weeks 10 and 16). At a very negative $\psi_{residue}$ (< -30.0 MPa), the residue θ_g was quite similar between decomposed and undecomposed red clover residues. Cereal rye residue decomposition and water retentive capacity

followed the same pattern as that of red clover (Figure 2.1b). At a given $\psi_{residue}$, the highest θ_g was found in the least decomposed cereal rye residues (week 2) and the lowest θ_g in the highly decomposed cereal rye residues (week 18). Cereal rye residues collected at week 5 had intermediate values of residue θ_g.

Decomposition-associated changes in residue water retention properties were directly linked to changes in residue chemical characteristics. We found that the maximum residue θ_g decreased linearly with increasing residue lignin concentrations (Figure 2.2a). Similarly, parameter 'a' of the characteristic moisture release curve also decreased linearly with the increase in residue lignin concentrations (Figure 2.2b). Conversely, parameter 'b' of the characteristic moisture release curve increased linearly with the increase in residue lignin concentrations (Figure 2.2c). These results indicate a common set of equations for both red clover and cereal rye residues can be used to predict maximum residue θ_g and parameters 'a' and 'b' of the characteristic moisture release curves.

Diurnal variations in surface residue decomposition: Effect of residue moisture and temperature

Air, residue, and soil temperatures exhibited similar diurnal patterns such that they increased between 06:00 and 16:00 h and decreased between 16:00 and 06:00 h on each day (Figure 2.3 and 2.4). The amplitudes of the diurnal patterns also varied substantially between study periods. We observed greater diurnal fluctuations in the temperature of surface residues than surface soils. Residue temperature consistently

increased to values higher than soil temperature during daytime and decreased to values similar to or lower than soil temperature during nighttime.

The diurnal patterns of ψ_{air} followed the patterns of air RH (Figure 2.3 and 2.4). Similarly, the diurnal patterns of the $\psi_{residue}$ followed the diurnal patterns of ψ_{air} such that the maximum values of the $\psi_{residue}$ were observed early in the morning at 06:00 h and then sharply decreased to reach daily minimums at 15:00 h. These patterns were completely opposite to those observed for soil, residue, and air temperatures. In addition, $\psi_{residue}$ had more extreme diurnal fluctuations during June than July or August. During Jun, the $\psi_{residue}$ of red clover fluctuated between -0.95 and -147.6 MPa while that of cereal rye fluctuated between -0.08 and -118.5 MPa (Figure 2.3a and 2.4). The $\psi_{residue}$ of red clover fluctuated between -5.15 and -68.4 MPa during July and between -2.36 and -73.7 MPa during August (Figure 2.3b and 2.3c).

Diurnal patterns of the residue θ_g were similar to those of $\psi_{residue}$ (Figure 2.3 and 2.4). The maximum values of the residue θ_g (red clover: 0.30 - 1.20 g g^{-1}; cereal rye: 0.37 - 2.58 g g^{-1}) were observed at 06:00 h on each day. After 06:00, residue θ_g sharply decreased during the daytime to reach its daily minimum values of 0.05 - 0.14 g g^{-1} for red clover and 0.04 - 0.07 g g^{-1} for cereal rye at 15:00 h. After 15:00, residue θ_g gradually increased during the nighttime. Conversely, surface soil θ_g and θ_v did not show diurnal variations and remained relatively constant throughout each study period.

Across all study periods, residue CO_2-C flux also showed diurnal fluctuations such that they decreased sharply between 06:00 and 12:00 h (morning), exhibited very little or undetectable CO_2-C flux between 12:00 and 18:00 h (daytime), and gradually increased between 18:00 and 06:00 h (afternoon and nighttime; Figure 2.3 and 2.4). The amplitudes of the diurnal patterns were observed at 06:00 h on each day; amplitudes decreased from one day to the next. For example, the peak CO_2-C flux from red clover residues during Jun. 3-5, 2019 decreased from 0.518 to 0.408 g m^{-2} hr^{-1} on day 1, down to 0.155 g m^{-2} hr^{-1} on day 2 (Figure 2.3a). Similarly, the peak CO_2-C flux from cereal rye residues decreased from 0.197 at day 0 to 0.085 to 0.072 g m^{-2} hr^{-1} on days 1 and 2, respectively (Figure 2.4). Similar observations were made during July and August study periods, though magnitudes were smaller. Diurnal variations in residue CO_2-C flux strongly tracked diurnal variations in $\psi_{residue}$ and residue θ_g.

Figure 2.5 shows the relationship between residue CO_2-C flux and (a) $\psi_{residue}$ and (b) residue θ_g for each study period. Residue CO_2-C flux increased exponentially with the $\psi_{residue}$, while a positive linear relationship was found between residue CO_2-C flux and residue θ_g. Conversely, residue CO_2-C flux decreased with increasing temperature (Figure 2.6). We also examined the effect of residue type and the extent of decomposition on moisture sensitivity of surface residue decomposition. The slopes and intercepts of the linear models (residue CO_2-C flux *vs.* residue θ_g) were significantly higher for red clover compared to cereal rye (Table 2.2). To examine the effect of the extent of decomposition on moisture sensitivity of residue decomposition, data from red clover residues were compared

between three study periods (June, July, and August). Although the intercepts of the linear models did not vary between these study periods, the slope was significantly higher for June compared to July and August (Table 2.2). The slopes for July and August study periods were not significantly different.

Discussion

Residue chemistry changes during decomposition

Cover crop residues differ greatly in their chemical composition, which in turn will affect their decomposition rate under given soil and climatic conditions (Cabrera et al., 2005; Poffenbarger et al., 2015; Thapa et al., 2018b). Several studies have suggested that residue C pool sizes sequentially decompose such that carbohydrates are degraded before holo-cellulose (cellulose + hemi-cellulose) and holo-cellulose before lignin (Gunnarsson et al., 2008; Gunnarsson and Marstorp 2002, Harman et al., 2008F). Studies have also suggested the occurrence of simultaneous decomposition of residue C pools, with the rate of decomposition decreasing in the following order: carbohydrate > holo-cellulose > lignin (Woodruff et al., 2018). Nonetheless, differences in the time and rate of decomposition of residue C pools will change the chemical composition of the remaining residues during decomposition.

In this study, we observed a sharp decrease in the carbohydrate concentration of red clover tissue until week 4, perhaps due to faster decomposition of readily decomposable carbohydrate fractions (Table 2.1). This concomitantly increased cellulose and hemi-cellulose concentrations in the red clover residue. Although hemi-cellulose concentrations initially increased, they decreased at later stages of

decomposition for both red clover and cereal rye residues. In contrast, residue lignin concentrations increased over time, probably due to degradation of carbohydrate and holo-cellulose fractions and the resultant increase in the recalcitrant lignin fractions via microbial by-products during decomposition. Our results are consistent with many previous studies that found decomposing crop residue lignin concentrations increased over time (Gao et al., 2016; Harman et al., 2008; Jahanzad et al., 2016; Kriauciuniene et al., 2008).

Changes in physical characteristics of CC residues were not evaluated in this study. However, studies have suggested that decomposition of cellulose and hemi-celluloses leads to formation of macropores within decomposed tissues (Iqbal et al., 2013; Maloney and Paulapuro, 1999). This loss of cellular components over time would alter the pore size distribution such that the decomposed residues have an increase in macropores. Such changes in the physical and chemical characteristics of CC residues during decomposition would strongly influence water retention properties, which impacts not only decomposability, but also water exchange processes between soil-residue-air interfaces.

Changes in residue water retention properties during decomposition were linked to changes in residue lignin concentrations

We observed that the maximum residue θ_g decreased with increasing decomposition for both CC species (Table 2.1). In sharp contrast, Iqbal et al. (2013) found that the decomposition of maize stems increased residue water retentive capacity and suggested that the increase in maximum θ_g was due to an increase in porosity during decomposition. Differences between these studies could be explained

by the distinct morphological characteristics of the maize stems. Maize stems are characterized by the presence of pith (the inner, sponge-like porous material) and bark (the outer, hard envelope). Since water is mostly stored in pith within maize stems, it may be possible that the increase in the volume of macropores during decomposition allowed pith to absorb more water in decomposed maize stems (Iqbal et al., 2013). However, CC residues used in this study were devoid of pith and hence, the water molecules may have been preferentially stored in the cell walls of decomposing tissues as bound water. Water molecules are bound or adsorbed to OH groups present in cellulose, hemi-cellulose, and lignin by the H-bonding force (Jiang et al., 2019). Jiang et al. (2019) further suggested that the availability of OH groups increased with increasing cellulose and hemi-cellulose fractions and decreased with increasing lignin fractions in the cell wall. Therefore, the changes in water retention properties of the decomposing CC residues likely may have been due to decomposition-associated changes in the residue chemical characteristics. Supporting this hypothesis, we found that the maximum residue θ_g was inversely related to lignin concentrations in the decomposing CC residues (Figure 2.2a).

The characteristic moisture release curves of the CC residues were also strongly influenced by the extent of decomposition (Figure 2.1). At any given $\psi_{residue}$, the θ_g of both red clover and cereal rye residues decreased as residue decomposed. In other words, residue θ_g of the decomposed residues dropped sharply even with a slight decline in $\psi_{residue}$, which was probably due to the presence of large volumes of macropores. From a modelling perspective, it is critical to determine the decomposition-associated changes in the characteristic moisture release curves

(parameters 'a' and 'b') because it helps us understand the rate at which the water is transferred among soil-residue-air interfaces under a given environmental condition (Dann et al. in prep.). In this study, we found that the decomposition-associated changes in characteristic moisture release curves can be best predicted as a function of residue lignin concentrations (Figure 2.2b and 2.2c). Given that the lignin concentrations in the CC residues can be quickly and easily determined using near infra-red spectroscopy (NIRS) technique, we propose the use of lignin as a proxy for water retention properties (maximum residue θ_g and parameters 'a' and 'b' of the moisture release curves) of the decomposing CC residues.

Diurnal variations in surface residue decomposition: Effect of residue moisture and temperature

Surface CC residues can influence the soil physical environment in no-till cropping systems. Residue acts as a physical barrier that intercepts solar radiation and thus reduces the maximum soil temperature (Bristow, 1988; Teasdale and Mohler, 1993). Consistent with previous studies, we found that the residue layer experienced greater temperature extremes than the underlying surface soil in the daytime (Figure 2.3 and 2.4). The maximum temperature in the CC residue layer and surface soil differed by as much as 2.2 to 10 °C. During nighttime, both soil and residue temperature declines and the rate of cooling of residue layers can be sometimes faster than that of surface soils (Figure 2.3 and 2.4). For instance, the temperature in the red clover residue layer was 2.1 °C lower than that in surface soil during early June. Therefore, CC residues experienced greater diurnal fluctuations in temperature than surface soils below the CC residues.

Our study further highlights that CC residues experience extreme diurnal fluctuations in residue θ_g or $\psi_{residue}$ and hence, undergo frequent dry-wet cycles: the residue θ_g declines below soil θ_g during the day (extreme drying) and rises above soil θ_g during the night (wetting) (Figure 2.3 and 2.4). The condensation of water vapor into dew, resulting from cool nights and high humidity at the study site, led to water absorption by CC residues during the nighttime. The underlying residue layer that is in contact with the soil can also serve as a sponge for water absorption from moist soil surfaces (Kutlu et al., 2018). The effect of soil water content on residue water content likely increased as decomposition progressed due to increase in soil-residue contact. As the sun rises, the water is rapidly lost to the atmosphere from CC residues via evaporation. The rate at which water is gained or lost from CC residues depends on the water potential gradient among soil-residue-air interfaces, which in turn is regulated by air temperature, RH, and soil moisture (Dann et al., in prep.). Although not quantified, we noticed that the topmost residue layer gained or lost water more rapidly compared to the underlying residue layer that is in direct contact with the soil. Therefore, depending on the residue thickness, a vertical moisture gradient exists such that different residue layers may decompose at different rates in the field.

To our knowledge, there is no study that measured diurnal variations in surface residue decomposition in no-till cropping systems. For the first time, we found that residue decomposition in no-till cropping systems exhibits distinct diurnal patterns that are strongly related to residue θ_g or $\psi_{residue}$ (Figure 2.3 and 2.4). Residue CO_2-C fluxes were typically observed during the nighttime, when residues gained moisture from the atmosphere (Figure 2.3 and 2.4). Depending on CC species

and the extent of decomposition, residue θ_g or $\psi_{residue}$ explained 70-89% of the diurnal variations in residue decomposition rate (Figure 2.5a, 2.5b; Table 2.2). Decomposition of red clover residues was more sensitive to residue θ_g than cereal rye residues. This suggests that CC residues of a recalcitrant nature (high C:N ratio and less carbohydrate fractions) decompose more slowly under the given environmental conditions. Moreover, we observed that the moisture-sensitivity of residue decomposition decreased as decomposition progressed. The slopes of a linear model (CO_2-C flux vs residue θ_g for red clover) were significantly higher for June as compared to the July and August 2019 study periods (Table 2.2). The earlier decomposition (June) reduced the amount of readily decomposable material available for each successive measurement period. In addition, residue quantity decreased over time, resulting in significantly lower CO_2-C flux (g m^{-2} hr^{-1}) during late-stage of decomposition. Another factor may be decomposition-associated changes in residue water retention properties, as discussed earlier.

Although the positive response of residue decomposition to temperature has been frequently reported in laboratory incubation studies (Quemada and Cabrera, 1997; Stott et al., 1986; See Chapter 3), residue decomposition decreased with increasing temperature under field conditions (Figure 2.6). This was because the increase in residue temperature resulted in the decrease of residue θ_g or $\psi_{residue}$ to values that substantially limited microbial decomposition of CC residues (Figure 2.3 and 2.4). Based on these findings, we can conclude that the decomposition of CC residues in no-till fields is strongly moisture-limited on dry days.

Conclusions

This study, to our knowledge, provides the first in-situ evidence that the water retention properties of CC residues change during decomposition in response to changes in residue physical and chemical characteristics. As decomposition of CC residues progressed over time, the maximum residue θ_g decreased. Characteristic moisture release curves of the CC residues were also strongly influenced by decomposition such that the propensity of the residues to lose moisture (decrease in residue θ_g relative to decrease in $\psi_{residue}$) increased with increasing decomposition. Results further suggest that the water retention properties (maximum residue θ_g, as well as the parameters 'a' and 'b' of the characteristic moisture release curves) of the CC residues at any stage of decomposition can be determined based on lignin concentrations in the decomposing residues.

In addition, this study demonstrated that CC residues in no-till fields experienced extreme diurnal fluctuations in moisture (θ_g or $\psi_{residue}$) and temperature compared to underlying soils. Surface residue decomposition also showed distinct diurnal patterns that were strongly coupled to residue moisture. Increases in residue temperature, however, decreased residue decomposition because microbial activity was limited by moisture at elevated temperatures under field conditions. Based on these findings, we can conclude that the decomposition of CC residues in no-till fields is strongly controlled by residue moisture, which in turn depends on environmental conditions and the water retention properties of CC residues. Therefore, accurate simulation of surface residue decomposition in no-till fields will require mechanistic

models that can accurately predict residue moisture based on information easily available from weather stations.

Acknowledgments

This work was supported by the Northeast Sustainable Agriculture Research and Education (SARE) graduate student grant (award # GNE17-160-31064) awarded to Resham Thapa and the USDA Natural Resources Conservation Services (Conservation Innovation Grant # 8042-21660-004-36-R). We express our sincere thanks to the technical staff of the Sustainable Agricultural Systems Laboratory, USDA-ARS, Beltsville Agricultural Research Center, Beltsville, MD for managing the long-term cover crop systems project. We would also like to acknowledge Dr. Jude Maul for providing the EGM-4 infrared gas analyzer system, Alondra Thompson for providing the data logger system used in this experiment, and Dr. Victoria Ackroyd for proof-reading the manuscript.

Tables and Figures

Table 2.1 Biochemical characteristics of red clover and cereal rye residues at various stages of decomposition in 2019.

Residue	Study period	C	N	C:N ratio	Carbohydrate	Cellulose	Hemi-cellulose	Lignin
		----------%----------			----------%----------			
Red clover	May (0 week)	43.2	2.58	16.8	50.8	29.9	8.8	5.6
Red clover	June (4 week)	42.3	2.61	16.2	33.5	37.4	12.6	10.2
Red clover	July (10 week)	43.8	2.89	15.2	32.2	37.9	12.0	12.7
Red clover	August (16 week)	43.3	3.02	14.3	34.0	36.3	10.2	13.9
Cereal rye	May (2 week)	43.8	0.96	45.5	21.6	38.6	30.7	7.4
Cereal rye	June (5 week)	44.9	0.99	45.2	22.4	43.0	26.2	9.0
Cereal rye	September (18 week)	45.2	1.19	38.0	24.8	44.2	20.9	11.3

Table 2.2 Parameters of regression models fitted between residue decomposition rate (CO_2-C flux) and (a) residue water potential ($\psi_{residue}$) and (b) residue moisture content (θ_g) for each study period in 2019. Residue CO_2-C flux was exponentially related to $\psi_{residue}$ and linearly related to residue θ_g.

Residue	Study period	(a) Residue water potential $CO_2 - C\ flux = a \cdot exp^{(b \cdot \psi_{residue})}$			(b) Residue moisture content† $CO_2 - C\ flux = m \cdot \theta_g + c$		
		a	*b*	R^2	slope (m)	Intercept (c)	R^2
Red clover	June (4 week)	0.5917	0.1827	0.85	0.5078 Aa	-0.0594 aA	0.86
Red clover	July (10 week)	0.1751	0.2584	0.75	0.2405 b	-0.0429 a	0.70
Red clover	August (16 week)	0.1181	0.2679	0.84	0.2513 b	-0.0453 a	0.83
Cereal rye	June (5 week)	0.1838	0.3531	0.83	0.0741 B	0.0080 B	0.89

† Different lowercase letters within a column represent significant differences between study periods for red clover residue. Different uppercase letters within a column represent significant differences between red clover and cereal rye residues for June study period. Significant differences were determined at $p<0.05$.

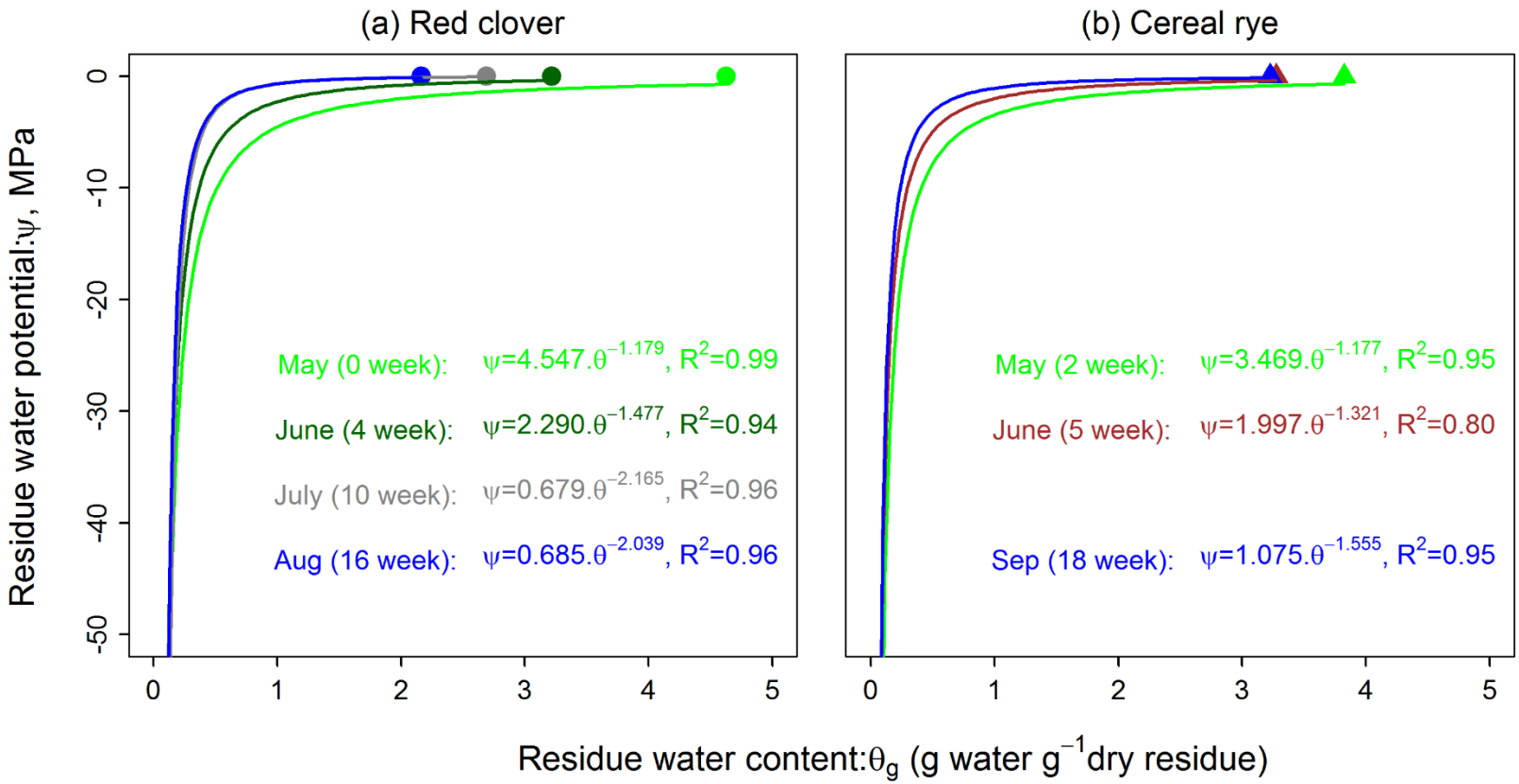

Figure 2.1 Characteristic moisture release curves for (a) red clover and (b) cereal rye residues at various stages of decomposition in 2019. The curves were fitted using the power function presented in equation [2] and the fitted equations are presented in subsequent figures. Solid points in the figures represent the actual maximum residue water content as determined in the laboratory. For clarity purposes, other points, indicating residue water potential values for corresponding gravimetric water contents, are not shown in the graphs.

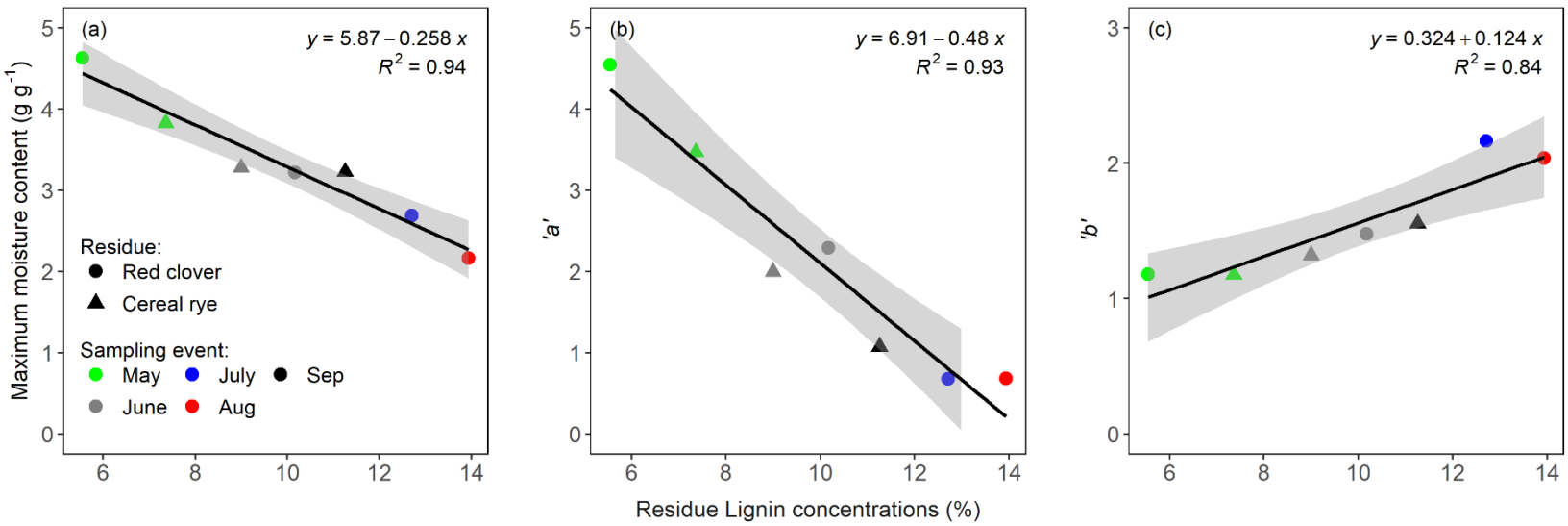

Figure 2.2 Water retention properties of decomposing cover crop residues as a function of residue lignin concentrations: (a) actual maximum residue moisture content, (b) parameter 'a' of the characteristic moisture release curves, and (c) parameter 'b' of the characteristic moisture release curves. The 'a' represents the plateau of the moisture release curve (estimated maximum residue water contents) and 'b' represents the shape of the moisture release curve (propensity of the residue to lose moisture as it dries, i.e. as $\psi_{residue}$ decreases). The equation of the linear models and their corresponding R^2 values are presented. Grey bands represent the 95% confidence interval of the modeled lines.

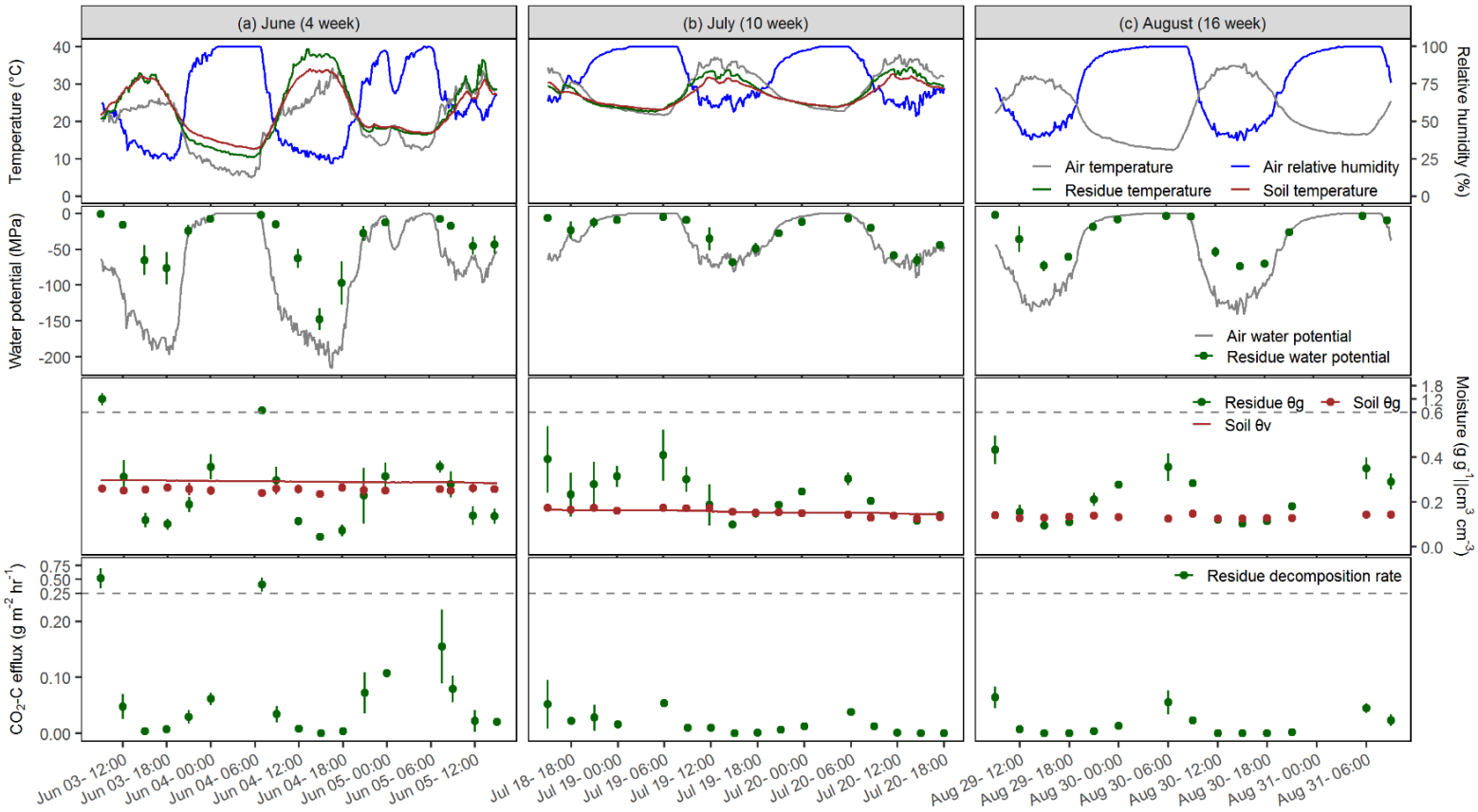

Figure 2.3 Diurnal variations in red clover residue decomposition rate (CO_2-C flux) and soil-residue-air environmental conditions for the (a) June (4 weeks after termination), (b) July (10 weeks after termination), and (c) August (16 weeks after termination) study periods in 2019. Residue CO_2-C flux, residue and soil gravimetric moisture content (θ_g), and residue water potential ($\psi_{residue}$) were measured at approximately 0:00, 6:00, 9:00, 12:00, 15:00, 18:00, and 21:00 hours each day. Air relative humidity (RH), soil-residue-air temperatures, and soil volumetric moisture content (θ_v) were continuously monitored at 10 min intervals throughout the study duration. Dashed lines indicate change in Y-axis scale for moisture and CO_2-C flux graphs.

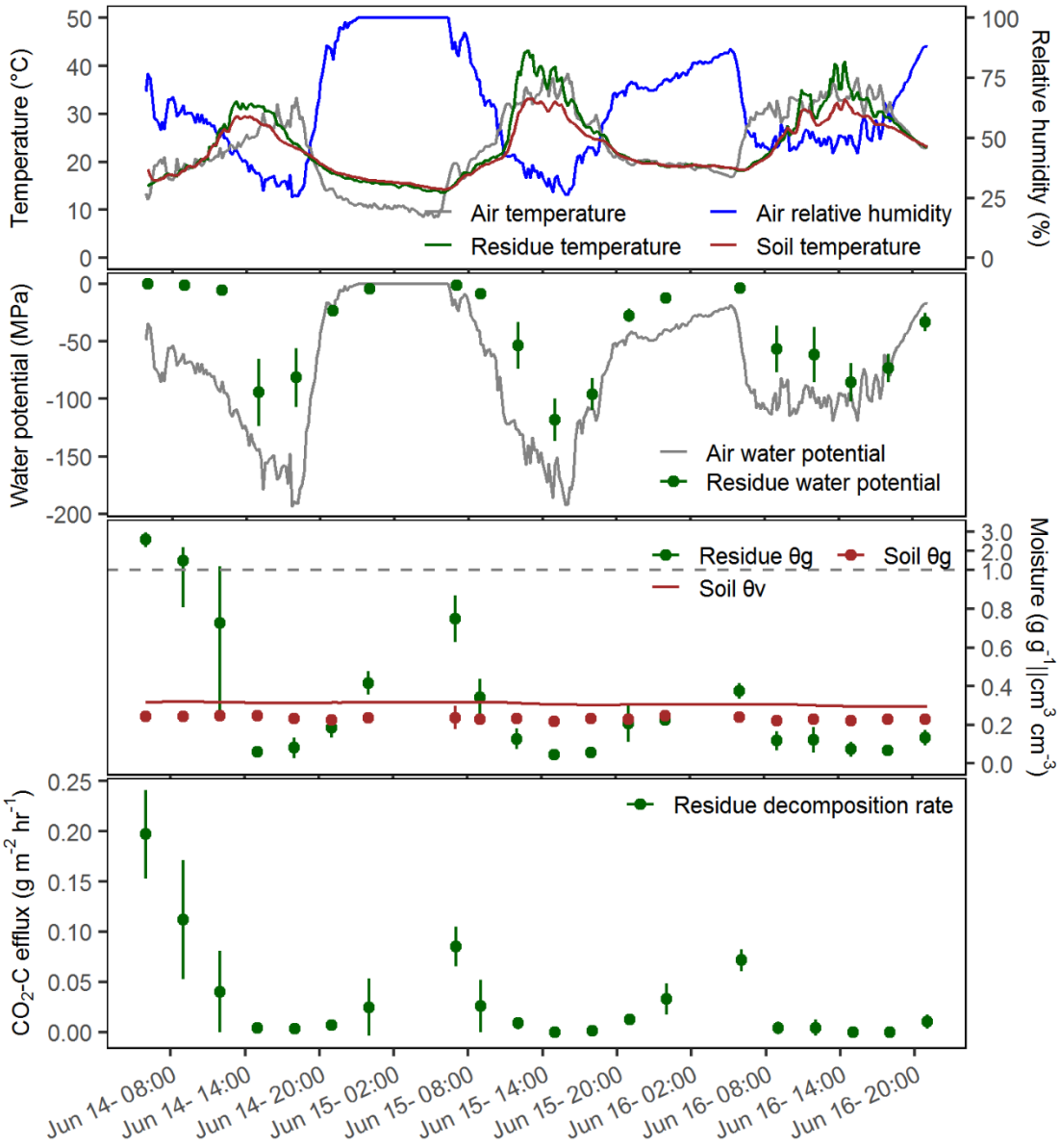

Figure 2.4 Diurnal variations in cereal rye residue decomposition rate (CO_2-C flux) and soil-residue-air environmental conditions during the June 14-16, 2019 (5 weeks after termination) study period. Residue CO_2-C flux, residue and soil gravimetric moisture content (θ_g), and residue water potential ($\psi_{residue}$) were measured at 0:00, 6:00, 9:00, 12:00, 15:00, 18:00, and 21:00 hours each day. Air relative humidity (RH), soil-residue-air temperatures, and soil volumetric moisture content (θ_v) were continuously monitored at 10 min intervals throughout the study duration. Dashed lines indicate change in Y-axis scale for moisture and CO_2-C flux graphs.

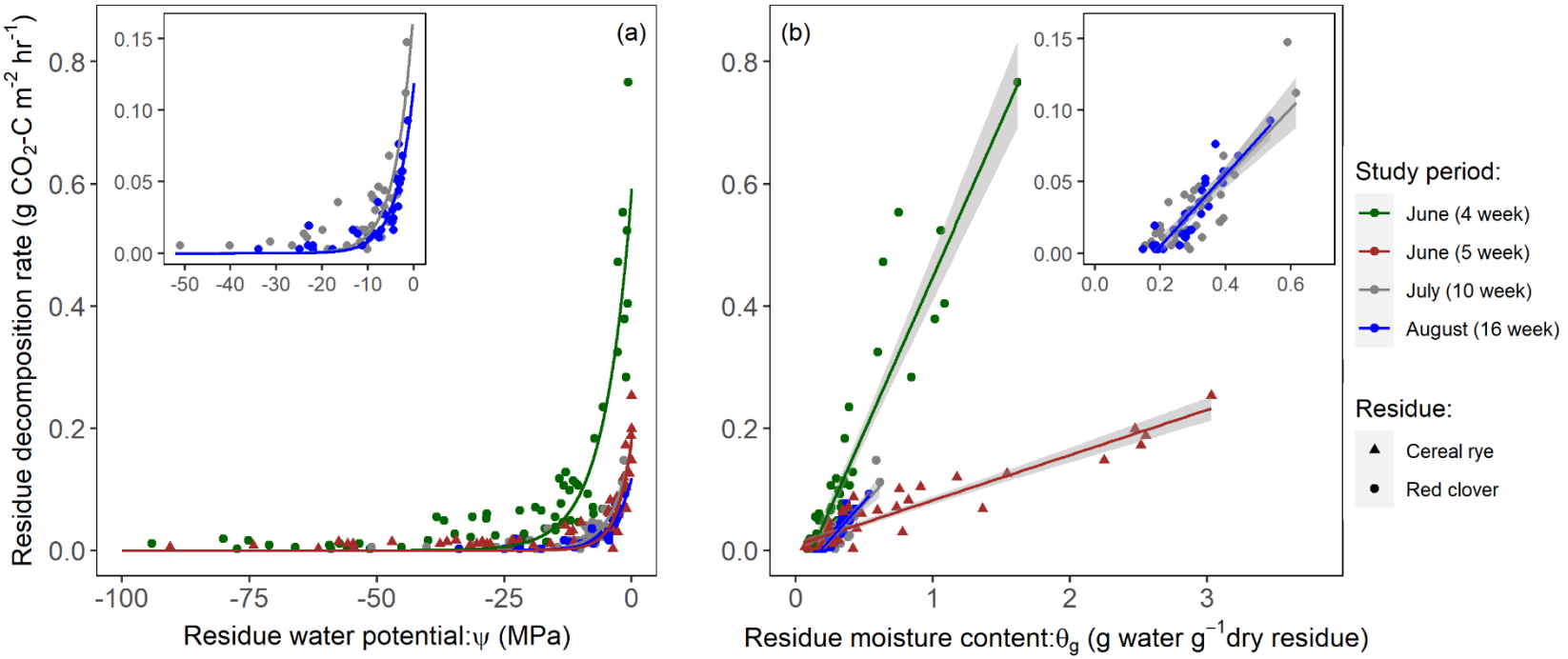

Figure 2.5 Relationship between surface residue decomposition rate (CO_2-C flux) and (a) residue water potential ($\psi_{residue}$), and (b) residue moisture content (θ_g) for each study period in 2019. Different colors represent different study periods; different shapes represent different cover crop residue types. Note that measurements where CO_2-C flux was equal to zero were excluded during analysis. Parameters of the model fits are presented in Table 2.2. Grey bands represent 95% confidence intervals.

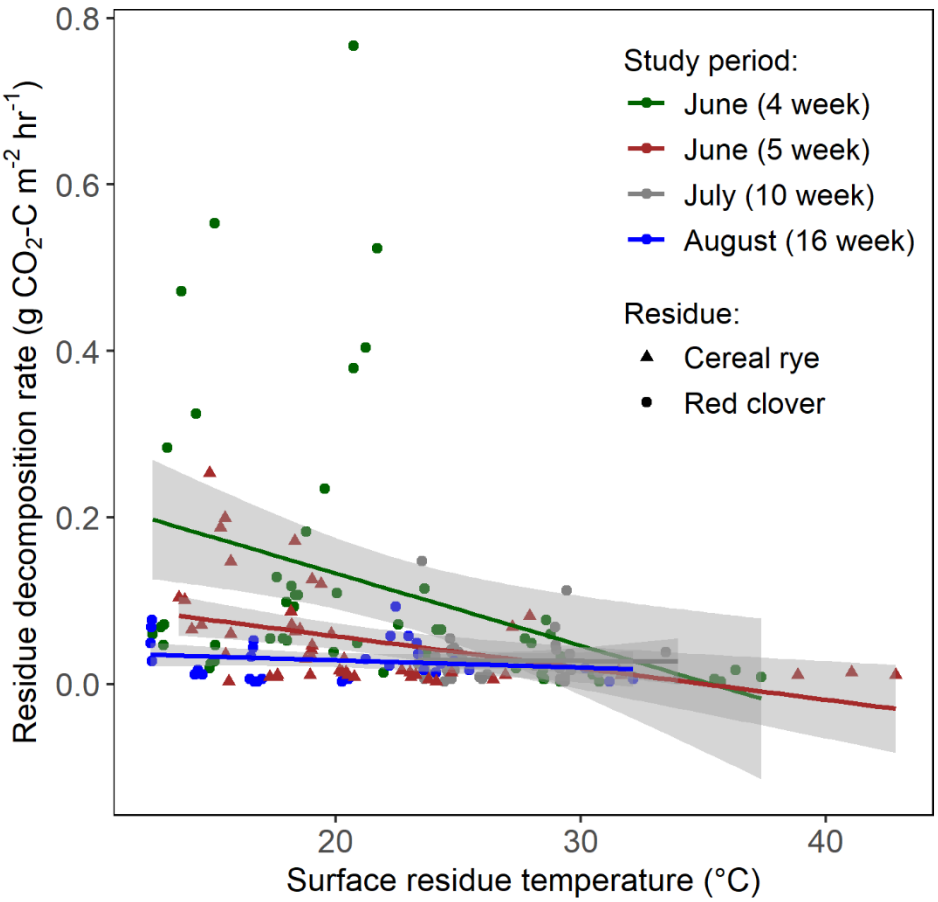

Figure 2.6 Relationship between surface residue decomposition rate (CO_2-C flux) and residue temperature for each study period in 2019. The decrease in surface residue CO_2-C flux with increasing residue temperature was due to decrease in moisture availability for microorganisms in the surface residue layers as temperature increases in no-till fields. Different colors represent different study periods; different shapes represent different cover crop residue types. Due to the failure of a data logger, we used air temperature at 75 cm height instead of residue temperature for the August study period. Note that measurements where CO_2-C flux was equal to zero were excluded during analysis. Grey bands represent 95% confidence intervals.

Chapter 3: Effects of moisture and temperature on C and N mineralization from surface-applied cover crop residues

Resham Thapa [a, b*], Katherine L. Tully [a], Miguel L. Cabrera [c], Carson Dann [c], Harry H. Schomberg [b], Dennis Timlin [d], Chris Reberg-Horton [e], Julia Gaskin [c], Brian W. Davis [b,f], and Steven B. Mirsky [b]

[a] Department of Plant Science and Landscape Architecture, University of Maryland

[b] Sustainable Agricultural Systems Laboratory, USDA-ARS

[c] Department of Crop and Soil Sciences, University of Georgia

[d] Adaptive Cropping Systems Laboratory, USDA-ARS

[e] Department of Crop and Soil Sciences, North Carolina State University

[e] Department of Environmental Science and Technology, University of Maryland

Forms the basis of a manuscript submitted to Biology and Fertility of Soils

Highlights

- Total C and N mineralized from surface residues were adequately described by first-order rate kinetic model.
- Net N immobilization was observed in late-killed rye residue.
- C and N mineralized from surface residues increased exponentially with increasing ψ from -10.0 to -0.03 MPa.
- Increasing temperature (T) enhanced ψ effect on C and N mineralization.
- The interaction effect between ψ and T on C and N mineralized from surface residues was modeled.

Abstract

Cover crop (CC) decomposition and subsequent release of nitrogen (N) in no-till systems is highly influenced by residue water potential (ψ) and temperature (T). To evaluate how carbon (C) and N mineralization from surface-applied CC residues responds to changes in ψ and T, a controlled microcosm experiment was conducted for 150 d with three CC residues [early-killed cereal rye (*Secale cereale* L.), late-killed cereal rye, late-killed crimson clover (*Trifolium incarnatum* L.), and a soil-alone control] under different ψ (-0.03, -1.5, -5, and -10 MPa) and T (15, 25, and 35 °C) conditions. Headspace gas was sampled periodically to determine carbon dioxide (CO_2) and nitrous oxide (N_2O) emissions. Soil inorganic N was determined by destructive sampling at 15, 30, 60, 100, and 150 d. Temporal dynamics in C and N mineralization from surface-applied CC residues were adequately described by first-order rate kinetic models. Early-killed rye and crimson clover (low C:N ratio) residues decompose quickly and mineralized N, whereas, late-killed rye residue (high fiber content and C:N ratio) immobilized N. The normalized values of C and N mineralized from surface-applied CC residues increased exponentially with increasing ψ from -10.0 to -0.03 MPa. Increasing T from 15 to 35 °C further amplified the effect of ψ, suggesting a strong interactive effect of ψ and T on C and N mineralization from CC residues. Mathematical equations were developed to describe these interactive effects. Existing computer simulation models (e.g. CERES-N) could be improved by integrating these equations to simulate the effect of environmental conditions on surface-applied CC residue decomposition and N mineralization.

Key words: Cover crops, Moisture, Temperature, C and N mineralization, Reduction factors

Abbreviations: CC, cover crops; ψ, water potential; T, temperature; *MTRF*, moisture-temperature reduction factor

Introduction

The rate and amount of nitrogen (N) released from cover crop (CC) residues during decomposition has consequences for N availability to the subsequent cash crop. While non-legume CC increases N fertilizer requirements due to N immobilization, legume CC decreases N fertilizer requirements due to fixed N (Poffenbarger et al. 2015; Otte et al. 2019; Thapa et al. 2018b; Williams et al. 2018). Farmers and agricultural professionals typically don't know the exact amount and timing of N availability from CC residues, resulting in N fertilizer recommendations based on expert opinion instead of a significant body of knowledge. As a result, they end up using more or less N fertilizer than required by the succeeding cash crop. Accurate predictions of plant-available N from decomposing CC residues are needed to improve N fertilizer recommendations in order to reduce environmental losses of N while meeting cash crop N needs (Gaskin et al. 2019).

Predicting plant-available N from decomposing CC residues is highly challenging because of the multiple factors involved in residue decomposition. These factors include residue chemistry (N content, C:N ratio, biochemical composition), residue placement (surface vs. incorporated), environmental conditions (water and temperature), and soil characteristics (Cabrera et al. 2005; Joshi et al. 2019;

Poffenbarger et al. 2015; Vigil and Kissel 1991; Wagger et al. 1998). Moreover, residue chemistry is impacted by management decisions such as CC species and mixture composition, planting and kill dates, and timing of termination (Alonso-Ayuso et al. 2014; Otte et al. 2019; Thapa et al. 2018b; Wagger 1989). Computer simulation models provide an operational approach to incorporate this complexity to simulate decomposition and concomitantly, C and N mineralization from crop residues.

A number of computer simulation models estimate crop residue decomposition and N mineralization under field conditions: Phoenix (McGill et al. 1981); NCSOIL (Molina et al. 1983); Verbene (Verbene et al. 1990); ecosys (Grant et al. 1993); CERES-N (Quemada and Cabrera 1995); APSIM (Thorburn et al. 2001); PASTIS (Findeling et al. 2007); and PNM (Melkonian et al. 2017). Decomposition models generally use initial CC biomass, residue chemistry (C or N content, C:N ratio, and residue C pool sizes), and environmental variables (soil water and temperature) as inputs. For example, CERES-N model partitions residue into three C pools (carbohydrate, holo-cellulose, and lignin) each having a specific decay rate (k values) under non-limiting conditions. Suboptimal environmental water (θ_g) and temperature (T) conditions are accounted for by applying θ_g and T reduction factors (MF and TF) to the k values. Accurate simulation of C and N mineralization from crop residues depends on the capacity of models to correctly estimate MF and TF. Although existing models are effective in simulating decomposition and N mineralization from incorporated residues, they often overpredict N mineralization from surface-applied crop residues (Melkonian et al. 2017; Quemada et al. 1997;

Schomberg and Cabrera 2001; Woodruff et al. 2018). Overprediction may be the result of estimating MF and TF based on soil θ_g and T, which may not reflect the true state of surface-applied crop residues. This hypothesis is supported by several laboratory and field studies showing that surface-applied CC residues experience greater fluctuations in θ_g or water potential (ψ) and T than surface soils (Coppens et al. 2006, 2007; Findeling et al. 2007; See Chapter 2). In a series of diurnal experiments, Thapa et al. (See Chapter 2) found that C mineralization from surface-applied red clover (*Trifolium pratense* L.) and cereal rye (*Secale cereale* L.) residues closely followed the pattern of residue θ_g or ψ, suggesting that residue decomposition in no-till systems is highly influenced by residue environment. Basing MF and TF on the residue environment (residue ψ and T) could, therefore, greatly improve estimation of C and N mineralization in existing models.

Response of surface-applied CC residue decomposition directly to residue ψ and T have rarely been studied together. In a 30-day incubation experiment, Stott et al. (1986) examined independently the effect of residue ψ or T on C mineralization from surface-applied wheat (Triticum aestivum L.) residue. In their study, response to ψ or T was determined while keeping the other variable constant. Quemada and Cabrera (1997) investigated the combined effect of ψ and T on C mineralization from surface-applied crimson clover (*Trifolium incarnatum* L.) residue over a 21-d period. They found that C mineralization increased exponentially with increase in ψ from -5.0 to -0.003 MPa and that the effect of ψ on C mineralization increased with increasing T. The interactive effects of ψ and T on C mineralization were different between unamended soil and soil with surface-applied crimson clover residue. Both

incubation studies were conducted for < 30 days. To our knowledge, no study has evaluated the interactive effects of ψ and T on decomposition of surface-applied CC residues of varying qualities for a full crop cycle (> 120 days). Moreover, limited data are available in the literature to evaluate the interaction between MF and TF for C and N mineralization from surface-applied CC residues across the continuum of ψ and T. For example, the lowest water potential studied by Quemada and Cabrera (1997) was -5 MPa, but our preliminary data show that residue decomposition can occur at even lower water potentials. Defining these relationships is crucial to simulate the effect of environmental conditions on surface residue decomposition and N mineralization in existing computer simulation models.

We investigated the interactive effect of ψ and T on C and N mineralized from surface-applied CC residues over 150 d. Our objectives were (i) to describe and quantify how C and N mineralization-immobilization kinetics from surface-applied CC residues were affected by changes in residue ψ and T; (ii) to evaluate the effect of CC species and kill date, i.e. the effect of residue chemistry, on the relationship between residue ψ and T; and (iii) to develop mathematical equations to describe the interaction between MF and TF for application in crop residue decomposition simulations.

Materials and Methods

Soil and cover crop residue characteristics

Soil for the incubation was collected in 2017 (0-10 cm) from a corn crop production field mapped as Russett (Fine-loamy, mixed, semiactive, mesic Aquic Hapludults)-Christiana (Fine, kaolinitic, mesic Aquic Hapludults) complex (Soil

Survey Staff 2020) at the Beltsville Agricultural Experiment Station (Beltsville, MD, USA; 39°01'12.6"N 76°56'33.8"W). Immediately after sampling, field-moist soil was sieved through 4-mm sieve, roots were manually removed, and the soil was homogenized. The soil was then air-dried, ground, passed through a 2-mm sieve, and stored at room temperature until beginning the incubation experiment. The processed soil contained 164 g kg^{-1} clay, 314 g kg^{-1} silt, 522 g kg^{-1} sand, 1.28 g N kg^{-1} and 13.0 g C kg^{-1}.

Cover crop (CC) residues for the incubation were collected at different vegetative growth stages: (i) early-killed cereal rye (tillering stage; Zadoks 30; Zadoks et al. 1974), (ii) late-killed cereal rye (anthesis; Zadoks 60), and (iii) late-killed crimson clover (full bloom stage). Residues were oven-dried at 60°C for 2 days, leaves and stems separated, and then stored at room temperature until future use. Fixed proportion of leaves and stems in crimson clover, early-killed cereal rye, and late-killed cereal rye, (0.4 and 0.6; 0.4 and 0.6; and 0.2 and 0.8; leaves and stems, respectively based on their relative proportions in the dried biomass), were used for establishing microcosms described below.

Water content of residues for use in microcosms were adjusted to four ψ (-10.0, -5.0, -1.5, and -0.03 MPa) prior to adding to the incubation units using the following procedure. Dried residue parts, cut into 0.5-cm long pieces, were saturated with distilled water overnight, and then allowed to drain for 10 minutes. After 10 minutes, residues assigned to -0.03 MPa were stored in air-tight plastic zippered bags. Remaining wet residues were spread on trays to air-dry under room ambient conditions (low RH and temperature of 24 to 26 °C). Periodically, ψ of the residue

was measured using a WP4C Dewpoint Potentiometer (METER Group, Inc., Pullman, WA). When the desired ψ was reached, sufficient residues for each treatment were stored in air-tight plastic zippered bags. Samples of residue at each ψ were oven-dried at 60°C for 48 h to determine the relationship between θ_g and ψ (Table 3.1).

The amount of total C and N, and structural carbohydrates remaining in the residues (following soaking and draining) were determined for a subset of residue samples from the process above. Residue subsamples were oven-dried, finely ground, and analyzed for total C and N using Elementar vario MAX Total Combustion Analyzer (Elementar Company, Langenselbold, Germany). Residue carbohydrate, cellulose, hemicellulose, and lignin concentrations were determined via near infra-red reflectance spectroscopy (NIRS) using scanning monochromator (model 6500; FOSS NIRSystems, Silver Spring, MD).

Preparation of microcosms

Approximately 40 kg of air-dried soil was wetted to field capacity (-0.03 MPa) with double deionized water and pre-incubated at 25°C for three weeks in closed containers to limit loss of moisture. The soil was mixed thoroughly every 2-3 days. Pre-incubation of soils was performed to deplete the initial flush of CO_2 from microbial activity caused by re-wetting of air-dried soil. After pre-incubation, soil was quickly sieved through a 2-mm sieve to avoid changes in moisture levels. The soil was divided and placed into four plastic bags. One plastic bag was sealed and immediately placed in a refrigerator at 4°C. Remaining soil was spread on trays and

air-dried with frequent turning to achieve θ_g equivalent to -10.0, -5.0, and -1.5 MPa, respectively (Table 3.1). Soil ψ was determined using the WP4C Dewpoint Potentiometer. Once a target ψ was achieved, another portion of soil was placed in a plastic bag and placed in the refrigerator, and duplicate 50 g soil subsamples were weighed and placed in an oven at 104°C for 48 h to determine θ_g (Table 3.1).

Microcosms for each target ψ were prepared in 100-mL plastic beakers (5.0 cm i.d.) using the previously prepared soil and residues. Beakers were packed with soil (50 g oven-dried equivalent) and CC residues (3000 kg ha^{-1} based on beaker surface area) were added to the soil surface (both soil and residue having the same ψ). Cover crop residues leaves and stems proportions added were predetermined as mentioned earlier. Microcosms of unamended soil were included for each moisture-temperature combination to determine C and N mineralization from soil organic matter.

Laboratory incubation

The experimental design was a split-split plot with T (15, 25, and 35°C) as main plot treatment, ψ (-10.0, -5.0, -1.5, and -0.03 MPa) as split-plot treatment within each main plot, and CC residue type (early-killed cereal rye, late-killed cereal rye, late-killed crimson clover, and soil-alone control) as split-split plot treatment. Each experimental unit was replicated three times. In total, 720 microcosms were prepared.

Microcosms were placed in a customized air-flow system that controlled the air relative humidity. This system was conducted in a set of CONVIRON E7/2 growth chambers (Controlled Environment Limited, Winnipeg, MB, Canada) set at

three different T: 15, 25, and 35°C. Four plastic chambers corresponding to four different ψ were held within each temperature unit. The relative humidity of the air in each plastic chamber was kept in equilibrium with the targeted ψ of the microcosms to minimize water loss during incubation and keep ψ constant. Humidified air was circulated through each plastic chamber by bubbling it through 10-L of deionized water or $CaCl_2$ solutions of specific osmotic potential (Calcium chloride handbook 2003). In addition, 2 L of deionized water or respective $CaCl_2$ solutions were added to the space below the microcosms in the plastic chamber. Air circulating into each chamber was regulated at 0.2 L min^{-1} using a flowmeter (Dwyer Instruments Inc., Michigan City, IN, USA).

An additional set of microcosms to determine CO_2 and N_2O emission rates was placed in 0.95-L mason jars containing 125 mL of deionized water or $CaCl_2$ solutions of specific osmotic potential. The jars were sealed with air-tight lids fit with butyl rubber septa to facilitate headspace gas sampling. The jars were opened daily and allowed to aerate for 30 min to avoid excessive buildup of CO_2. Gas samples were collected 29 times over the 150-d incubation period. Sampling was more frequent during the first 60 days and then at weekly or bi-weekly intervals for the rest of the incubation. Prior to gas sampling, headspace gas in each jar was thoroughly mixed three times by drawing and reinjecting 10 mL of headspace with a syringe. A 10-mL gas sample was transferred into 12-mL N_2-flushed glass vials (Labco Ltd., Lampeter, UK) fitted with butyl rubber septa. Vials were stored in a refrigerator at 4°C until analysis, within a week of collection, using a Varian GC450 gas chromatograph (Agilent Technologies, Santa Clara, CA) equipped with a thermal

conductivity detector for CO_2 and an electron capture detector for N_2O. Various concentrations of CO_2 and N_2O gas standards were prepared from a tank (Airgas Specialty Gases, 2.30 ppm N_2O, 2.99 ppm CH_4, 1.00% CO_2, balance N_2) on each sampling day and analyzed along with gas samples. Gas concentrations were converted into emission rates using the ideal gas law, headspace volume, time of gas accumulation in the headspace, and surface area of the microcosms. Cumulative CO_2 and N_2O emissions were calculated by linear interpolation of CO_2 and N_2O emission rates between the measurement dates (Thapa et al. 2015).

A set of microcosms were destructively sampled at 15, 30, 60, 100, and 150 d and analyzed for total inorganic N ($NH_4^+ + NO_3^-$). The contents of the microcosms were extracted with 500 mL of 1 mol L^{-1} KCl (1:10 soil:extractant ratio) after overnight shaking in 1-L plastic bottles. The KCl extracts were filtered through Whatman No. 42 filter paper and a 30-mL subsample was stored at -18°C until analyzed colorimetrically for NH_4^+ and NO_3^- using a SEAL AutoAnalyzer 3 High Resolution (SEAL Analytical Inc., Mequon, WI).

Data analysis

Cumulative N mineralized for each microcosm unit was calculated as the sum of inorganic N ($NH_4^+ + NO_3^-$) and cumulative N_2O emitted during that period. Total C or N mineralized from CC residue was estimated by subtracting the cumulative values of CO_2 emitted or N mineralized in unamended (control) treatments from values measured in residue-amended treatments. Total C and N mineralized over 150-d were compared by two-way analysis of variance performed separately for each residue using *agricolae* package in R (Mendiburu 2019). Significant differences

among treatment means were determined using least significant difference (LSD) tests at α value of 0.05.

We investigated C or N mineralized from each CC residue type as a function of time using a single-pool first-order rate kinetic model. Models parameters were determined using the *nlme* package in R (Pinheiro et al. 2017):

$$C_{min} = C_0(1 - e^{-k \cdot t}) \quad \text{Eq. [1]}$$

$$N_{min} = N_0(1 - e^{-k \cdot t}) \quad \text{Eq. [2]}$$

where C_{min} or N_{min} are C or N mineralized in time t (g m^{-2}), C_0 or N_0 represents potentially mineralizable C or N (g m^{-2}), and k the mineralization rate constant (d^{-1}). The first-order rate kinetic models were fit independently for each ψ and T combination.

Instead of separately estimating MF and TF, we used the approach of Quemada and Cabrera (1997) to model the interactive effects of ψ and T on C and N mineralization using a normalized factor, hereafter referred to as the moisture-temperature reduction factor ($MTRF$). For each residue ψ and T combination, $MTRF$ is calculated by dividing the total C and N mineralized at the end of the incubation period (150 d in our study) by the value determined under optimum conditions (-0.03 MPa and 35 °C). The $MTRF$ is a dimensionless scaling factor ranging from 0 to 1. The following exponential model was used to relate $MTRF$ at a given T (15, 25, and 35°C) to ψ (-0.03 to -10.0 MPa):

$$MTRF(T) = a \cdot e^{b \cdot \psi} \quad \text{Eq. [3]}$$

Where $MTRF(T)$ is the residue moisture-temperature reduction factor at a given T (°C), 'a' and 'b' are empirical constants. Estimates for 'a' and 'b' in Eq. [3] were determined for each CC residue type using the *nls* function in R. Additionally, the two-dimensional response surface model equations described in the manuscript were fit to describe $MTRF$ as a function of the interaction between ψ and T. The response surfaces were plotted using *scatterplot3D* package in R (Ligges and Mächler 2003).

Results and Discussion

Cover crop quality

Structural and nonstructural carbohydrates and total C and N of the various CC residues are provided in Table 3.2. Compared to cereal rye, crimson clover had higher N and soluble carbohydrates but was lower in structural C (cellulose + hemi-cellulose; Table 3.2). Compared to the early-killed rye, the residue N concentrations and labile carbohydrate fractions were lower in late-killed rye, while the recalcitrant lignin fractions and slowly-degradable cellulose and hemi-cellulose fractions were greater (Table 3.2). Similar declines in cereal rye quality from early tillering to anthesis have been observed globally (Alonso-Ayuso et al. 2014; Otte et al. 2019; Wagger 1989). Differences in residue N concentrations were also reflected in tissue C:N ratio, which increased in the order: crimson clover < early-killed rye < late-killed rye (Table 3.2).

C mineralization

The CO_2 emission curves indicate that C mineralization from CC residues was very rapid initially and then decreased to a relatively slow and steady rate of residue

decomposition (Figure 3.1). This pattern was more pronounced at higher ψ and T as microbial activity quickly depleted the readily available substrates. The rapid initial phase of residue decomposition is represented by a steep slope in the CO_2 emission curves (Figure 3.1). Across all three CC residues, decreases in either ψ or T decreased overall CO_2 emissions and delayed time when the plateau was observed. The greatest and earliest peaks in CO_2 emissions were observed under conditions considered optimum for residue decomposition, i.e. -0.03 MPa and at 35°C (Quemada and Cabrera 1997; Schomberg et al. 1994). At the lowest ψ (-10.0 MPa) and T (15°C), maximum CO_2 emissions occurred much later (15-20 d after initialization depending on CC residue type). The CO_2 emissions decreased following their peak to a somewhat steady state, as indicated by the flat line in the CO_2 emission curves (Figure 3.1).

The patterns of cumulative CO_2 emission differed across CC residue types (Figure 3.1). The total C mineralized by 150 d was greater from early-killed rye residues compared to late-killed rye across all ψ and T combinations (Table 3.3). Several studies have reported that late-killed CC residues decomposed more slowly and mineralized less C than early-killed CC residues (Alonso-Ayuso et al. 2014; Otte et al. 2019; Wagger 1989). This was due to low N and carbohydrate concentrations and high lignin content in late-killed rye residues (Table 3.2). Although residues of crimson clover had higher N concentrations than the rye residues, total C mineralized was intermediate between early- and late-killed rye (Table 3.3). This could be attributed to the intermediate levels of cellulose and lignin compared to the two rye

residue types (Table 3.2). These results highlight the importance of residue chemical composition in regulating kinetics of C mineralization from CC residues.

We found that the total C mineralized by 150 d from surface-applied CC residues was significantly affected by ψ, T, and ψ × T interactive effects (Table 3.3). Across all three residues, total C mineralized by 150 d increased with increasing ψ or T or both and the response to T was generally greater at high ψ (Table 3.3; Figure 3.1). Increasing incubation T from 15 to 35°C proportionally increased total C mineralized from residues probably due to enhanced enzymatic activity at higher T, which led to greater break-down of freshly-added residue substrate (Stott et al. 1986; Roper 1985; Quemada and Cabrera 1997; Yanni et al. 2018). At all temperatures, total C mineralized increased sharply with the increase in ψ from -10.0 to -0.03 MPa (Table 3.3). Decreases in residue C mineralization at lower ψ could be attributed to a combination of physical, biochemical, and physiological effects associated with low moisture availability. For example, as the residue dries, 1) the solubility and diffusivity of labile C from residues decreases, leading to poor substrate availability (physical effect); 2) the activity of extracellular enzymes necessary for substrate breakdown diminishes (biochemical effect); and 3) the activity of decomposer communities diminishes due to dehydration of microbial cells at lower ψ (physiological effect) (Griffin 1981; Manzoni et al. 2012; Moyano et al. 2013; Skopp et al. 1990; Schjonning et al. 2003).

In this study, considerable amounts of C mineralized were observed even at relatively dry surface residue conditions. Depending on the incubation T, the total C

mineralized at -10.0 MPa from early-killed rye, late-killed rye, and crimson clover residues were 27-37%, 7-8%, and 10-14% of the total C mineralized at -0.03 MPa, respectively. Thus, our data suggest that microbial decomposition of surface-applied CC residues can occur until water potentials fall below -10.0 MPa (e.g. threshold dynamic). In line with our findings, several researchers have reported that the microbial decomposition of surface residues will cease at ψ between -38.0 to -22.8 MPa (Manzoni et al. 2012, Moore 1986; Moyano et al. 2013). This is considerably drier than the water stress threshold value for most bacteria ($\leq$ -2.0 MPa) (Manzoni et al. 2012). Fungi, on the other hand, are more tolerant to water stress than bacteria and have very low water stress threshold values ranging between -60.0 to -4.0 MPa (Griffin 1981). Therefore, we hypothesize that fungi are primarily responsible for the decomposition of surface-applied residues. Previous studies have also demonstrated that fungi are the primary decomposers of surface-applied crop residues because of their ability to produce a wide variety of extracellular enzymes, accumulate osmoregulatory solutes, and form extensive hyphal networks between soil and surface residues (Frey et al. 2000; Griffin 1977; Holland and Coleman 1987; Wells et al. 2017). The hyphal bridges permit fungi to exploit resources (water and nutrients) from both soil and surface-applied crop residues. In our study, extensive growth of hyphal networks was visually observed particularly in microcosms amended with early-killed rye residues. We hypothesized that the cell walls of early-killed rye residues may not be structurally rigid and have water-filled pores that allowed greater solubility and diffusivity of readily available C, extracellular enzymes, and other metabolic products resulting in enhanced fungal growth and activity. Differences in

physical characteristics of the CC residues may explain part of the differences in C mineralization observed between early- and late-killed CC residues, especially at low ψ.

N mineralization-immobilization kinetics

Net N mineralization from crimson clover and early-killed rye residues was observed at all ψ and T combinations, whereas late-killed rye exhibited a pattern of N immobilization (Figure 3.2). Most of the N mineralization from crimson clover and early-killed rye occurred within the first 15 days. Depending on ψ and T, the amount of net N mineralized by 15 d ranged from 0.5-25% of the total residue N (Figure 3.2). Early period net N mineralization from CC residues has been reported previously for surface-applied (Quemada and Cabrera 1995) and incorporated CC residues (Kuo and Sainju 1998; Lawson et al. 2012; Poffenberger et al. 2015a). The pattern of net N mineralization from crimson clover and early-killed rye residues were quite similar at all environmental conditions (Figure 3.2). This suggests that early-killed rye, which has a comparable C:N ratio as crimson clover, decomposes and mineralizes N in a similar manner.

The cumulative net N mineralized by 150 d from surface-applied crimson clover and early-killed rye residues is shown in Table 3.3. Depending on ψ and T combinations, cumulative net N mineralized ranged from 2.0 to 47% of the total N in crimson clover residue and from 1.5 to 45% of the total N in early-killed rye residue. Cumulative %N mineralized was linearly related to cumulative %C mineralized for both crimson clover (R^2 = 0.96) and early-killed rye residues (R^2=0.88). This indicates that the ψ and T effects on net N mineralization from surface-applied CC

residues were like those expressed above for C mineralization and the response was similar for these two types of CC residues (Table 3.3, Figure 3.2).

The pattern of net N immobilization observed for surface-applied late-killed rye residues was most pronounced at -0.03 MPa at 15 or 25 °C. For these ψ and T combinations, the amount of net N immobilized progressively increased throughout the incubation (Figure 3.2). By 150 d, the amount of N immobilized was equivalent to 49% of the total residue N at 15 °C, whereas it was 41% of the total residue N at 25 °C (Table 3.3; Figure 3.2). However, at 35 °C, net N immobilization persisted for a shorter period and reached a maximum value (32-36% of residue N) at 30 to 60 d of incubation. This coincided with periods of high C mineralization (Figure 3.1 and 3.2). After 60 d in the -0.03 MPa and 35 °C treatment, N began to be mineralized from the late-killed rye (Figure 3.2). By 150 d, 11% of the total residue N was mineralized.

Several studies have reported the decomposition of residues with low N concentrations and high C:N ratio immobilizes N from the system (Kuo et al. 1997; Kuo and Sainju 1998; Poffenbarger et al. 2015a; Quemada and Cabrera 1995; Schomberg et al. 1994; Williams et al. 2018). The critical value of C:N ratio above which N immobilization occurred varied across studies, ranging between 20 and 40 (Frankenberger and Abdelmagid 1985; Kuo et al. 1997; Reberg-Horton et al. 2012; Vigil and Kissel 1991). The C:N ratio of late-killed rye applied in our study (C:N ratio = 87.7) was above this critical range. Fungal translocation of soil N to decomposing surface-applied CC residues is a primary mechanism for N immobilization (Frey et al. 2000; Holland and Coleman 1987). Our observation of

fungal hyphae on CC residues in the microcosms would indicate this as a probable mechanism facilitating N immobilization by the late-killed rye.

Our observation at -0.03 MPa and 35°C of a change from N immobilization to mineralization indicates a decrease in the C:N ratio of the late-killed rye residue over time based on work of Quemada and Cabrera (1995) and Nicolardot et al. (2007). Quemada and Cabrera (1995) found that the C:N ratio of surface-applied residues of cereal rye, wheat and oat (*Avena sativa* L.) stems decreased over time resulting in net N mineralization after 60-96 d of incubation. Nicolardot et al. (2007) also reported net N immobilization by surface-applied wheat straw (C:N ratio = 66) during the initial 14-84 d of incubation followed by net N mineralization until the end of the incubation (168 d).

The relative proportion of NH_4^+N and NO_3^-N in net N mineralized from surface-applied CC residues varied across incubation conditions (Figures A1, A2, and A3). At very dry surface residue conditions (ψ = -5.0 or -10.0 MPa), mineralized N was primarily in the form of NH_4^+N with nil to negligible concentrations of NO_3^-N throughout the incubation period. This suggests that the process of nitrification (conversion of NH_4^+N to NO_3^-N) was suppressed at ψ lower than -5.0 MPa, likely due to physiological stress on nitrifiers (Stark and Firestone, 1995). At -1.5 MPa, a time lag in nitrification was observed with conversion of NH_4^+N to NO_3^-N beginning 15 to 30 d after starting the incubation (Figures A1 and A2). This was probably due to limited NH_4^+N diffusivity and slow growth rate of nitrifiers at -1.5 MPa. Stark and Firestone (1995) found that the nitrification activity is greatly reduced at ψ below -0.6 MPa due to the adverse physiologic effects of cell dehydration, whereas substrate

limitation is the major inhibiting factor at ψ above -0.6 MPa. Accordingly, the maximum rate of nitrification in this study was achieved at -0.03 MPa where net N mineralized or immobilized from surface-applied CC residues was primarily in the form of NO_3^-N with nil to negligible amounts of NH_4^+N throughout the incubation. The net N_2O emitted from surface-applied CC residues also showed a pattern similar to those described above for NO_3^-N production (Figures A1, A2, and A3). At -0.03 MPa, both NO_3^-N and N_2O sharply increased immediately following residue addition. Whereas at -5.0 and -10.0 MPa, the amount of NO_3^-N mineralized and N_2O emitted from residues were minimal throughout the incubation. In a similar fashion, we observed a time lag in N_2O emissions at -1.5 MPa which coincides with the period when the conversion of NH_4^+N to NO_3^-N started. Therefore, nitrification may have been the dominant pathway for N_2O emissions from surface-applied CC residues across the environmental conditions studied.

Pool size and rate constants for C and N mineralization

At all ψ and T combinations, the single-pool first-order rate kinetic model adequately described temporal dynamics in C (R^2 ranged between 0.85 to 0.99) and N (R^2 ranged between 0.33-0.95) mineralized from surface-applied CC residues (Fig. 1, 2). Model parameters for potentially mineralizable C and N (C_0 and N_0) and rate constants (k values) estimated using first-order kinetics for the different CC residues are presented in Table 3.4 and 3.5. The C_0 and N_0 pool size reflected the cumulative C and N mineralized by 150 d across all ψ and T conditions (Tables 3.3, 3.4, and 3.5). The C_0 and N_0 values increased with response to increase in ψ and T.

Because there is an inverse relationship between k and C_0 or N_0 in the single-pool first-order rate kinetic model (Paustian and Bonde 1987), we chose to calculate ψ - and T-dependent k values following the method outlined by Wang et al. (2003). This method is based on the hypothesis that C_0 and N_0 represent residue intrinsic properties and are independent of ψ and T. Values of C_0 and N_0 obtained under optimum conditions of ψ (-0.03 MPa) and T (35 °C) were used as fixed values in the first-order rate kinetic model to determine k values at all other remaining ψ and T combinations. The ψ- and T- dependent k values determined in this way clearly showed an increasing response with increase in ψ and T, suggesting a faster decomposition of surface-applied CC residues under wetter and warmer conditions.

Modelling moisture-temperature interactive effects on C and N mineralization

Our results show ψ and T effects on decomposition and N mineralization from surface-applied CC residues interact. This suggests that MF and TF should be combined to express their overall effect on these processes. Quemada and Cabrera (1997) combined MF and TF into a single function labeled as $MTRF$ using a response surface. The response surfaces are scaled based on the total amounts of C or N mineralized compared to those at optimum conditions and thus, represents the relative activity. The relative activity normalizes the data and allows fitting a single response surface model across different CC residue types.

Results from fitting an exponential function estimating $MTRF$ for C and N mineralization at a given T (15, 25, and 35°C) over the range of ψ (-0.03 to -10.0 MPa) are given in Figure 3.3 and Table 3.6. For both C and N mineralization, the

value of 'a' for Eq. [3] increased linearly with T. Likewise, the value of 'b' for Eq. [3] was linearly related to the inverse of temperature (T^{-1}), suggesting the enhanced effect of ψ on C and N mineralization from surface residues with increasing T. Therefore, the interactive effects of ψ and T on C and N mineralized from surface-applied CC residues were estimated by the following two-dimensional response surface model (Quemada and Cabrera, 1997):

$$MTRF(T,\psi) = (c + d \cdot T) \cdot e^{(f + g \cdot T^{-1}) \cdot \psi} \qquad \text{Eq. [4]}$$

where, $MTRF(T,\psi)$ is the residue moisture-temperature reduction factor at a given residue ψ (MPa) and T (ºC), and 'c',' d',' f', and 'g' are empirical constants of the model. The fitted two-dimensional response surface models for predicting $MTRF$ for C and N mineralized from CC residues are presented in Fig. 4.

For C mineralized from surface-applied CC residues:

$$MTRF(T,\psi) = (0.384 + 0.018 \cdot T) \cdot e^{(0.142 + 0.628 \cdot T^{-1}) \cdot \psi} \text{ ; } R^2 = 0.91 \qquad \text{Eq. [5]}$$

For net N mineralized from surface-applied CC residues:

$$MTRF(T,\psi) = (0.184 + 0.023 \cdot T) \cdot e^{(0.199 + 0.929 \cdot T^{-1}) \cdot \psi} \text{ ; } R^2 = 0.97 \qquad \text{Eq. [6]}$$

The response surfaces developed in our work, Eq. [5] and Eq. [6], were then used to predict $MTRF$ values for C and N mineralization using residue ψ and T values from a similar laboratory study conducted by Quemada and Cabrera (1997) that only ran for 21-d. The predicted values generated from our model were then compared against the $MTRF$ values calculated from Quemada and Cabrera (1997)

measured data over 21-d (C or N mineralized/Maximum C or N mineralized). For C mineralization, we found that the response surface (Eq. [5]) overpredicted $MTRF$ at lower values and the relationship between measured and predicted $MTRF$ tended to converge at higher values (Figure 3.5). This is not surprising as it takes longer time for all the C to be lost at lower ψ and T because of the suboptimal residue environmental conditions for microbially-mediated processes. Given the very short period of decomposition (21-d), Quemada and Cabrera (1997) suggested that the readily decomposable C fraction of crop residues were mainly decomposed. In contrast, the response surfaces developed in our study were based on a 150-d incubation study during which both labile and recalcitrant C fractions may all have been decomposed. These results show the dependencies of response surfaces predicting $MTRF$ for C mineralization to changes in residue chemistry during decomposition. The response surface model (Eq. [6]) predicted $MTRF$values for N mineralization much better than Eq. [5] did for $MTRF$values for C mineralization (Figure 3.5). This was probably because most of the net N mineralized from surface-applied CC residues occurred early and may have been mostly associated with the decomposition of readily available labile C fractions (Figure 3.2). Therefore, our results showed greater promise towards using the two-dimensional response surface model developed in this study to predict $MTRF$ for modeling N mineralization from surface-applied CC residues. In future work, these response surfaces will be integrated into existing residue decomposition models to test their applicability in modelling C and N mineralization from surface-applied CC residues under field conditions.

Conclusions

Our findings show that surface-applied residue decomposition was mainly influenced by the residue environment (ψ and T). The first-order rate, kinetic model can be used to adequately describe the temporal dynamics of C and N mineralization during surface-applied residue decomposition. Depending on ψ and T, residues of crimson clover and early-killed rye decomposed quickly and released significant amounts of N, i.e. 1.5-47% of the total residue N by 150 d. Late-killed rye residue, on the other hand, decomposed slowly and immobilized N owing to its high fiber content and high C:N ratio.

This study further highlights the presence of strong interaction between residue ψ and T in mineralizing C and N from surface-applied CC residues. The normalized values of C and N mineralized in 150 d increased exponentially with increase in ψ from -10.0 to -0.03 MPa, suggesting greater sensitivity of surface residue decomposition to residue moisture. Moreover, the effect of ψ on C and N mineralization was amplified when the T increased from 15 to 35 °C. The two-dimensional response surface equations, which included ψ and T as variables, adequately described the interactive effect of these variables on C and N mineralized from surface-applied CC residues (R^2 = 0.91-0.97). This work served to enhance the mechanistic understanding of CC decomposition kinetics and how ψ and T interact to drive C and N cycling. Future efforts should be directed towards integrating these response surfaces into the existing computer simulation models and testing the efficiency of the modified models in predicting C and N mineralized from surface-applied residues under field conditions.

Acknowledgements

This research is part of a regional collaborative project supported by the USDA Natural Resources Conservation Services (Conservation Innovation Grant # 8042-21660-004-36-R), USDA National Institute of Food and Agriculture (Award # 2018- 68011-28372), and the Northeast Sustainable Agriculture Research and Education (SARE) graduate student grant (Award # GNE17-160-31064). We express our sincere thanks to research interns and technical staff of the Sustainable Agricultural Systems Laboratory, USDA-ARS, Beltsville Agricultural Research Center, Beltsville, MD for their laboratory assistance.

Tables and Figures

Table 3.1 Gravimetric water content of cover crop (CC) leaves and stems and soil used in the incubation experiment.

Water potential (ψ)	Gravimetric water content (θ_g)						
	Crimson clover		Early-killed rye		Late-killed rye		Soil
	Leaves	Stems	Leaves	Stems	Leaves	Stems	
	----------g g^{-1}----------						
MPa							
-10.0	0.370	0.374	0.701	0.664	0.679	0.468	0.033
-5.0	0.954	0.899	1.142	1.159	1.181	0.951	0.044
-1.5	1.980	2.103	2.319	2.164	2.309	2.520	0.069
-0.03	5.331	4.022	3.675	2.703	4.106	3.263	0.221

Table 3.2 Bio-chemical constituents of cover crop (CC) residues used in incubation study.

Cover crops	N	C	C:N ratio	Carbo hydrate	Cellulose	Hemi-cellulose	Lignin	ADF†	NDF‡
	-----%-----			----------%----------					
Crimson clover	2.90	48.5	16.7	46.1	32.7	10.1	6.0	38.7	48.8
Early-killed rye	2.24	48.0	21.5	39.7	24.7	29.7	2.7	27.4	57.1
Late-killed rye	0.56	49.2	87.7	18.5	42.5	31.4	8.4	50.9	82.3

† Acid detergent fiber.

‡ Neutral detergent fiber.

Table 3.3 Effect of residue water potential (ψ) and temperature (T) on total C and N mineralized in 150 d from different cover crop (CC) residues.

Residue water potential (ψ)	C mineralized†			N mineralized†		
	15°C	25°C	35°C	15°C	25°C	35°C
MPa	---------- g m^{-2} ----------					
	Crimson clover					
-10.0	5.3 ± 0.6‡	7.8 ± 0.6	11.8 ± 0.4	0.2 ± 0.0	0.2 ± 0.1	0.5 ± 0.3
-5.0	17.4 ± 2.1	27.6 ± 3.5	30.7 ± 1.6	0.4 ± 0.2	0.8 ± 0.2	1.3 ± 0.4
-1.5	46.4 ± 2.5	51.7 ± 3.2	68.5 ± 2.3	1.9 ± 0.2	2.1 ± 0.6	2.7 ± 0.2
-0.03	54.4 ± 1.1	68.0 ± 1.2	85.4 ± 2.0	2.2 ± 0.3	2.5 ± 0.1	4.1 ± 0.2
$LSD_{0.05}$		5.76			0.77	
	Early-killed rye					
-10.0	19.6 ± 0.9	21.8 ± 0.5	37.2 ± 7.1	0.1 ± 0.0	0.1 ± 0.0	0.4 ± 0.3
-5.0	38.0 ± 1.5	55.2 ± 0.9	71.4 ± 1.1	0.5 ± 0.1	0.5 ± 0.1	0.8 ± 0.2
-1.5	59.0 ± 2.9	72.3 ± 2.0	88.4 ± 2.4	1.1 ± 0.1	1.6 ± 0.2	2.4 ± 0.5
-0.03	68.5 ± 0.3	81.3 ± 4.2	101.7 ± 1.5	1.7 ± 0.3	2.0 ± 0.1	3.0 ± 0.3
$LSD_{0.05}$		8.16			0.63	
	Late-killed rye					
-10.0	3.1 ± 0.6	4.2 ± 0.6	6.3 ± 1.0	0.2 ± 0.0	0.1 ± 0.0	0.1 ± 0.1
-5.0	11.8 ± 1.0	19.1 ± 1.9	23.7 ± 1.4	0.0 ± 0.0	0.0 ± 0.0	0.1 ± 0.1
-1.5	42.1 ± 1.3	51.8 ± 1.5	67.8 ± 3.8	-0.2 ± 0.1	-0.2 ± 0.1	0.1 ± 0.0
-0.03	46.8 ± 1.2	58.5 ± 1.3	77.5 ± 3.5	-0.8 ± 0.0	-0.7 ± 0.1	0.2 ± 0.3
$LSD_{0.05}$		5.03			0.29	

† Total C and N mineralized from surface-applied cover crop residues was determined on an area basis (surface area of microcosm = 19.6 cm^2).

‡ Values are mean ± 1 standard error (n=3).

Table 3.4 Effect of residue water potential (ψ) and temperature (T) on potentially mineralizable C (C_0) and decay rate constant (k values) estimated using first-order kinetic models for different cover crop (CC) residues.

Residue water potential (ψ)	Potentially mineralizable C (C_0)			Rate constant (k values)		
	15°C	25°C	35°C	15°C	25°C	35°C
MPa	----------g C m^{-2}----------			----------d^{-1}----------		
			Crimson clover			
-10.0	5.58	7.86	11.64	0.0248	0.0411	0.0611
-5.0	15.36	24.89	28.08	0.0271	0.0349	0.0603
-1.5	44.91	49.20	65.22	0.0357	0.0617	0.0651
-0.03	51.15	63.91	81.70	0.0506	0.0625	0.0764
			Early-killed rye			
-10.0	23.59	23.59	40.81	0.0152	0.0152	0.0376
-5.0	38.69	53.41	67.81	0.0253	0.0399	0.0560
-1.5	58.39	70.11	86.15	0.0406	0.0640	0.0770
-0.03	65.36	79.48	99.79	0.0522	0.0719	0.0851
			Late-killed rye			
-10.0	4.05	4.60	6.48	0.0151	0.0306	0.0507
-5.0	11.85	19.56	22.04	0.0177	0.0162	0.0345
-1.5	44.36	51.11	66.25	0.0203	0.0315	0.0377
-0.03	50.06	57.60	75.75	0.0178	0.0298	0.0378

Table 3.5 Effect of residue water potential (ψ) and temperature (T) on potentially mineralizable N (N_0) and decay rate constant (k values) estimated using first-order kinetics for different cover crop (CC) residues.

Residue water potential (ψ)	Potentially mineralizable N (N_0)			Rate constant (k values)		
	15°C	25°C	35°C	15°C	25°C	35°C
MPa	----------g m^{-2}----------			----------d^{-1}----------		
			Crimson clover			
-10.0	0.32	0.27	0.65	0.0379	0.0858	0.1006
-5.0	0.35	0.89	1.21	0.0442	0.0467	0.0504
-1.5	1.95	2.20	2.72	0.0241	0.0300	0.0436
-0.03	2.25	2.57	3.68	0.0353	0.0397	0.0498
			Early-killed rye			
-10.0	0.13	0.20	0.42	0.0511	0.0507	0.0428
-5.0	0.42	0.58	0.75	0.0180	0.0306	0.0312
-1.5	1.17	1.54	2.09	0.0260	0.0375	0.0375
-0.03	1.65	1.96	2.80	0.0285	0.0510	0.0360

Note: Model fit was not performed for late-killed rye residue where net N immobilization was observed.

Table 3.6 Parameters of the exponential model fitted between normalized C and N mineralized in 150 d from different surface-applied cover crop (CC) residues against residue water potential (ψ) at different temperatures (T).

Temperature, T	$^{\dagger}MTRF(T) = a.e^{b.\psi}$					
	C mineralization			N mineralization		
°C	a	b	R^2	a	b	R^2
			Crimson clover			
15	0.672	0.216	0.98	0.567	0.258	0.95
25	0.806	0.194	0.99	0.644	0.227	0.98
35	1.027	0.198	0.99	0.984	0.225	0.99
			Early-killed rye			
15	0.685	0.123	0.99	0.558	0.265	0.99
25	0.828	0.110	0.96	0.693	0.250	0.99
35	1.011	0.091	0.98	1.036	0.225	0.98
			Late-killed rye			
15	0.653	0.238	0.95			
25	0.808	0.217	0.97		ND[‡]	
35	1.067	0.222	0.97			

[†] $MTRF(T)$ is the residue moisture-temperature reduction factor at a given temperature T (ºC) and residue water potential ψ (MPa). It represents the normalized values of C and N mineralized in 150-d from a given surface-applied cover crop residues at a specific residue water potential ψ (MPa) and temperature T (ºC) when compared at optimum conditions (-0.03 MPa and 35 °C) for surface residue decomposition.

[‡] ND, not determined.

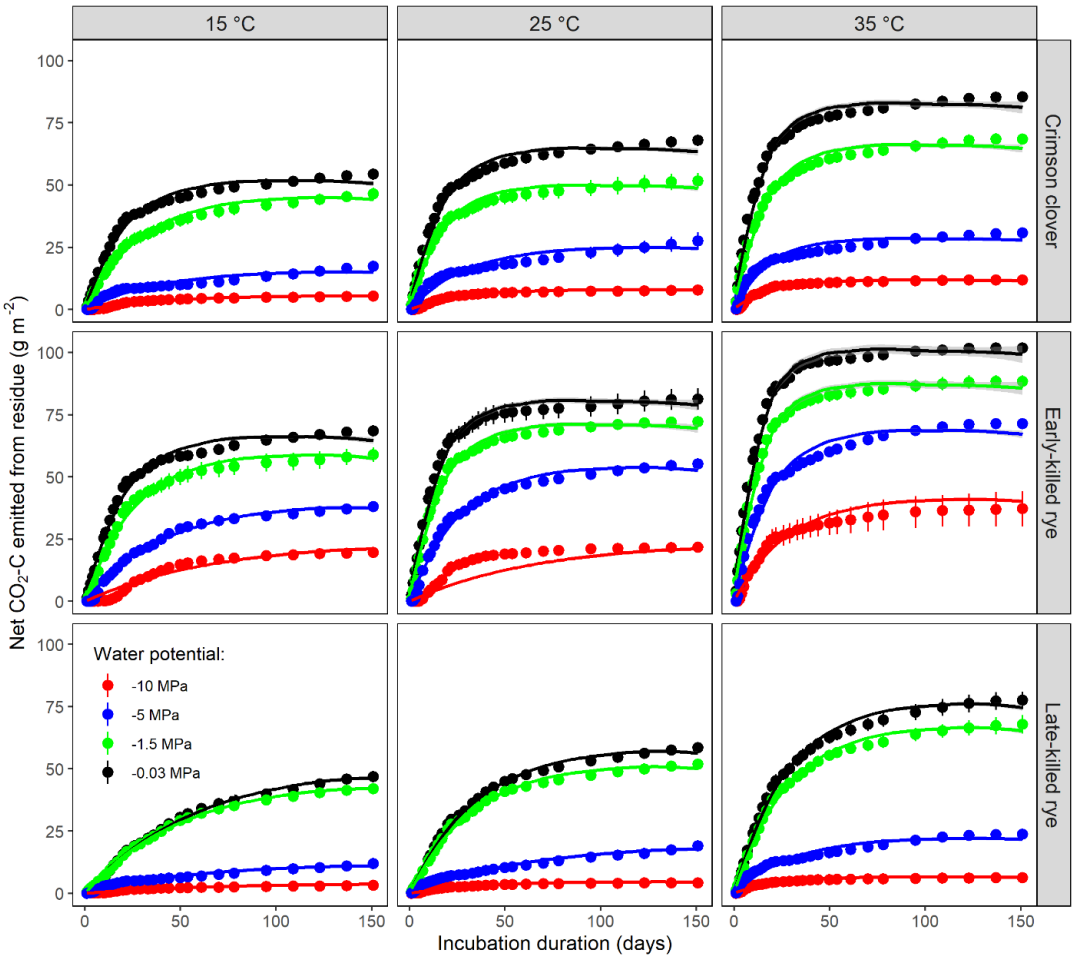

Figure 3.1 Total C mineralized from different surface-applied cover crop (CC) residues during a 150-d incubation experiment at different residue water potential ψ (MPa) and temperature T (°C). Solid lines are best fits from a single-pool first order rate kinetic model. The error bars are ± 1 standard error (n=3).

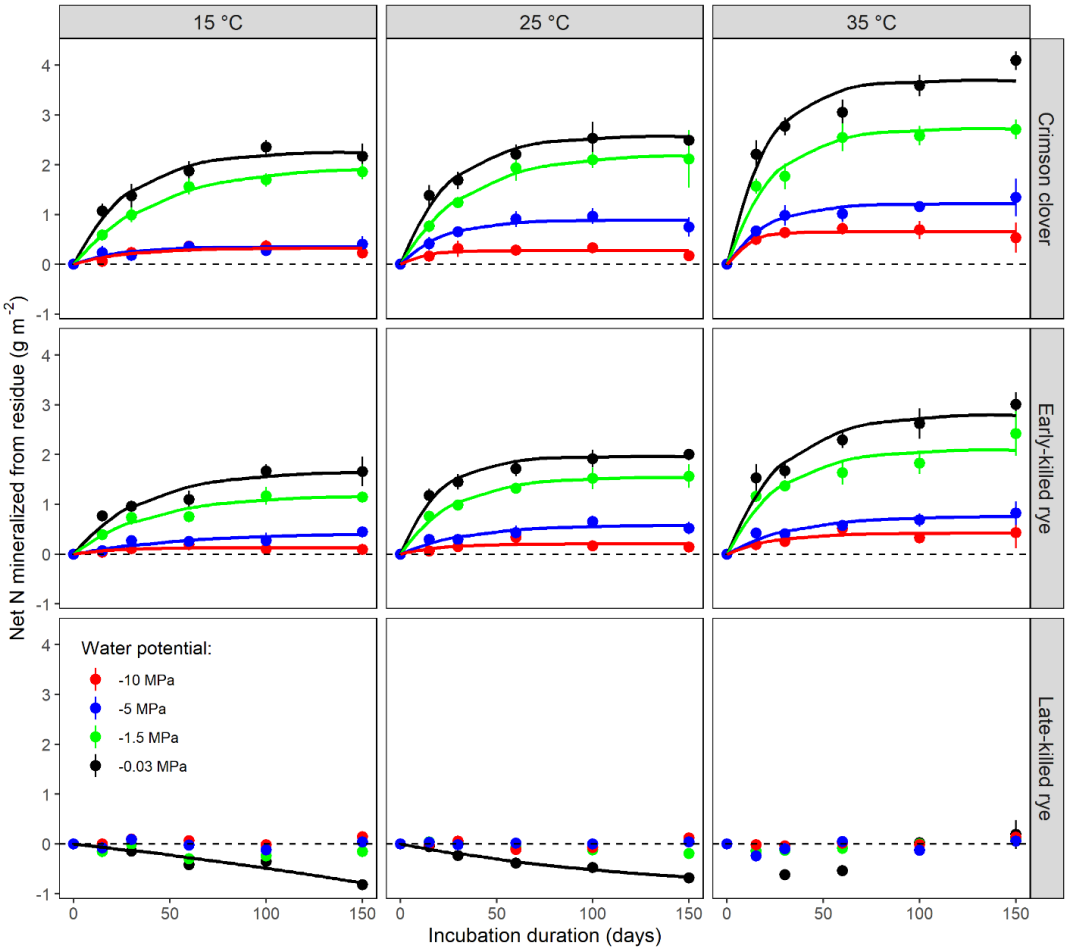

Figure 3.2 Net N mineralized from different surface-applied cover crop (CC) residues during a 150-d incubation experiment at different residue water potential ψ (MPa) and temperature T (°C). Solid lines are best fits from a single-pool first order rate kinetic model. Negative values in late-killed rye residue represent net N immobilization during decomposition. The error bars are ± 1 standard error (n=3).

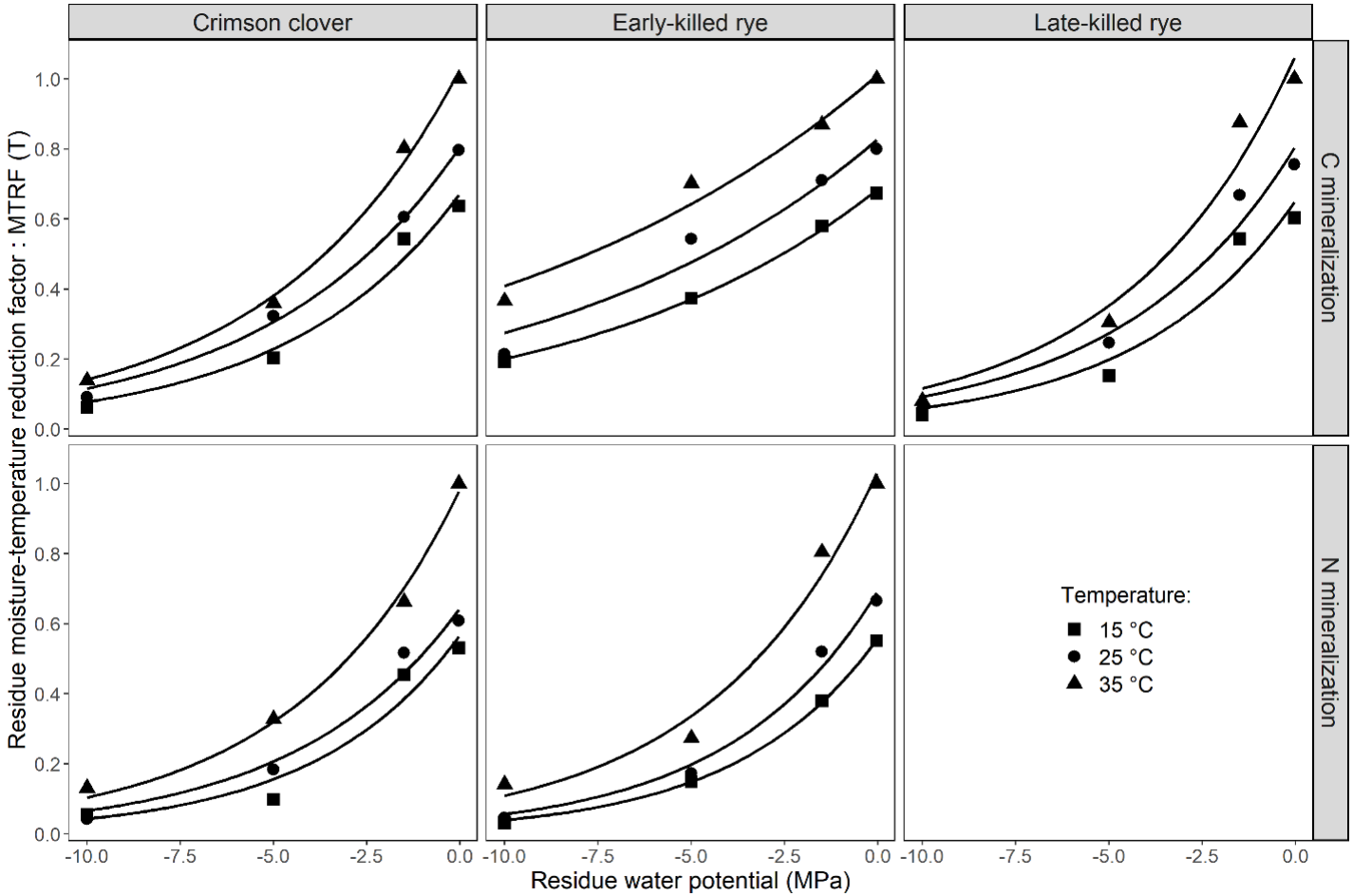

Figure 3.3 Relationship between residue water potential ψ (MPa) and the normalized residue moisture-temperature reduction factor, $MTRF$, for C and N mineralization from different surface-applied cover crop (CC) residues at three temperatures T (°C). The $MTRF$ represents the normalized values of C and N mineralized in 150-d at a specific residue water potential ψ (MPa) and temperature T (ºC) when compared at optimum conditions for surface residue decomposition (-0.03 MPa and 35 °C).

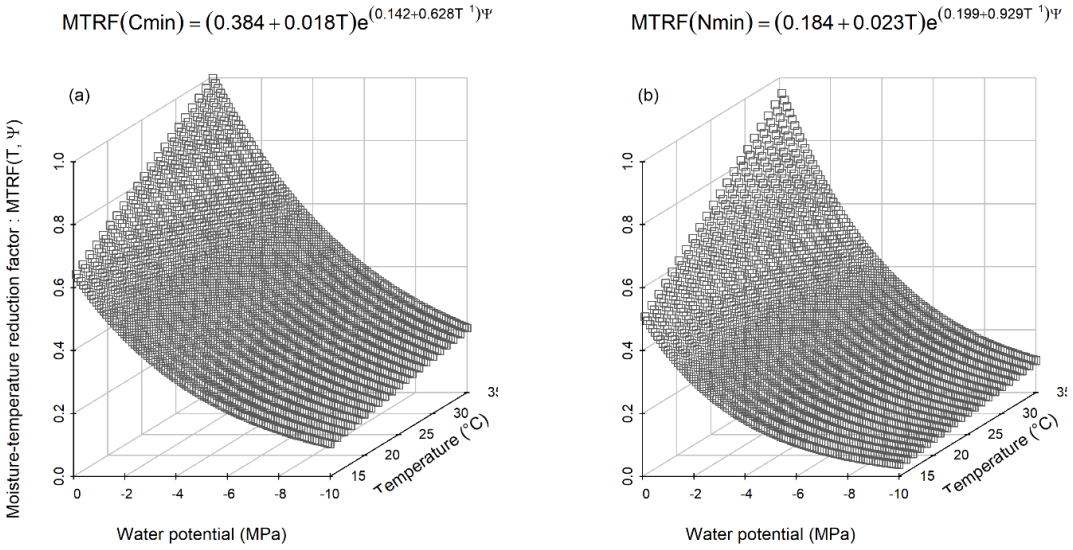

Figure 3.4 Response surface models depicting the interactive effect of residue water potential ψ (MPa) and temperature T (°C) on (a) C mineralization and (b) N mineralization from surface-applied cover crop (CC) residues.

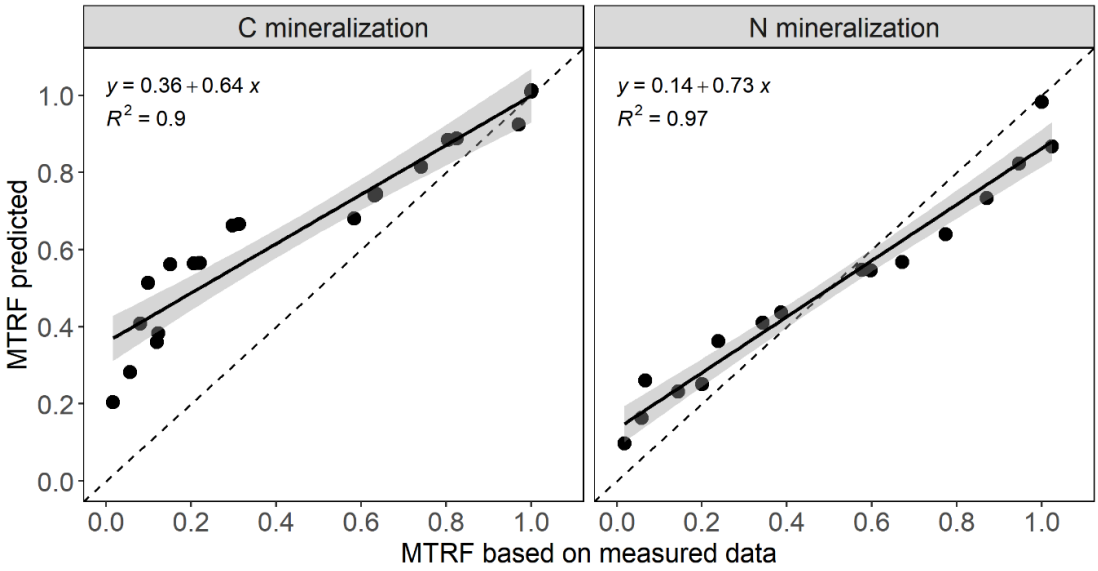

Figure 3.5 Comparisons between residue moisture-temperature reduction factor, $MTRF$, predicted based on the response surface models developed in this study with $MTRF$ calculated based on Quemada and Cabrera (1997) measured C and N mineralized data over 21-d.

Chapter 4: Microbial processes and community structure as influenced by cover crop residue type and location during repeated dry-wet cycles

Resham Thapa [a, b*], Katherine L. Tully [a], Nora Hamovit [c], Stephanie A. Yarwood [c], Harry H. Schomberg [b], Miguel L. Cabrera [d], Chris Reberg-Horton [e], and Steven B. Mirsky [b]

[a] Department of Plant Science and Landscape Architecture, University of Maryland

[b] Sustainable Agricultural Systems Laboratory, USDA-ARS

[c] Department of Environmental Science and Technology, University of Maryland

[d] Department of Crop and Soil Sciences, University of Georgia

[e] Department of Crop and Soil Sciences, North Carolina State University

Manuscript in preparation for submission to Applied Soil Ecology

Highlights

- Residues of crimson clover had higher water storage capacities than cereal rye.
- Residue water dynamics explained the majority of the effect of residue location on C and N mineralization during repeated dry-wet cycles.
- Residue chemistry influenced soil microbial diversity, community structure, and their potential functionality.
- Incorporated residues are more colonized by soil prokaryotes and saprophytic fungi.

Abstract

Soil microorganisms play a critical role in cover crop (CC) residue decomposition and nutrient cycling in agroecosystems. However, the impact of CC residue management and dry-wet cycles on soil and residue microbiota and their potential ecosystem functions is largely unknown. To fill these knowledge gaps, an incubation experiment was conducted with two CC residues, crimson clover (*Trifolium incarnatum* L.) and cereal rye (*Secale cereale* L.), and two residue locations (incorporated vs surface-applied). Each CCs by location treatment was subjected to four dry-wet cycles (20-d each) for a total of 80-d. Crimson clover residues had higher water storage capacities than cereal rye, and the rate at which water was lost from surface-applied CC residues increased after each successive wetting event. Rapid drying of surface-applied CC residues quickly suppressed CO_2 fluxes, which increased immediately upon rewetting. Incorporated CC residues maintained water content for longer duration than surface-applied residues and showed greater colonization by soil prokaryotes and saprophytic fungi. Thus, significantly more C and N were mobilized from incorporated residues by 80-d than from surface-applied residues ($p<0.05$). Due to differences in residue chemistry, CC residue types have a stronger impact on soil N levels than residue location. Thus, residue chemistry strongly influenced soil prokaryotic and fungal diversity, community structure, and functionality. While crimson clover-amended soils (N-rich environments) were dominated by copiotrophs, oligotrophs dominated cereal rye-amended soils (N-poor soil environments). On the other hand, residue location may have a greater effect than residue type in determining residue microbiota, particularly

prokaryotes. Based on these findings, we can conclude that the effect of residue location on C and N mineralization during repeated dry-wet cycles is primarily explained by differences in water dynamics between incorporated and surface-applied CC residues.

Key words: Cover crops, Residue location, Dry-wet cycles, Decomposition, C and N mineralization, Microbial community, Metabolic functions

Abbreviations: CCs, cover crops

Introduction

Across the globe, climate change is expected to alter rainfall patterns and increase flood and drought intensity and duration (Trenberth et al., 2014). Many regions in the US have already experienced wetter springs and drier summers, and an increased frequency of extreme rainfall events (Konrad and Fuhrmann, 2013; Mourtzinis et al., 2016). This will alter dry-wet cycles with huge consequences for carbon (C) and nitrogen (N) cycling in agroecosystems. Farmers are increasingly using cover crops (CCs) to support crop productivity and resilience to changing climate through enhanced agroecosystem functions such as nutrient cycling and C storage. Therefore, we need to better understand the mechanisms behind changes in nutrient cycling processes due to repeated dry-wet cycles to better adapt our CC-based crop production systems to imminent changes in rainfall regimes under future climate change scenarios.

Organic matter decomposition generally spikes following soil rewetting, a phenomenon known as the “Birch effect” (Birch 1958). The ‘Birch effect’

phenomenon has also been consistently observed in studies investigating the influence of repeated dry-wet cycles on the decomposition of CC residues (Coppens et al., 2006; Franzluebbers et al., 1994; Kruse et al., 2004). However, the rate of C and N mineralization from CC residues during dry-wet cycles could vary depending on its location in the soil. Cover crop residues are either incorporated into soil or left on the soil surface depending on tillage practices. In general, incorporated CC residues decompose quickly, and C and N are mineralized faster as compared to surface-applied CC residues (Poffenbarger et al., 2015a; Schomberg et al., 1994). During dry-wet cycles, moisture conditions can greatly vary between incorporated and surface-applied CC residues, thus affecting decomposition rates. While surface-applied CC residues are subjected to extreme drying between dew, rainfall or irrigation events in the field, incorporated CC residues, on the other hand, experience more stable moist environments for a longer duration (Coppens et al., 2006; Lee et al., 2014; Poffenbarger et al., 2015a).

To date, a limited body of research has investigated how changes in C and N mineralization rates during dry-wet cycles were modified by CC residue incorporation in soil. For example, Curtin et al. (1998) reported that the CO_2 pulse released from surface-applied wheat (*Triticum aestivum* L.) straw (C:N ratio > 100) following its rewetting was smaller than incorporated wheat straw. In sharp contrast, Coppens et al. (2006) suggested that the rain regime has a stronger impact on the decomposition of surface-applied CC residues. They observed higher CO_2 pulses after rewetting when oilseed rape (*Brassica napus* L.) residues (C:N ratio = 29) were surface-applied vs. incorporated into the soil. Therefore, the existing body of

knowledge on the effect of repeated dry-wet cycles on C and N mineralization from decomposing CC residues is unsettled. As CCs are multi-functional tools that provide numerous agroecosystem services, a better understanding of the interactions between dry-wet cycles and residue location on microbially-mediated processes will assist farmers and land managers to effectively manage residue decomposition and hence, targeted agroecosystem services in CC-based cropping systems.

Both bacteria and fungi are key decomposers, and their relative contributions can be influenced by residue quality and its location in the soil (Holland and Coleman, 1987; Frey et al., 1999; Wells et al., 2017). Fungi are the main decomposers of surface-applied residues, while bacteria are the primary decomposers of incorporated residues. Residue type and therefore chemistry, also leads to divergence in bacterial and fungal communities. In a 11-month field study, Pascault et al. (2010) observed that the genetic structure of bacterial communities colonizing incorporated wheat, rape, and alfalfa (*Medicago sativa* L.) residues were significantly different. Similarly, Kerdraon et al. (2019) found different bacterial and fungal communities colonizing in surface-applied wheat and rape residues. Within the soil, microbial communities also have distinctly different bacterial and fungal components that are influenced by residue quality and location (Clocchiatti et al., 2020; Detheridge et al., 2016; Maul et al., 2014; Nevins et al., 2018). To our knowledge, only one study simultaneously evaluated the effect of CC residue type and its location on soil as well as residue microbiota (Nicolardot et al., 2007). They concluded that the soil and residue contributed distinct trophic and functional niches for microorganisms. However, the soil and residue microbiota in the study by Nicolardot

et al. (2007) did not experience drought stress. In reality, microorganisms are frequently subjected to drought stress in cropping systems. Our current understanding on how microbes respond to dry-wet cycles is limited and primarily based on studies that only measured total microbial biomass and/or activity (Fierer and Schimel, 2003; Franzluebbers et al., 1994). The differential response of microbial functional groups to drought stress has not yet been documented. Since each microbial species has specific physiological requirements and roles in residue decomposition and nutrient cycling, it is critical to understand how residue management shifts soil and residue microbiota and their potential functionality when subjected to repeated dry-wet cycles.

An experiment was designed to increase our understanding on how dry-wet cycles and residue management strategies influence microbial community structure and function. Our main objectives were to evaluate the effect of CC residue type and its location on: (i) C and N mineralization, and (ii) soil and residue microbial communities and their potential functionalities, during repeated dry-wet cycles. Since global cropping systems are more frequently experiencing extreme heat, drought, and rainfall events than anytime in the past, this work will serve to help optimize residue management decisions in agricultural fields under future climate change scenarios.

Materials and Methods

Soil and cover crop residue characteristics

The soil used in this incubation experiment was obtained from a sorghum (*Sorghum bicolor* L.) field at the Beltsville Agricultural Research Center (Beltsville, MD, USA; 39°01'08.9"N 76°56'33.0"W) in 2018. The field was mapped as Codorus

(Fine-loamy, mixed, active, mesic Fluvaquentic Dystrudepts) and Hatboro (Fine-loamy, mixed, active, nonacid, mesic Fluvaquentic Endoaquepts) soils (Soil Survey Staff, 2020). Field-moist soil (0-10 cm) was collected and immediately sieved through a 4-mm sieve to remove rocks, crop roots, and undecomposed residue parts. The soil was then air-dried, ground, sieved through a 2-mm sieve, and stored in a refrigerator at 4 °C until the experiment started. The gravimetric water content of the soil at field capacity (-0.03 MPa) was determined using pressure chamber apparatus. A subsample of soil was analyzed for texture using a hydrometer method. The total C and N in soil was determined using Leco TruMac CN Analyzer (LECO Corporation, St. Joseph, MI). The soil contained 1.32 g N kg^{-1} and 14.1 g C kg^{-1}, and consisted of 24% clay, 58% silt, and 18% sand.

Cover crop residues used in this experiment were: crimson clover (*Trifolium incarnatum* L; full bloom stage) and cereal rye (*Secale cereale* L.; anthesis stage Zadoks 60; Zadoks et al., 1974). Residues were oven-dried at 60 °C for 2 days, leaves and stems separated, and then stored at room temperature. Residues used in each microcosm consisted of fixed proportions of leaves and stems (0.4 and 0.6, respectively). Dried residue parts, cut into 0.5-cm long pieces, were soaked in distilled water overnight and then allowed to drain for 10 minutes before preparing microcosms. A sub-sample of residue prepared in this way was oven-dried, finely ground, and analyzed for total C and N using Leco TruMac CN Analyzer (LECO Corporation, St. Joseph, MI). The biochemical composition of the residue (percent lignin, carbohydrate, cellulose, and hemi-cellulose) was determined via near infra-red reflectance spectroscopy (NIRS) using scanning monochromator (model 6500; FOSS

NIRSystems, Silver Spring, MD). Total C, total N, C:N ratio, and biochemical characteristics of both residues is provided in Table 4.1.

Preparation of microcosms

Sieved, air-dried soil was wetted to 0.26 g H_2O g^{-1} with double deionized water [gravimetric water content (θ_g) at -0.03 MPa]. The soil was pre-incubated for three weeks to deplete initial flush of CO_2 caused by re-wetting of air-dried soil. During pre-incubation, the soil was mixed every 2-3 days. Following pre-incubation, soil was sieved through a 2-mm sieve and 50 g oven-dried equivalent of pre-incubated soil was packed in 100 mL plastic beakers (5.0 cm i.d.). Cover crop residue parts were either placed on the soil surface or thoroughly mixed (i.e., incorporated) with soil at the rate of 3000 kg ha^{-1}. Therefore, treatments were factorial combination of two CC residues (crimson clover or cereal rye) and two residue placement strategies (surface-applied or incorporated). A soil-alone control treatment was also included.

Dry-wet experiment

Microcosms were subjected to four dry-wet cycles in a set of CONVIRON E7/2 growth chambers (Controlled Environment Limited, Winnipeg, MB, Canada) at 25 °C. In each dry-wet cycle, microcosms were dried for 16 d in a drying chamber. At the end of each drying period, 12 mL of double deionized water was quickly added using a pipette to raise θ_g from 0.02 to 0.26 g H_2O g^{-1} (Figure 4.1a). Microcosms were then transferred to an identical high-humidity chamber (hereafter, referred as wetting chamber) and maintained at field capacity for 4 d. The relative humidity of the air in the wetting chamber was kept at ~95% by placing 2 cm of double deionized

water and bubbling air through it. Air flow was regulated at 0.2 L min^{-1} using a flowmeter (Dwyer Instruments Inc., Michigan City, IN, USA).

At the end of each dry (16, 36, 56, and 76 d) and wet (20, 40, 60, and 80 d) period, three microcosms were destructively sampled for each treatment to determine N mineralization/immobilization from CC residues. Microcosms were extracted with 500 mL of 1 mol L^{-1} KCl (1:10 soil:extractant ratio) after overnight shaking in 1-L plastic bottles. The KCl extracts were filtered through Whatman No. 42 filter paper and a 30-mL subsample was stored at -18 °C until analysis. The NH_4^+ and NO_3^- contents were determined colorimetrically using a SEAL AutoAnalyzer 3 High Resolution (SEAL Analytical Inc., Mequon, WI) using sodium salicylate and cadmium reduction method, respectively.

An additional 20 microcosms (5 treatments × 4 replicates) were prepared to determine the rate of C mineralization from CC residues. These microcosms were prepared as described above. To determine CO_2 and N_2O emission rates, microcosms were transferred into 0.95-L mason jars and the jars were sealed with air-tight lids for 1 hr. Headspace gas was thoroughly mixed three times and a 10-mL of gas was sampled into 12-mL N_2-flushed glass vials (Labco Ltd., Lampeter, UK). Vials were stored in a refrigerator at 4 °C until analysis. During the wetting period, first gas sample was collected at hr 6 and then every 1-2 d thereafter. During the drying period, gas sampling was performed every day for a week and then at every 2-3 d thereafter. Gas samples were analyzed on a Varian GC450 gas chromatograph (Agilent Technologies, Santa Clara, CA) within a week of collection. Various concentrations of CO_2 (range: 0.011-0.678%) and N_2O (range: 0.025-1.551 ppm) gas

standards were prepared from a tank (Airgas Specialty Gases, 2.30 ppm N_2O, 2.99 ppm methane (CH_4), 1.00% CO_2, balance N_2) on each sampling day and analyzed along with gas samples. Gas concentrations were converted into emission rates using the ideal gas law, headspace volume, time of gas accumulation in the headspace, and surface area of the microcosms.

To determine changes in the θ_g of surface-applied residues during dry-wet cycles, eight additional microcosms were constructed for each CC residue. The residues were placed in customized cups sealed with nylon mesh from the bottom. Residue cups were detached from the microcosms during each gas sampling day and the weights were recorded. Two residue cups were destructively sampled for each CC residues 1 d after the wetting event, and the oven-dried mass of the surface-applied CC residues was determined for use in θ_g calculations. The change in the θ_g of incorporated residues was not determined in this study.

DNA extraction, Illumina sequencing library preparation, and bioinformatics

At the end of four dry-wet cycles, microcosms used for CO_2 flux measurements were also used for microbial DNA extractions. Residue pieces were separated from the soil using sterilized tweezers and stored separately in centrifuge tubes in a freezer at -80 °C. Microbial DNA from soil and residue samples were extracted separately using the Qiagen DNeasy PowerLyzer PowerSoil and PowerPlant kit (Qiagen, Hilden, Germany), per the manufacturer's recommendations. DNA extracted from each sample was quantified using a Qubit 2.0 fluorometer (Invitrogen) and stored at -20 °C. When needed, DNA was diluted to 5ng/µl for PCR

amplification. Prokaryotic 16S rRNA gene and fungal ITS gene regions were targeted using the primers 515F/806R and ITS1f/ITS2r, respectively (Coporaso et al., 2011; White et al., 1990). Illumina sequencing was performed according to the 16S metagenomic sequencing library preparation manual (Part number 1504423 rev. B, Illumina, Inc.). PCR cleanup and indexing was carried out using AMPure CP beads (Beckman Coulter, Pasadena, CA) and Nextera XT 96 index kit (Illumina, Inc.), respectively. Samples were pooled; the amplicon library size was verified using a Bioanalyzer 2100 DNA chip (Agilent Technologies). Library was quantified using qPCR and the final library was run on an Illumina MiSeq using a 600-cycle v3 cartridge.

The R package *dada2* (version 1.14.1; Callahan et al., 2016) was used for processing fastq files returned from Illumina Sequencing (filter and trim, dereplication, sample inference, merging pair-end reads, and removing chimeras). Prior to *dada2* workflow, sequences containing 'N' values (unreadable bases) were pre-filtered and the forward and reverse primers were removed using *cutadapt* (version 2.9; Martin, 2011). Taxonomy was assigned to the chimeric-free sequence table with the *dada2* native implementation of the naïve Bayesian classifier method. The SILVA (version 132; Quast et al., 2013) and UNITE (release 10.10.2017; Nilsson et al., 2019) databases were used as reference sequences for the identification of prokaryotic 16S rRNA genes and fungal ITS gene amplicon sequence variants (ASV), respectively. The ASV tables were converted into phyloseq objects using the R *phyloseq* package (McMurdie and Holmes, 2013). Before performing microbial community analysis, features with ambiguous phylum annotation (phylum classified

as ‘NA’) and phylum with low-prevalence were removed. In addition, ASVs available in less than 10% of the total samples were discarded; low-performing samples with total sequence reads less than 1000 were also discarded. This removed most of the rye residue samples from the prokaryotic 16S rRNA gene data and hence, we excluded all rye residue samples from statistical tests. To account for differences in sequencing depth across samples, samples were rarefied by randomly sub-sampling the minimum number of sequence reads present in the sample (prokaryotic 16S = 24,608; fungal ITS = 31,403). All statistical analyses were performed on rarefied datasets for soil and residue samples separately, unless otherwise stated.

Statistical analysis

Total C mineralized during each dry-wet cycle was calculated by linear interpolation of CO_2 flux data over time. Similarly, total N mineralized or immobilized was calculated by summing total inorganic N and cumulative N_2O emitted during the same period. Significant differences in total C and N mineralized or immobilized between residue treatments was determined by one-way analysis of variance (ANOVA) at a α value of 0.05. Whenever necessary, data were log-transformed to meet ANOVA assumptions. Only when the overall treatment effect was significant, Tukey-adjusted pairwise comparisons were performed using the *emmeans* package in R (Lenth, 2020).

The Shannon diversity index was calculated as a measure of α-diversity using the R *phyloseq* package. The Bray-Curtis dissimilarity was calculated after transforming the count data into relative abundances. Non-metric multidimensional scaling (NMDS) ordination plots based on Bray-Curtis dissimilarity were constructed

to visualize differences on prokaryotic and fungal community structure between residue treatments. The effect of residue treatments on microbial community structure was statistically tested using the permutational multivariate ANOVA (PERMANOVA) with 1000 permutations via the *adonis* function of the R *vegan* package (Oksanen et al., 2019). To check the assumption of PERMANOVA, permutation-based test of multivariate homogeneity of group dispersions was performed using the *betadisper* and *permutest* functions of the *vegan* package. If the overall treatment effect was significant based on PERMANOVA, pairwise treatment comparisons were performed using the *pairwiseAdonis* package in R (Martinez Arbizu, 2019). The associations between the most abundant taxa and the microbial community structure was investigated using the *envfit* function of the R *vegan* package, and the taxa that showed significant correlations were fitted to the NMDS plots. The *VennDiagram* package in R was used to construct venn diagrams to depict the number of unique and shared ASVs between soil and residue samples for each CC residue treatments (Chen, 2018). The potential metabolic functionality of the prokaryotic community was predicted based on 16S rRNA gene data using the *t4f* (Tax4Fun) function of the R *themetagenomics* package and the Kyoto Encyclopedia of Genes and Genomes (KEGG) pathway database (Woloszynek et al., 2017). The relative gene abundances were calculated by summing all KEGG orthologs associated to a specific C degradation and N metabolism pathways (Lüneberg et al., 2018). Similarly, *FUNGuild* was used for functional guild and trophic mode assignments to the ITS gene data (Nguyen et al., 2016). For simplicity, we re-classified the assigned trophic modes into four categories: Pathotrophs (plant pathogens, fungal parasites),

Saprotrophs, Pathotroph-Saprotrophs, and others (animal pathogens, symbiotrophs). As recommended by *FUNGuild* developer's, only trophic modes assigned with 'highly probable' or 'probable' confidence ranking were reported. Kruskal-Wallis and Dunn's test was used to statistically test the effect of residue treatments on microbial diversity and potential microbial functionality of the soil and residue microbiota using the R *rstatix* package (Kassambara. 2020). Significant differences were determined at α value of 0.05, unless otherwise stated.

Results and Discussion

Change in the water content of surface-applied residues during dry-wet cycles

At time t_0, crimson clover and cereal rye residues had 4.74 and 3.54 g H_2O g^{-1}, respectively (Figure 4.1b). Averaged across four dry-wet cycles, residue θ_g was 0.26 ± 0.06 g H_2O g^{-1} before each rewetting event. After rewetting, the θ_g of crimson clover and cereal rye residues increased to 2.97 ± 0.13 and 2.32 ± 0.13 g H_2O g^{-1}, respectively (Figure 4.1b). Residues of crimson clover had greater water storage capacity than cereal rye, likely due to greater soluble carbohydrate fractions in crimson clover residues (Table 4.1). Other studies have observed that the water storage capacity of CC residues is directly proportional to soluble carbohydrate concentrations (Quemada and Cabrera, 2002) and inversely proportional to lignin concentrations (See Chapter 2).

The rate at which water was lost from CC residues increased after each successive wetting event (Figure 4.1b). While it took approximately seven days for wet residue to dry in the 1st dry-wet cycle, it only took 2-3 days in the remaining dry-

wet cycles (2^{nd}, 3^{rd}, and 4^{th}). The observed change in the rate of drying during successive dry-wet cycles was probably due to changes in the residue physical and chemical characteristics. As decomposition progressed, dissolution of cellulose and hemi-cellulose fractions can lead to the formation of macropores in decomposed tissues (Maloney and Paulapuro, 1999). Moreover, decomposition increases hydrophobicity of CC residues by increasing residue lignin fractions and concomitantly, decreasing residue carbohydrate and holo-cellulose fractions (See Chapter 2). Therefore, changes in residue physical (increased porosity) and chemical (hydrophobicity) characteristics during decomposition most likely caused the increased rates of water loss from CC residues during successive drying periods.

Influence of residue type and its location on C mineralization

Carbon mineralization from CC residues was influenced by dry-wet cycles (Figure 4.2). Irrespective of the residue type and its location, CO_2 fluxes decreased during the drying period. This was probably due to reduced microbial activity as water becomes limited during the drying period. Rewetting sharply increased residue θ_g, resulting in quick CO_2 pulses within 6 h. In accordance with our results, multiple studies have also observed a flush of C mineralization following rewetting of surface-applied and incorporated residues (Borken et al., 2003; Coppens et al., 2006; Miller et al., 2005). Our results further highlighted that the temporal differences in CO_2 fluxes between surface-applied and incorporated residues during dry-wet cycles was primarily due to differences in residue θ_g. Although not quantified, we believe that the rate of water lost from incorporated residues was much slower than surface-applied residues during the drying phase. Thus, CO_2 fluxes were greater when CC

residues were incorporated rather than surface-applied during the drying period. However, surface-applied residues had higher CO_2 fluxes than incorporated residues following rewetting. This pattern was consistent for both CC residues. Coppens et al. (2006) also observed similar results while examining the effect of residue location on the decomposition of rape residues subjected to dry-wet cycles. Our results further indicated that the increase in the rate of C mineralization from surface-applied residues during a 4-d wetting period compensated for the decrease in C mineralization during a 16-d drying period. Thus, we saw no significant differences in the cumulative CO_2 released between surface-applied and incorporated residues during 2^{nd}, 3^{rd}, and 4^{th} dry-wet cycles (Table 4.2). In natural field settings, however, the frequency, intensity, and duration of dry-wet cycles vary greatly; frequent light rains might accelerate the decomposition of surface-applied CC residues. Sparse and heavy rainfall events, on the other hand, might stimulate the decomposition of incorporated CC residues. In addition, changes in micro-climatic conditions such as the air relative humidity, air temperature, and dewfall causes θ_g of surface-applied CC residues to fluctuate more dramatically and results in diurnal fluctuations in the decomposition of surface-applied CC residues in fields (See Chapter 2).

Irrespective of their location, the initial CO_2 fluxes were higher from residues of crimson clover than cereal rye (Figure 4.2). This translated into significantly higher cumulative C mineralized from crimson clover than cereal rye residues during 1^{st} dry-wet cycle ($p<0.05$; Table 4.2). Differences in C mineralization between residue types was associated with differences in residue quality (Table 4.1). The lower C:N ratio and higher soluble carbohydrate fractions in crimson clover residues led to its faster

decomposition under both surface-applied and incorporated conditions. After four repeated dry-wet cycles, incorporated CC residues mineralized 11.6 g m^{-2} more C than surface-applied CC residues for both residue types ($p<0.05$; Table 4.2). As discussed earlier, greater C mineralization from CC residues following incorporation was mostly due to a more stable, moist environment favoring microbial activity. Incorporation of CC residues also increased the area of contact between soil and residues, resulting in enhanced microbial attack and faster decomposition of incorporated CC residues (Poffenbarger et al., 2015a; Schomberg et al., 1994). Another factor that may influence the rate of decomposition between incorporated and surface-applied CC residues could be changes in diversity, community structure, and functional capabilities of the microbes, as discussed below.

Influence of residue type and its location on N mineralization-immobilization

While crimson clover decomposition led to net N mineralization, cereal rye decomposition, on the other hand, immobilized N ($p<0.05$; Figure 4.3). Cereal rye residues, which have high C:N ratio, did not meet microbial N requirements and thus, microbes assimilate soil inorganic N and reduce N pool size during its decomposition to meet their stoichiometric demands. These results confirm the findings of other research that showed CC residues with high C:N ratio immobilized N during its decomposition and vice-versa (Otte et al., 2019; Poffenbarger et al., 2015a; Williams et al., 2018).

As expected, the amount of N mineralized or immobilized during residue decomposition was significantly affected by its location in the soil ($p<0.05$; Figure

4.3). After four repeated dry-wet cycles, incorporated crimson clover residues mineralized 28% of the CC N, whereas surface-applied crimson clover residues mineralized 21% of the CC N. Similarly, cereal rye residues immobilized significantly more N when incorporated than surface-applied. We found that, after four repeated dry-wet cycles, incorporated and surface-applied cereal rye residues immobilized 76 and 57% of the CC N, respectively. As discussed earlier, residues became more accessible to soil microorganisms and were subjected to a more favorable environment for microbial activity when incorporated into rather than left on the soil surface. Thus, incorporated residues decomposed and mineralized C rapidly, thereby increasing the amount of N mineralized or immobilized during its decomposition.

We observed that the differences in N mineralized or immobilized between incorporated and surface-applied CC residues mostly occurred during the 1st dry-wet cycle ($p<0.05$; Figure 4.3). For the remaining dry-wet cycles, differences in the soil inorganic N pool size between incorporated and surface-applied CC residues remained relatively constant. These results were like those observed above for C mineralization, indicating that C and N mineralization-immobilization from CC residues were coupled processes and were tightly linked to each other. Supporting this hypothesis, the flush of CO_2 after rewetting was accompanied by an increase in both net N mineralization from crimson clover residues and net N immobilization from cereal rye residues (Figure 4.2 and 4.3). It is possible that rewetting dissolved and translocated some of the organic C and N from CC residues to microbial sites in the soil layers. Such redistribution of added C and N following rewetting events

probably enhanced microbial activity (as evidenced from CO_2 pulses in Figure 4.2) and concomitantly, more N was mineralized or immobilized upon rewetting. Since soil microbes have poor access to surface-applied CC residues than incorporated CC residues, this phenomenon may be critically important for the decomposition of CC residues left on the soil surface.

Influence of residue type and its location on microbial composition and diversity

In this study, the quality-filtered and rarefied dataset contained 2,881 unique ASVs for prokaryotes (1,678,448 sequence reads) and 618 unique ASVs for fungi (2,994,404 sequence reads). The most abundant bacterial sequences in both soil and residue samples were putatively identified as phylum *Proteobacteria* (*Alphaproteoobacteria, Gammaproteobacteria*), *Actinobacteria* (*Actinobacteria, Thermoleophilia*), *Firmicutes* (*Bacilli*), *Bacteroidetes* (*Bacteroidia*), *Chloroflexi* (*Chloroflexia*), *Planctomycetes* (*Planctomycetacia*), and *Verrucomicrobia* (*Verrucomicrobiae*) (Figure A4). These bacterial classes, altogether, accounted for 61-63 and 72-73% of the identified sequences in cereal rye and crimson clover-amended soils, respectively. Similarly, they accounted for 91 and 99% of the prokaryotic sequence abundance in incorporated and surface-applied crimson clover residues, respectively. Sequences belonging to the phylum *Acidobacteria* (*Acidobacteriia*, *Subgroup 6*, *Subgroup 4*), *Chloroflexi* (*KD4-96*, *Ktedonobacteria*), and *Gemmatimonadetes* (*Gemmatimonadetes*) were only present in soil samples and accounted for 9.4-21% of the soil prokaryotic sequences (Figure A4). The only dominant archaeal class that was solely present in the soil samples was *Nitrosophaeria* (7.7-13%). The most abundant ITS DNA sequences were putatively

identified as *Ascomycota* (orders: *Hypocreales*, *Sordariales*, *Chaetothyriales*, and *Pleosporales*). *Ascomycota* was the dominant phylum in both soil (40-55%) and residue (69-89%) samples (Figure A4). Sequences belonging to the phylum *Basidiomycota* (orders: *Phallales*, *Tremellales*, and *Filobasidiales*) and *Mortierellomycota* were only detected in soil samples and accounted for 37-50% of the soil fungal community.

The soil microbial communities were more diverse than those found in the residue samples, suggesting that the decomposition of CC residues were carried out by a specific group of bacterial and fungal communities. When crimson clover residues were incorporated into the soil, 33% of the prokaryotic ASVs were shared between soil and residue samples (Figure A5). However, only 17% of the prokaryotic ASVs were shared between soil and surface-applied crimson clover residues. On the contrary, the number of shared ASVs in the fungal community between soil and residue samples were slightly higher when residues were surface-applied (crimson clover: 43%; cereal rye: 37%) than incorporated into the soil (crimson clover: 36%; cereal rye: 35%). Therefore, we can conclude that the rapid decomposition and N mineralization from incorporated CC residues, as observed in this study, was likely due to enhanced microbial colonization of incorporated residues by the soil prokaryotic community. Surface-applied CC residues, on the other hand, were colonized more by soil fungal rather than prokaryotic communities, which is in line with the findings of several other studies in no-tillage agroecosystems (Frey et al., 2000; Holland and Coleman, 1987; Wells et al., 2017). The invasion of surface-

applied CC residues by soil fungi was probably due to their ability to form filamentous hyphae that can grow into surface-applied CC residues.

Both the prokaryotic and fungal α-diversity in the soil samples were significantly affected by the residue treatments ($p<0.05$, Figure 4.4). The prokaryotic Shannon diversity index was significantly lower in crimson clover incorporated soils as compared to that in cereal rye incorporated soils (Figure 4.4a). Similarly, the fungal Shannon diversity index was also significantly lower in crimson clover incorporated soils as compared to the control soils (Figure 4.4b). All other remaining treatments exhibited similar soil microbial diversity. These results suggest that the increased availability of labile C and N in soils incorporated with crimson clover residues led to the enrichment of specific prokaryotic and fungal populations, thereby reducing the overall soil microbial diversity (Table 4.2; Figure 4.2 and 4.3). These types of microorganisms have been classified as r-strategists (Pianka, 1970) or copiotrophs (Fierer et al., 2007), since they preferentially consume labile organic C pools, have high nutrient requirements, and exhibit high growth rates when resources are abundant. In the residue samples, the prokaryotic Shannon diversity index was significantly higher when crimson clover residues were incorporated than surface-applied ($p<0.05$, Figure 4.4a). As mentioned earlier, increased prokaryotic diversity in incorporated crimson clover residues was probably the result of a greater invasion of incorporated residues by new colonizers from the soil. In addition, it is possible that the easily degradable labile C fractions disappeared from incorporated crimson clover residues after four successive dry-wet cycles, thereby increasing the proportion of recalcitrant C fractions in the remaining residues. The accumulation of recalcitrant

C fractions over time may have stimulated the growth of a more diverse bacterial population that can degrade it (Bastian et al., 2009; Zhong et al., 2020). Therefore, residue location has variable effects on microbial diversity between soil and residue, such that the incorporation of residues likely increased microbial diversity in the residue but decreased microbial diversity in the surrounding soil.

Influence of residue type and its location on microbial community structure

The NMDS ordination plot based on Bray-Curtis distances illustrates the significant effect of residue treatments on soil prokaryotic community (PERMANOVA test: R^2=0.62, p<0.001; Figure 4.5a). Irrespective of the residue location, points on the NMDS plot separated the soil prokaryotic community structure between CC residue types (Table 4.3; Figure 4.5a). The genetic structure of soil prokaryotic community may be more influenced by CC residue type than by its location, which is in line with the observations made by Nicolardot et al. (2007). It can be hypothesized that the relatively higher proportion of readily decomposable C fractions and lower C:N ratio of crimson clover residues resulted in C and N-rich soil environments, thereby supporting the growth of copiotrophs in crimson clover-amended soils (Figure 4.3). According to the copiotrophy-oligotrophy concept outlined by Fierer et al. (2007), *Alphaproteobacteria*, *Gammaproteobacteria*, *Actinobacteria*, and *Chloroflexia* can be considered as copiotrophs since these bacterial classes were positively associated with the prokaryotic community structure in crimson clover-amended soils (Figure 4.5a). The bacterial class *KD4-96*, *Gemmatimonadetes*, and those belonging to the phylum *Acidobacteria* (*Acidobacteria, Subgroup 6*, *Subgroup 4*) were positively associated with the

prokaryotic community structure in cereal rye-amended soils, suggesting that they thrive in N-poor environments and can be considered oligotrophs (Figure 4.5a).

Residue location significantly affected the prokaryotic community structure in the residue samples (PERMANOVA test: R^2=0.63, $p<0.05$; Figure 4.5b). In accordance with other studies, the dominant taxa involved in residue decomposition were *Alphaproteobacteria*, *Gammaproteobacteria*, and *Actinobacteria* (Figure A4; Banerjee et al., 2016; Bastian et al., 2009; Pascault et al., 2010; Zhong et al., 2020). Among them, the effect of *Actinobacteria* was significant and they were found to be positively associated with surface-applied crimson clover residues (Figure 4.5b). On the other hand, low abundance bacterial classes, such as *Verrucomicrobiae*, *Thermoleophilia*, *Planctomycetacia*, and *Chloroflexia*, were better correlated to prokaryotic community structure in incorporated crimson clover residues (Figure 4.5b). These results suggest that the copiotrophic taxa, such as *Actinobacteria*, exhibit high growth rates and were favored in surface-applied residues following its rewetting.

The soil fungal community composition was also significantly affected by CC residue treatments (Figure 4.6a; PERMANOVA test: R^2=0.55, $p<0.001$). Pairwise comparisons further suggested that the soil fungal community structure was significantly different between incorporated and surface-applied CC residues (Table 4.3; Figure 4.6a). However, the soil fungal community structure was significantly different between CC residue types, only when residues were incorporated (Table 4.3; Figure 4.6a). Among the dominant fungal order belonging to the phylum *Ascomycota*, *Sordariales* and *Pleosporales* were positively associated with the fungal community

structure in cereal rye-incorporated soils (Figure 4.6a). These fungal orders consist of saprophytic fungi and were known to effectively decompose cellulose over lignin (Banerjee et al., 2016; Harreither et al., 2011; Voriskova and Baldrian, 2013; Zhong et al., 2020). *Mortierellales* was the second most dominant fungal order and was found to be better correlated to fungal community structure in crimson clover-incorporated soils (Figure 4.6a). Similarly, Clocchiatti et al. (2020) and Detheridge et al. (2016) also observed increased abundance of *Mortierella*les in soils amended with legume CC residues. Based on these results, we can conclude that the increase in soil N levels due to legume CCs, stimulated the growth of *Mortierella*les. Regarding phylum *Basidiomycota*, the fungal orders *Phallales* and *Filobasidiales* were more abundant in the control soils and *Tremellales* was more abundant in cereal rye-incorporated soils (Figure 4.6a). Members of the phylum *Basidiomycota* play a major role in the decomposition of recalcitrant C pools such as lignocellulose complexes (Hiscox et al., 2018; Morrison et al., 2018; Voriskova and Baldrian, 2013). Based on the copiotrophy-oligotrophy framework discussed earlier for bacterial communities, *Mortierellales* can be considered copiotrophs because of its close association to N-rich soil environments, which in our case is crimson clover-amended soils. Similarly, the fungal orders *Sordariales* and *Pleosporales* and the phylum *Basidiomycota* can be considered oligotrophs due to their close association to N-poor soil environments and their ability to degrade recalcitrant C pools, such as those found in cereal rye-amended and control soils.

Surprisingly, both fungal diversity and community structure in the residue samples were not significantly affected by CC residue type and its location ($p>0.05$;

Figure 4.4b and 4.6b). This result differed from those observed by Nicolardot et al. (2007), which may be due to differences in incubation conditions or the timing of residue sampling. We observed convergence of fungal community composition when soils were subjected to repeated dry-wet cycles for longer duration. This could be due to the ability of fungi to colonize surface-applied residues as effectively as that of incorporated residues or could be linked to greater stress tolerance of fungi to moisture fluctuations in surface-applied residues. The dominant fungal colonizers in the CC residues were members of the phylum *Ascomycota*, suggesting their major involvement in residue decomposition. Members of the phylum *Basidomycota* were only found in crimson clover residues and accounted for 21 and 3.8% of the fungal community structure in incorporated and surface-applied crimson clover residues, respectively (Figure A4). It is likely that the faster decomposition of crimson clover residues led to greater accumulation of recalcitrant C fractions after four repeated dry-wet cycles, which likely have stimulated residue colonization by *Basidomycota* to further decompose it.

Influence of residue type and its location on potential microbial functionality

The potential functional capacity of the prokaryotic community, in relation to residue decomposition and N cycling, was predicted using the KEGG database. On average, 16 and 21% of the ASVs per sample were mapped to KEGG organisms for the soil and residue samples, respectively. This suggests that the functional predictions based on 16S rRNA gene data may not fully capture the functionality of soil and residue prokaryotic community. In addition, functional gene predictions of the fungal community are not currently available. Using FUNGuild, we were able to

gain a relative understanding of the overall functionality of the fungal community by assigning trophic modes to ITS gene data (Nguyen et al., 2016). FUNGuild, on average, assigned trophic mode to 84 and 73% of the sequence reads for the soil and residue samples, respectively. Of these, trophic mode was assigned to 28 and 48% of the sequence reads per sample at a confidence ranking of 'highly probable' or 'probable'.

Relative abundances of enzyme-encoding genes involved in residue decomposition and N cycling were significantly affected by the residue treatments (Figure 4.7). This suggests that the compositional shifts in soil and residue microbiota were partly responsible for the differences in C and N mineralization observed in this study. Significantly higher abundance of genes associated with cellulose and hemi-cellulose breakdown likely stimulated the decomposition of incorporated crimson clover residues (Figure 4.2 and 4.7). Because of the short duration of this study, we did not expect any differences in the relative abundances of genes involved in lignin breakdown. Surprisingly, surface-applied crimson clover residues had significantly higher lignin-associated genes. The abundances of genes involved in dissimilatory nitrate reduction, nitrification, denitrification, and anaerobic ammonium oxidation (annamox) were also more abundant in surface-applied crimson clover residues. This was probably due to decomposition-associated changes in residue chemistry. After four repeated dry-wet cycles, it is likely that the incorporated crimson clover residues had lost all or most of the easily-degradable labile C fractions because they were decomposed faster than surface-applied residues (Table 4.2). The limited availability of labile C in incorporated residues during the late stage of decomposition may have

resulted in the decrease of functional gene abundances for most of the N metabolic pathways (Cheneby et al., 2010; Zhong et al., 2018). However, assimilatory nitrate reduction is not limited by C availability and the gene abundances were higher in incorporated crimson clover residues likely due to greater NO_3^- availability. Although large shifts in the potential functionality of soil prokaryotes were not observed, relative abundances of the enzyme-encoding genes for C degradation and N metabolic pathways were typically lower in cereal rye-incorporated soils (Figure 4.7). This was probably because the recalcitrant cereal rye residues immobilized N from the soil resulting in both C and N limitations.

Relative to the control soils, the sequence abundances of fungal pathotrophs, saprotrophs, and pathotroph-saprotrophs were not significantly affected by residue additions (Figure 4.8). Among all treatments, saprophytic fungi were significantly more abundant in cereal rye-incorporated soils as compared to that in crimson clover surface-applied soils. This result suggest that the incorporation of more complex and recalcitrant CC residues in soils might stimulate saprophytic (particularly, *Basidiomycota*) fungi as they are known to produce extracellular enzymes and effectively decompose lignocellulosic materials (Clocchiatti et. al., 2020; Reardon and Wuest, 2006). It is also plausible that the pathotrophic fungi in the studied soils were copiotrophic and were stimulated due to greater N availability in crimson clover-amended soils. Although our study highlights the role that fungi play in decomposing surface-applied residues, fungi were equally important in decomposing incorporated residues. In fact, the saprophytic fungi, although not significantly different, were more abundant in soil and residue samples from incorporated residue

treatments as compared to those from surface-applied residue treatments (Figure 4.8). Therefore, incorporation of CC residues likely shifted the fungal community towards non-pathogenic, saprophytic groups which in turn resulted in the faster decomposition of incorporated residues.

Summary and Conclusions

During repeated dry-wet cycles, decomposition of CC residues was strongly influenced by the residue location in soil. Irrespective of the residue type, the rate of C mineralization following rewetting was higher when residues were surface-applied than incorporated, which decreased quickly as they entered the drying phase due to rapid loss of water. The extent to which CC residues mineralized or immobilized N also depends on its location in the soil. After four repeated dry-wet cycles, the total amount of C and N mineralized or immobilized from CC residues was higher when residues were incorporated than surface-applied. Our results suggest that residue water dynamics explains much of the effect of residue location on decomposition and subsequent N availability from CC residues. In other words, CC residue decomposition in fields is highly moisture-mediated; the frequency and intensity of rain events causes differences in residue θ_g and hence, the differences in the rate of C and N mineralization between surface-applied and incorporated residues.

Our study further demonstrated that soil nutrient availability, which was more affected by CC residue type than by its location, had a strong influence on soil microbiota. N-rich soil environments, crimson clover-amended soils in our case, decreased soil prokaryotic and fungal diversity due to dominance by copiotrophs. Similarly, N-poor soil environments, such as cereal rye-amended soils, were

dominated by oligotrophs. On the other hand, residue location may have a greater effect than residue type on determining residue colonizers. Incorporated residues were more colonized by soil prokaryotes resulting in significantly higher prokaryotic diversity. Fungal diversity and community structure in the residue samples were not significantly different. The compositional shifts in the soil and residue microbiota due to residue management appeared to shift its potential functionality, likely contributing to part of the observed differences in C and N mineralization between surface-applied and incorporated residues. Taken together, we can conclude that residue water dynamics has a greater control than microbial colonization on the decomposition and N mineralization from CC residues during repeated dry-wet cycles. More research is needed to confirm these findings under field conditions. Future studies should also investigate how microbes respond to residue management when subjected to variable intensities of dry-wet cycles, as typically observed in fields.

Acknowledgements

This work was supported by the Northeast Sustainable Agriculture Research and Education (NE SARE) graduate student grant (Award no. GNE17-160-31064) awarded to Mr. Resham Thapa and the USDA Natural Resources Conservation Services (Conservation Innovation Grant no. 8042-21660-004-36-R). We express our sincere thanks to research interns and technical staff of the Sustainable Agricultural Systems Laboratory (USDA-ARS), Beltsville Agricultural Research Center, Beltsville, MD for their laboratory assistance. We also thank Lindsay Wood and Martina Gonzalez Mateu for their guidance in Illumina Sequencing and microbial data analysis.

Tables and Figures

Table 4.1 Biochemical characteristics of the cover crop (CC) residues used in an incubation study.

Residue	N	C	C/N	Carbohydrate	Cellulose	Hemi-cellulose	Lignin
	-------%------			----------%----------			
Crimson clover	2.49	47.8	19.2	41.4	33.2	13.0	7.8
Cereal rye	0.61	48.7	79.3	20.0	40.4	31.6	8.0

Table 4.2 Total C mineralized during successive dry-wet (D-W) cycles as affected by cover crop (CC) residue type and placement.

Treatments	Cumulative CO_2-C emitted										Total C mineralized‡
	1st D-W cycle (0-20 d)		2nd D-W cycle (20-40 d)		3rd D-W cycle (40-60 d)		4th D-W cycle (60-80 d)		Total (0-80 d)		
	----------g C m^{-2}----------										% of C applied
Clover Incorporated	49.6 ± 1.9	a†	17.4 ± 2.0	a	14.1 ± 2.4	a	10.4 ± 0.9	ab	91.6 ± 4.4	a	35.5
Clover Surface-applied	40.9 ± 2.3	b	15.8 ± 1.7	a	13.9 ± 2.3	a	9.3 ± 2.2	bc	80.0 ± 6.3	b	28.6
Rye Incorporated	33.4 ± 3.0	c	19.0 ± 1.7	a	15.6 ± 1.9	a	12.9 ± 1.5	a	80.9 ± 4.4	b	28.6
Rye Surface-applied	24.5 ± 2.1	d	17.5 ± 0.6	a	15.1 ± 1.2	a	12.3 ± 2.7	ab	69.3 ± 3.5	c	21.8
Control	9.3 ± 1.3	e	8.7 ± 1.6	b	8.1 ± 0.9	b	6.2 ± 1.2	c	32.2 ± 4.6	d	

† Values are mean ± 1 standard deviation (n=4). Values followed by lowercase letters within each column were significantly different at the 0.05 level.

‡Total C mineralized from cover crop (CC) residues was calculated by dividing the difference in the cumulative CO_2-C emitted between residue amended and un-amended control treatments by the total C applied.

Table 4.3 Effect of cover crop (CC) residue type and placement on the soil prokaryotic and fungal community structure at the end of four repeated dry-wet (D-W) cycles.

Comparison pairs		Prokaryotic community		Fungal community	
		R^2	p-value	R^2	p-value
(a) Residue type effects					
Crimson clover vs Cereal rye	Surface-applied	0.48	0.023	0.28	0.131
	Incorporated	0.61	0.026	0.45	0.030
(b) Residue location effects					
Surface-applied vs Incorporated	Crimson clover	0.29	0.030	0.45	0.037
	Cereal rye	0.39	0.027	0.28	0.035

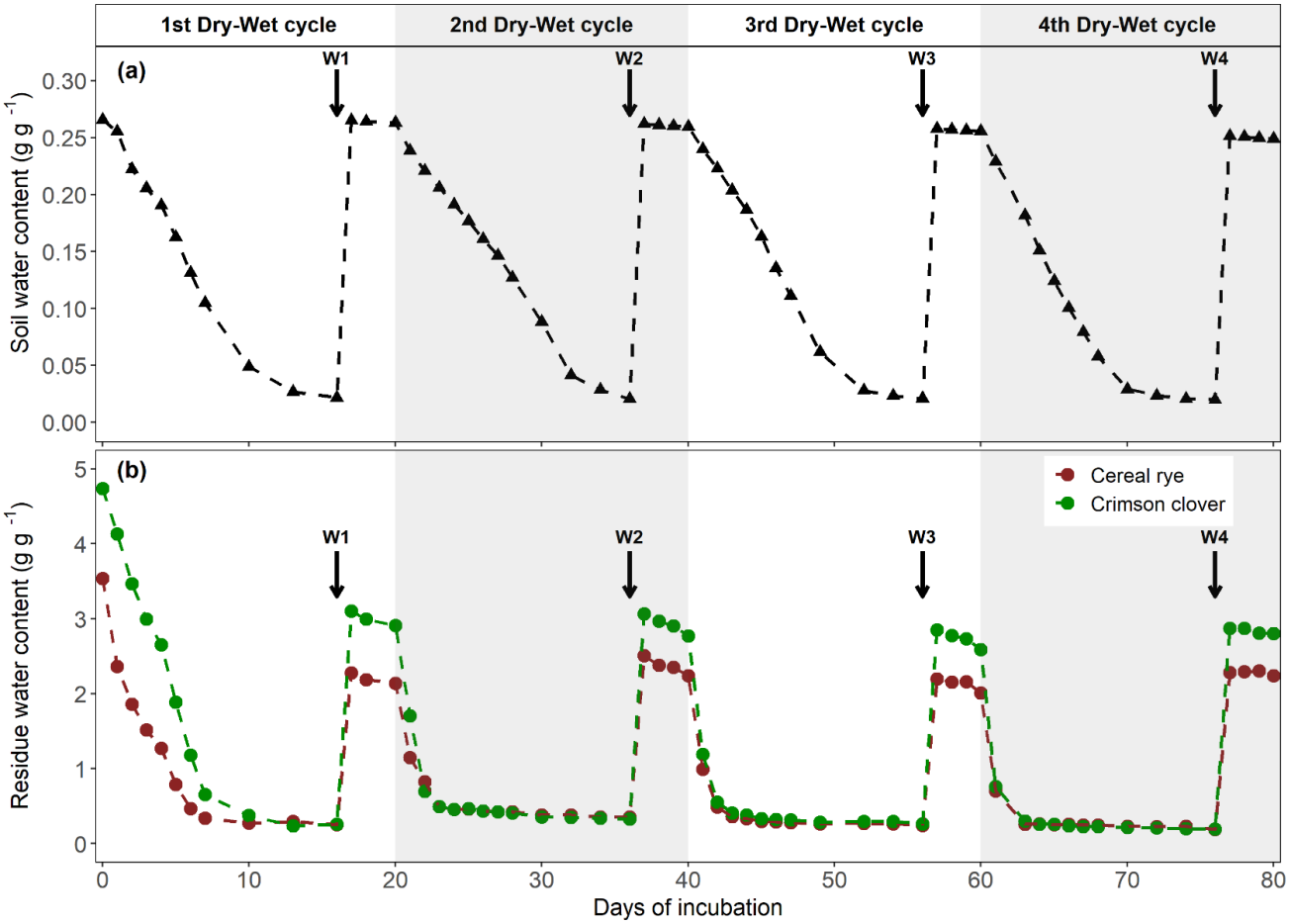

Figure 4.1 Change in the gravimetric water content of soil and surface-applied cover crop (CC) residues during four repeated dry-wet (D-W) cycles. Downward pointing arrows in each D-W cycle indicate the wetting events (W1, W2, W3, and W4).

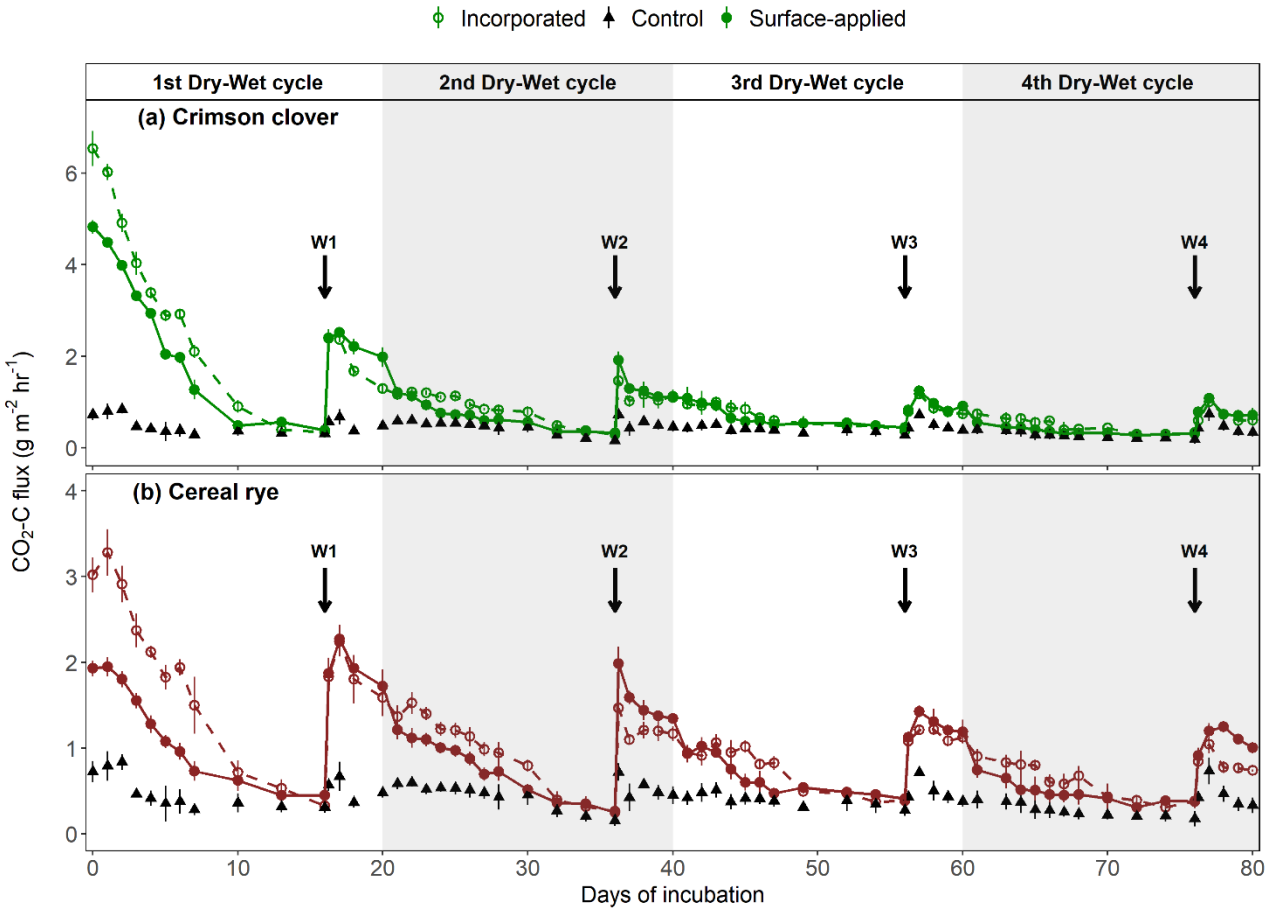

Figure 4.2 Change in the rate of (C) mineralization from surface-applied and incorporated cover crop (CC) residues during four repeated dry-wet (D-W) cycles. Downward pointing arrows in each D-W cycle indicate the wetting events (W1, W2, W3, and W4). The error bars are ± 1 standard error (n=4).

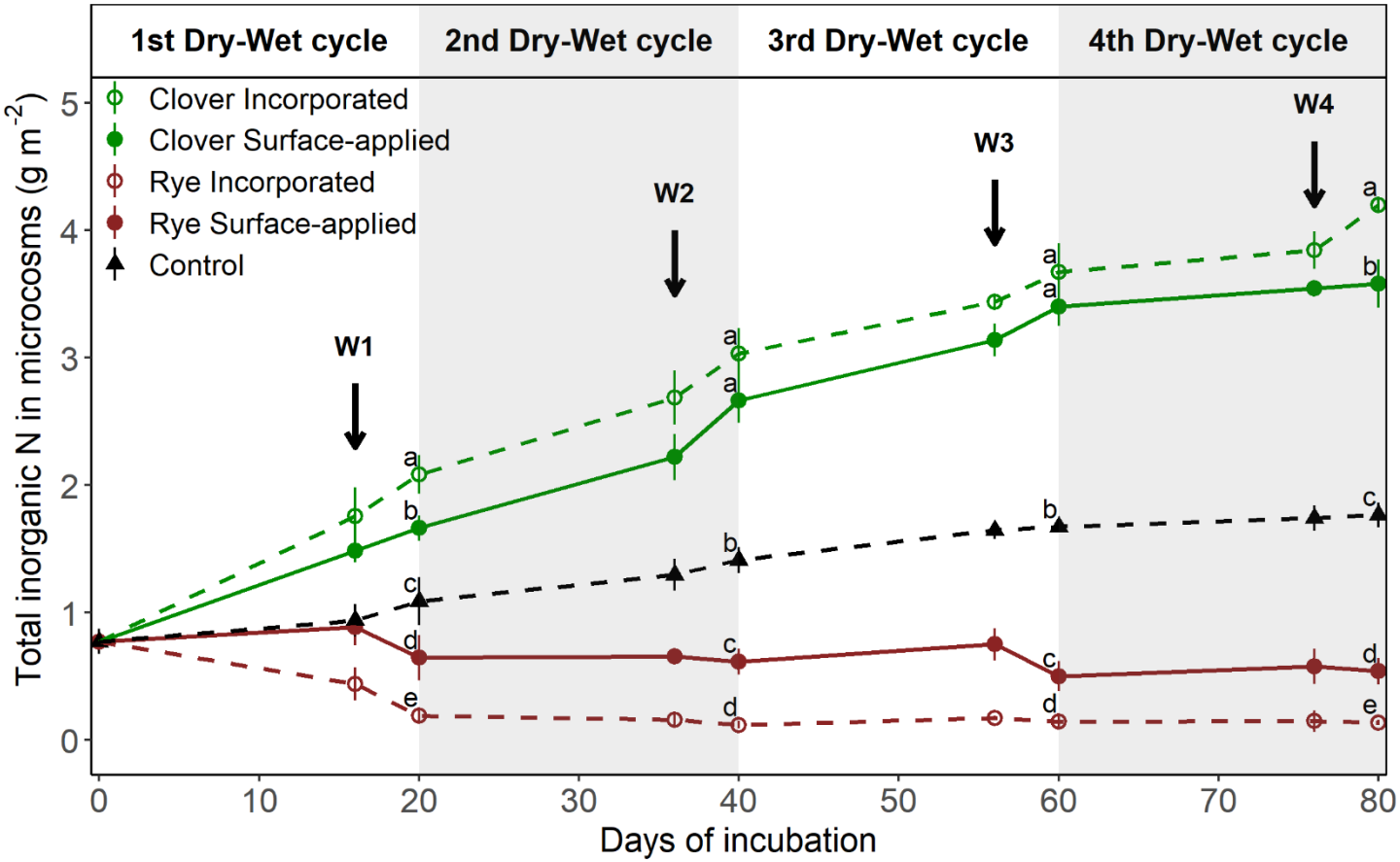

Figure 4.3 Effect of cover crop (CC) residue type and placement on total inorganic nitrogen (N) content during four repeated dry-wet (D-W) cycles. Measurements were performed at the end of each drying and wetting period. Downward pointing arrows in each D-W cycle indicate the wetting pulses (W1, W2, W3, and W4). Different lowercase letters represent significant differences between treatments at each measurement period. The error bars are ± 1 standard deviation (n=3).

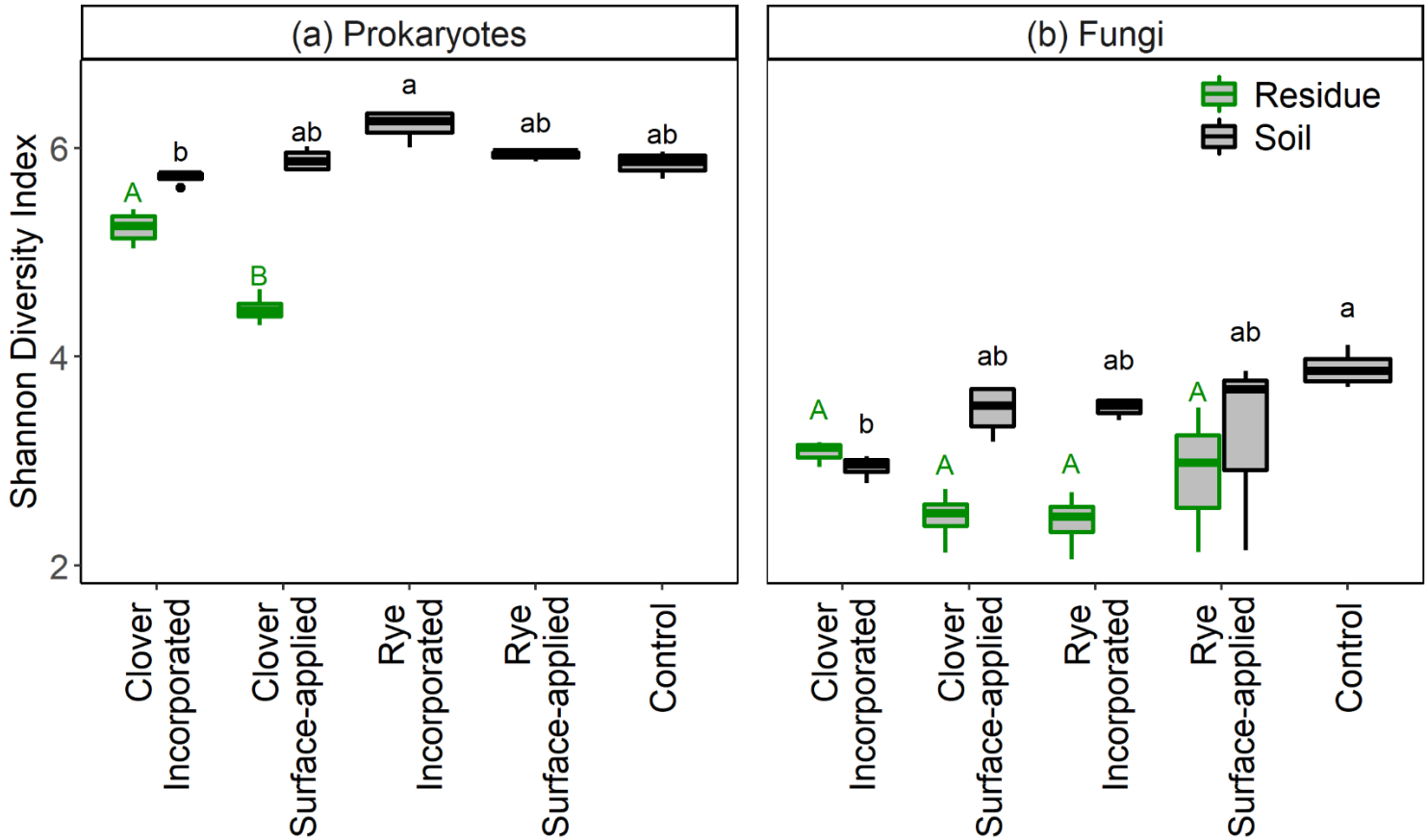

Figure 4.4 Box and whisker plot showing the Shannon diversity index of the (a) prokaryotic and (b) fungal communities in the soil and residue samples. Significant differences between treatments were indicated by lowercase letters for the soil samples and by uppercase letters for the residue samples. Note, most of the rye residue samples have very few sequence reads for the prokaryotic community and were discarded before analysis.

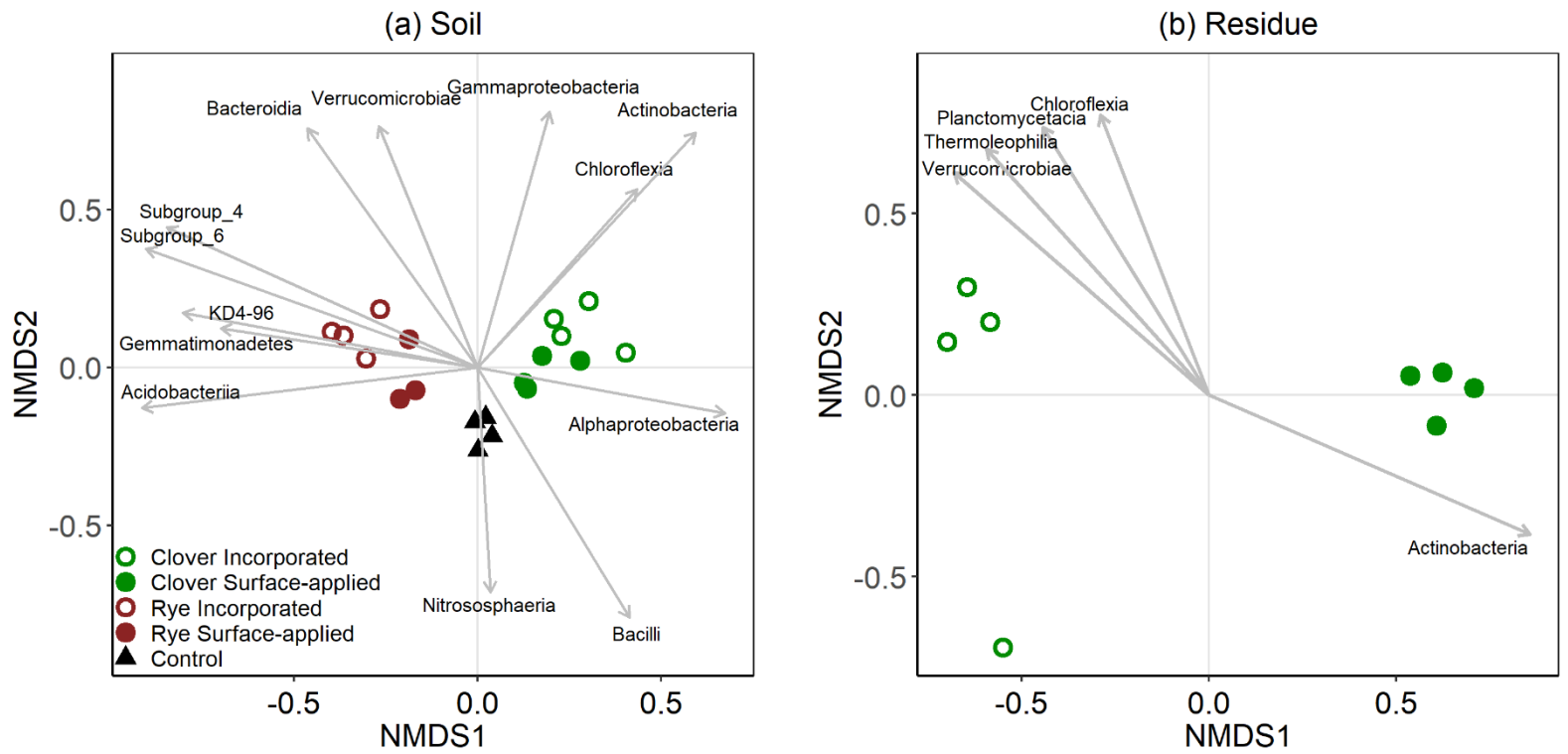

Figure 4.5 Non-metric multidimensional scaling (NMDS) ordination plots based on Bray-Curtis distances of the prokaryotic community structures in the (a) soil and (b) residue samples, respectively. Soil and residue samples were collected at the end of four repeated dry-wet (D-W) cycles. Different colors and shapes represent different treatments. The stress values were 0.07 and 0.17 for soil and residue samples, respectively. Vectors represent the correlation of the most abundant taxa to the prokaryotic community structure in the samples. Note: the bacterial class subgroup 4 and 6 belongs to the phylum *Acidobacteria*.

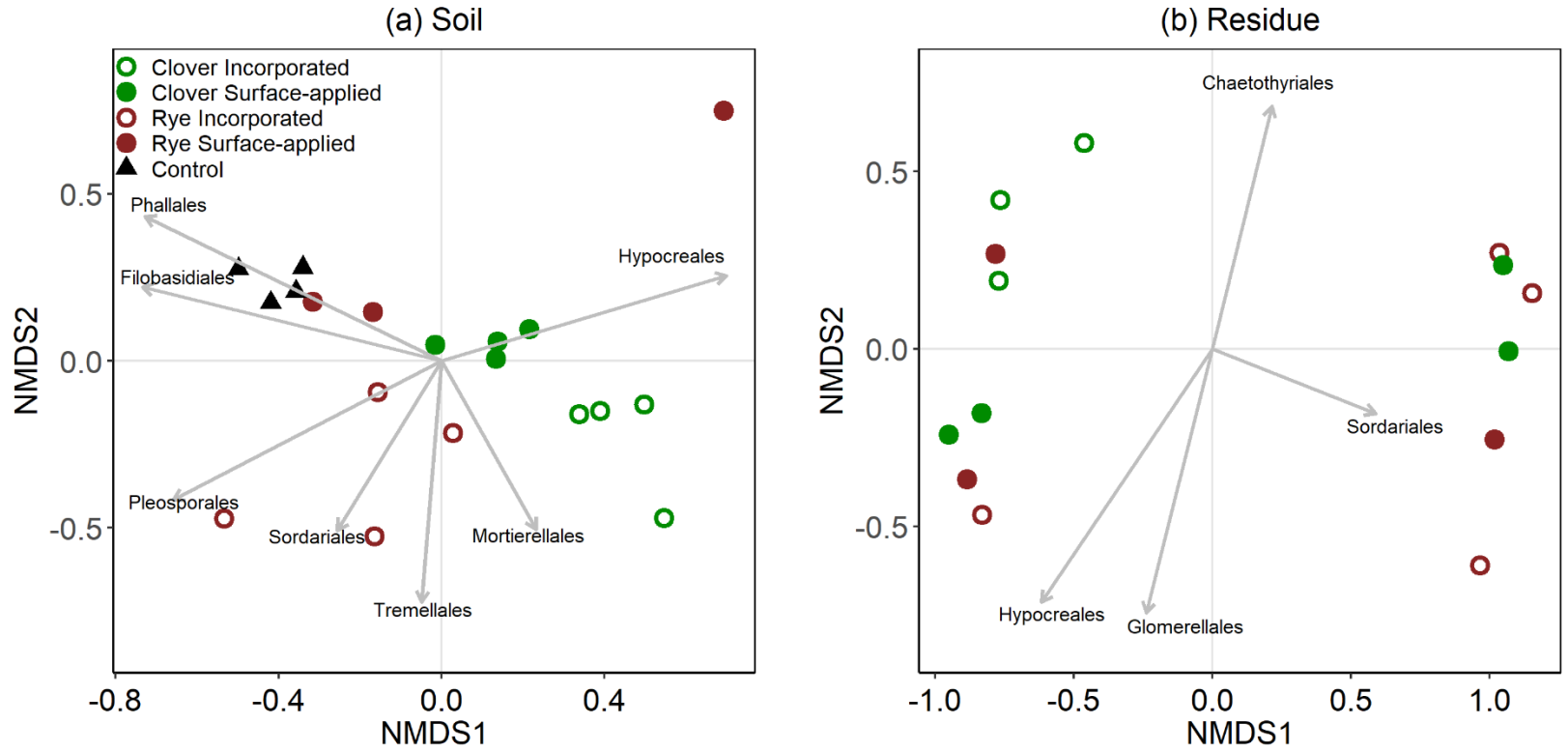

Figure 4.6 Non-metric multidimensional scaling (NMDS) ordination plots based on Bray-Curtis distances of the fungal community structures in the (a) soil and (b) residue samples, respectively. Soil and residue samples were collected at the end of four repeated dry-wet (D-W) cycles. Different colors and shapes represent different treatments. The stress values were 0.14 and 0.08 for soil and residue samples, respectively. Vectors represent the correlation of the most abundant taxa to the fungal community structure in the samples.

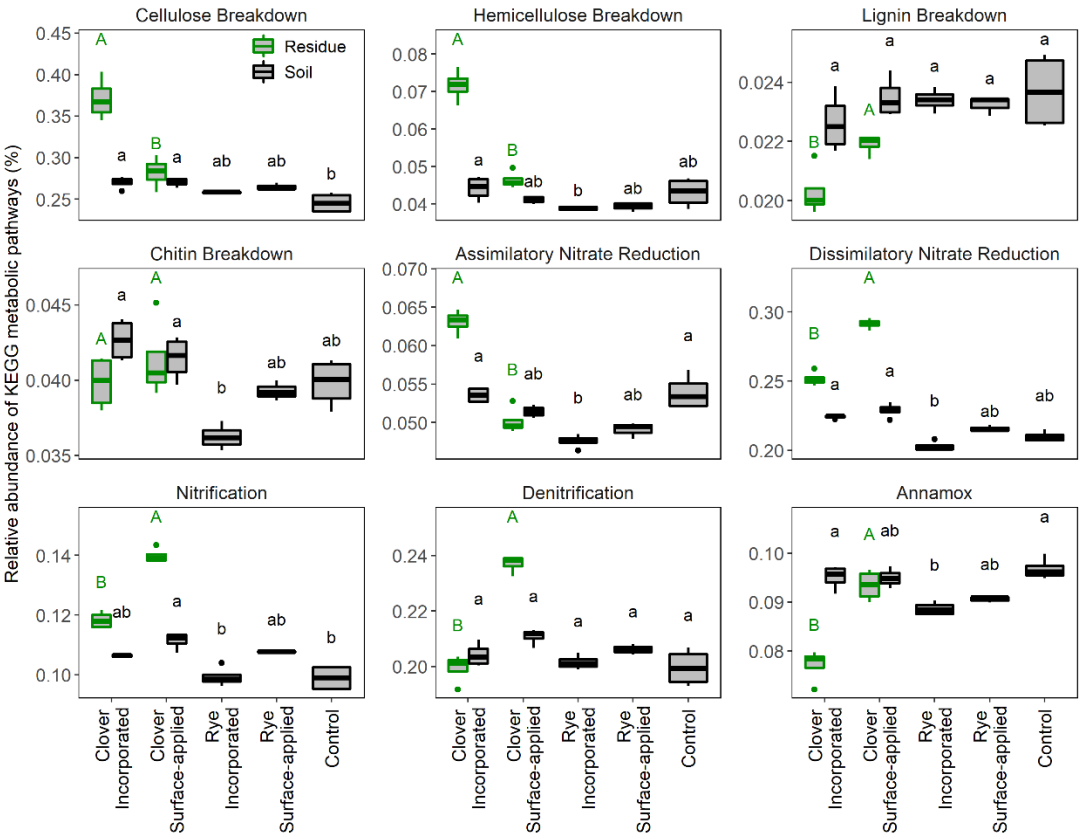

Figure 4.7 Box and whisker plots showing the relative abundances of the enzyme-encoding genes participating in carbon (C) degradation and nitrogen (N) cycling, based on Kyoto Encyclopedia of Genes and Genomes (KEGG) database. Black and green colors represent soil and residue samples, respectively. Significant differences between treatments were indicated by lowercase letters for the soil samples and by uppercase letters for the residue samples. Note, most of the rye residue samples have very few sequence reads for the prokaryotic community and were discarded before analysis.

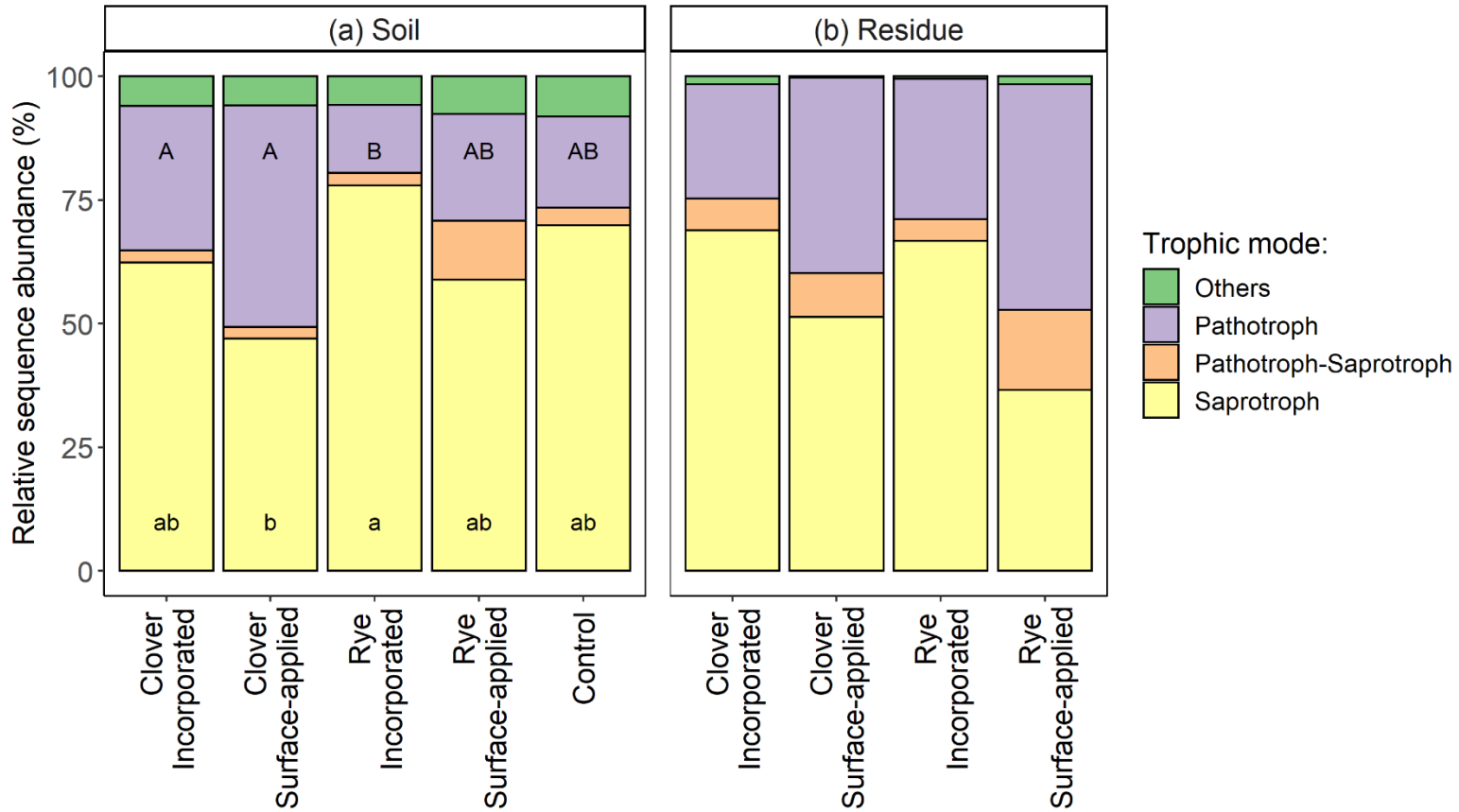

Figure 4.8 Relative proportion of the fungal sequence reads assigned to main trophic modes in the (a) soil and (b) residue samples, respectively, based on FUNGuild database. Only if the differences were significant, different lowercase and uppercase letters were used to indicate significant differences between residue treatments for the saprotrophic and pathotrophic modes, respectively.

Chapter 5: Cover crop residue decomposition in no-till corn systems: Insights from multi-state inter-site litter bag studies

Resham Thapa [a, b*], Katherine L. Tully [a], Chris Reberg-Horton [c], Harry H. Schomberg [b], Miguel L. Cabrera [d], Julia Gaskin [d], Brian W. Davis [a,e], Aurelie Poncet [c], Sarah A. Seehaver [c], Richard Hitchcock [d], Dennis Timlin [f], David Fleisher [f], and Steven B. Mirsky [b]

[a] Department of Plant Science and Landscape Architecture, University of Maryland

[b] Sustainable Agricultural Systems Laboratory, USDA-ARS

[c] Department of Crop and Soil Sciences, North Carolina State University

Department of Environmental Science and Technology, University of Maryland

[d] Department of Crop and Soil Sciences, University of Georgia

[e] Department of Environmental Science and Technology, University of Maryland

[f] Adaptive Cropping Systems Laboratory, USDA-ARS

Manuscript in preparation for submission to Proceedings for the National Academy of Sciences USA (PNAS)

Significance statement

Provisioning of agroecosystem services from cover crop (CC) residues depends on the rate at which they decompose, i.e. *k*-values. Yet, regional assessment of the factors controlling *k*-values are currently lacking. Here, we investigated the independent and combined effects of factors intrinsic to the field (latitude, soil, and climate) and extrinsic or management factors (CC quantity and quality) on *k*-values in no-till corn systems. The combination of CC residue quality (C:N and residue holo-cellulose concentrations) and climatic (mean daily relative humidity of the air and

number of rainy days) variables provided the best predictive model for k-values (70% variance explained). Results further suggest that CC residue quality has greater control over k-values than does climate in the mid-Atlantic and Southeastern US states.

Abstract

Cover crop (CC) residue decomposition influences the provisioning of agroecosystem services. While several laboratory and field studies have investigated processes and mechanisms of CC residue decomposition at specific point or plot scales, regional assessment of the factors controlling decomposition rates (i.e. k-values) in no-till corn (*Zea mays* L.) systems are currently lacking. Here, we conducted the first multi-state inter-site litter bag study over 105 site-years in the mid-Atlantic and Southeastern US states to determine the independent and combined effect of factors intrinsic to the field (latitude, soil, and climate) and extrinsic or management factors (CC quantity and quality) on k-values. The k-values increased along the latitudinal gradient in response to changes in climate and residue quality factors. Among climatic variables, mean daily relative humidity of the air (RHair) and number of rainy days showed stronger control on k-values than cumulative rainfall. This suggests faster decomposition of CC residues in humid environments and in site-years with frequent rain-events. Among extrinsic factors, the k-values decreased with higher CC biomass, C:N, residue holo-cellulose concentrations, and lignin:N, but increased with higher residue carbohydrate concentrations. The combination of CC residue quality (C:N and holo-cellulose) and climatic (RHair and rainy days) variables accounted in total for 70% of the variability in k-values. Results further

indicated that CC residue quality has greater control over k-values than does climate in the mid-Atlantic and Southeastern US states. Therefore, our study emphasizes the necessity to update current process-based decomposition models to explicitly consider CC residue quality (C:N, holo-cellulose) and climate factors (RHair, rainy days), when predicting CC residue decomposition in no-till cropping systems.

Keywords: Cover crops, Inter-site litter bag study, Controlling factors, Residue decomposition rates, No-till systems

Abbreviations: CCs, cover crops; RHair, air relative humidity; NIRS, near infra-red reflectance spectroscopy; k-values, residue decomposition rates

Introduction

Cover crops (CCs) are multi-functional tools that provide a broad suite of agroecosystem services in cropping systems (Mirsky et al., 2012). Historically, CCs were adopted to address the key challenges of conventional agriculture, such as soil conservation (Dabney et al., 2001; Dabney, 1998) and scavenge residual soil nitrogen (N) from being leached after the harvest of previous cash crops (Meisinger et al., 1991; Thapa et al., 2018a). Besides this, some CCs can fix atmospheric N and control weeds effectively, thereby reducing the dependence of agriculture on chemical inputs such as synthetic N fertilizers and pesticides (Mirsky et al., 2011; Poffenabarger et al., 2015b). Given some of the predicted effects of climate change on agriculture (increased flood and drought intensity and altered rainfall patterns), the water conservation benefits associated with CCs have recently gained considerable attention among farmers and agricultural professionals. In the long run, CCs can build soil

organic matter stocks, improve soil health, stabilize crop yields, and build resilient agricultural cropping systems (Mirsky et al., 2012; Poeplau and Don, 2015).

Agroecosystem services provisioned by CC residues depend on intrinsic (latitude, soil, and climate) and extrinsic (CC management decisions) factors, and the rate at which these residues decompose (k-values). For example, nitrate leaching reductions were more effective when CCs were planted early and higher biomass levels were achieved (Thapa et al., 2018a). In the same study Thapa et al. (2018a), it was further suggested that CC more effectively reduced nitrate leaching in coarse-textured soils and in drier years. Similarly, the k-values will determine the longevity of CC residues in no-till cropping systems. Slow decomposition rates (lower k-values) will maintain the CC residue mulch layer throughout the growing season, which in turn helps control weeds and conserve water more effectively. In the long-term, CC residues with small k-values will build up soil organic matter and nutrient stocks in the soil, thereby enhancing agricultural sustainability. On the other hand, CC residues with high k-values (fast decomposition rates) release nutrients, particularly N, quickly and help to meet all or part of the N requirements of the succeeding cash crops (Poffenbarger et al., 2015b; Thapa et al., 2018b). Therefore, it is crucial to determine key factors controlling k-values (i.e. residue decomposition rates) to design evidence-based management practices to optimize agroecosystem services from CCs.

Residue decomposition is a complex biogeochemical process in which the CC residues are broken down into simpler forms by soil microorganisms and animals.

Factors controlling the existence and activities of these organisms will ultimately control the rate of residue decomposition, i.e. k-values. These factors can be broadly categorized as factors intrinsic to the field and extrinsic or management factors. Intrinsic factors include latitude, soil, and climate. Environmental conditions have a strong influence on residue decomposition, with k-values accelerating proportionately with increasing moisture and temperature (Quemada and Cabrera, 1997; Stott et al., 1986; See Chapter 3). The moisture and temperature in surface CC residue layers, in turn, is driven by climatic variables such as the amount and distribution of rainfall, relative humidity of the air (RHair), and air temperature (Manstretta and Rossi, 2015; See Chapter 2). Extrinsic or management factors include CC residue quantity (biomass) and quality (N content, C:N, residue C chemistry such as carbohydrate, holo-cellulose, and lignin concentrations) (Cabrera et al., 2005; Otte et al., 2019; Poffenbarger et al., 2015a; Ranells and Wagger, 1992, 1996; Vigil and Kissel, 1991; Wagger et al., 1998; Williams et al., 2018). The quantity and quality of CC residues depend on latitude (Mirsky et al., 2017), climate during the CC growth period (Mirsky et al., 2011; Thapa et al., 2018b), farmers' management decisions such as CC species selection and mixture composition, and planting and termination dates/methods (Otte et al., 2019; Poffenbarger et al., 2015b; Ranells and Wagger, 1992; Thapa et al., 2018b; Wagger, 1989).

Much of our current understanding on the factors controlling k-values are either based on laboratory or small-scale field experiments, typically 2-3 site-years. While these studies provide the foundational knowledge on CC residue decomposition, reported evidence has not been conclusive in determining the

dominant factors controlling k-values in no-till cropping systems. First, past studies focused on determining the effect of CC management (CC species and mixture composition, planting and termination dates/methods) on residue decomposition and have linked the variations in k-values to differences in C:N (Otte et al., 2019; Poffenbarger et al., 2015a). The effect of residue chemistry (i.e. carbohydrate, holo-cellulose, and lignin) on residue decomposition has largely been ignored. Second, we have vague understanding on how climate affects k-values in natural field settings due to lack of decomposition studies across large temporal and spatial scales. Moreover, the nature of past studies did not provide the flexibility to investigate the combined effect of climate and CC residue quality on k-values. Therefore, findings from past studies were highly site-specific and cannot be extrapolated across large geographical regions.

In forest ecosystems, global or regional assessment of the factors controlling k-values have been conducted via meta-analyses (Aerts, 1997; Zhang et al., 2008; Zhang and Wang, 2015) and inter-site litter bag studies along elevation or latitudinal gradients (Paudel et al., 2015; Zhou et al.,2008). One of the major limitations of the meta-analytic approach is that individual studies likely have different litter bag decomposition protocols such as the usage of litter bags with different mesh sizes. Inter-site litter bag studies along elevation or latitudinal gradients, on the other hand, provide the benefit of having standardized methodology and can be used as a surrogate for long-term decomposition studies by capturing k-values across a range of environmental conditions. Moreover, inter-site litter bag studies provide the opportunity to understand the temporal response of decomposition to climate change

by providing ‘space-for-time substitutions’. Despite such benefits, regional assessment of CC residue decomposition in cropping systems is currently lacking due to considerable labor and financial requirements for conducting inter-site litter bag studies.

The CROWN (**C**over crops: **R**eal-time **O**bservation of **W**ater and **N**utrients) project was launched in 2017 to determine the immediate effects of CC adoption on soil water, nutrients, and succeeding cash crop yields. To our knowledge, this is the first multi-state inter-site litter bag decomposition study conducted in no-till cropping systems in the US. In this study, we measured decomposition of CC residues in no-till cropping systems using standardized methodology in which the proportion of CC biomass remaining over time was tracked during the succeeding cash crop season. In this paper, our main objectives were to (i) determine the independent and combined effects of factors intrinsic to the field (latitude, soil, and climate) and extrinsic or management factors (CC quantity and quality) on k-values, (ii) develop an empirical model to predict k-values for estimating CC residue decomposition in no-till corn (*Zea mays* L.) systems, and (iii) identify dominant factors controlling CC surface residue decomposition rates in the mid-Atlantic and Southeastern US states.

Materials and Methods

Description of the CROWN project

We established a network of CC adopters across the mid-Atlantic and Southeastern US states (Figure 5.1a). At each farm site, the experiment was conducted in a strip-plot design with CC and bare soil as adjacent treatments (Figure 5.1b). There were two subplots within each strip-plot (Figure 5.1c). Farmers were

required to leave a strip of bare soil at the time of CC planting or terminate a strip of CC within 10 d after its planting using herbicide. All other CC and cash crop management decisions were dictated by the farmers. They were free to plant any CC species and mixture composition, and have flexibility in their preferred CC planting and termination dates/methods. The only requirement to get enrolled in the CROWN project was to leave the CC mulch layer on the soil surface and plant subsequent cash crops using no-till methods. The subsequent cash crops were corn, soybean (*Glycine max* L.), or cotton (*Gossypium* sp.).

In this paper, our main objective was to quantify factors controlling CC decomposition kinetics in no-till corn systems. Hence, 101 site-years of data collected during 2017-2019, with corn as subsequent cash crop, were included from the CROWN project (Figure 5.1a). Detailed description on CC biomass sampling and decomposition kinetics is provided below. We also included four site-years of data collected during 2016-2017 from the long-term CC study conducted at the USDA-ARS Beltsville Agricultural Research Center in Beltsville, MD (Otte et al., 2019). Therefore, the final database contained 105 site-years of data across five states: Georgia (GA), North Carolina (NC), Delaware (DE), Maryland (MD), and Pennsylvania (PA) (Figure 5.1a).

Cover crop quantity and quality

Just prior to termination, CC biomass was collected by clipping two separate 1 m^2 areas in each of two subplots (Figure 5.1c, d). Biomass sampling procedure at each farm site was determined based on the CC planting method. For broadcasted CC, we used quadrants. If CC was drill-seeded, the number and length of drill lines to

harvest was determined by measuring the spacing between drill lines. The fresh weight of CC biomass from each subplot was recorded and was subsequently used for filling litter bags (see below). The time 0 litter bags were retained on the day of CC termination and then dried at 60 °C for at least two days to determine residue gravimetric water contents (θ_g). The field-measured fresh CC weights were converted into dry weights using θ_g. Dried CC biomass samples were mechanically ground to pass through a 1-mm sieve and analyzed for tissue C and N concentrations using dry combustion via Leco TruMac CN Analyzer (LECO Corporation, St. Joseph, MI). A 5-g subsample from each subplot was sent to the Agricultural and Environmental Services Labs at the University of Georgia (Athens, GA) to determine CC residue C chemistry [carbohydrate, holo-cellulose (cellulose plus hemi-cellulose), and lignin concentrations] via near infra-red reflectance spectroscopy (NIRS) using a scanning monochromator (model 6500; FOSS NIRSystems, Silver Spring, MD).

A few site-years had missing C and N data based on dry combustion analysis. In that case, we estimated tissue N concentrations based on NIRS analysis (%N-combustion = 1.21 × %N-NIRS – 0.76; Adj. R^2 =0.89; p<0.0001; Figure A6). This predictive equation was developed based on all other remaining data in the database. Similarly, the missing tissue C concentrations were estimated using a constant 42.6%, which was the average tissue C concentrations of all other remaining site-years of data in the database.

Litter bag decomposition protocol

Decomposition kinetics of the aboveground CC biomass were determined using nylon mesh litter bags (26 by 60 cm dimensions, 1-mm mesh size). Two separate 1 m^2 fresh CC biomass collected from each of the two subplots were mixed together and equally distributed among 12 litter bags. In total, 24 litter bags were prepared at each farm site which provided four sets of six litter bags. Out of six litter bags, one bag was retained on the same day and dried immediately as described above (Figure 5.1c). The remaining five bags were deployed on the soil surface using landscape staples (Figure 5.1e). In sites where CC was terminated prior to corn planting, the bags were placed in headlands of the field or nearby bare areas to avoid interference with farmers' cultural operations. Following corn planting, the litter bags were moved in between crop rows in their respective subplots. In sites where CC was terminated on the same day or after corn planting, i.e. planting green, litter bags were directly placed in between corn rows. The remaining five litter bags were collected at approximately 14, 30, 60, 90-120 d after CC termination, and finally at corn harvest at physiological maturity. Retrieved litter bags were oven-dried at 60 °C for at least 2 days and the weights were recorded after scraping any soil adhered to the outside of the bags. Residues from each litter bag were ground to pass through a 1-mm sieve. Soil contamination was determined by ashing 1-g subsample of ground residue at 550 °C for 4 h. The residue weights were finally adjusted to an ash-free basis.

Soil and climate data

Soil samples (0-30 cm depth) were collected, air-dried, and ground to pass through a 2-mm sieve. A 40-g subsample was used for soil textural analysis using a

hydrometer method (Gee and Bauder,1986). For sites in which the soil samples were not collected, soil textural data was extracted from the Web Soil Survey database (accessed on June 3, 2020).

Climatic variables of interest included cumulative rainfall, number of rainy days, mean daily air temperature, and mean daily RHair. These data were imported from the in-house weather API (Application Programming Interface) developed for the CROWN project. Our weather API contains hourly weather data generated by North American Land Data Assimilation System Phase-2 (NLDAS-2; Xia et al., 2012) and hourly rainfall data generated by Multi-Radar Multi-Sensor System (MRMS; Zhang et al., 2016). The hourly data were summarized to calculate daily rainfall, daily mean air temperature, and daily mean RHair using the R *dplyr* (Wickham et al., 2020) and *dbplyr* (Wickham and Ruiz, 2020) packages.

Data summarization and statistical analysis

The soil, climate, and CC data for the CROWN project is available in a centralized postgreSQL database. These data were imported into the R statistical environment for analysis using the *RPostgres* package (Wickham et al., 2019). Data summarization was performed using functions from the R *dplyr* and *dbplyr* packages. Mean values of CC quantity and quality (C:N, lignin:N, residue carbohydrate, holo-cellulose, and lignin concentrations) variables were calculated for each site-year. Similarly, we calculated cumulative rainfall, number of rainy days, mean daily air temperature, and mean daily RHair during the first 30, 60, 90 d after CC termination, and for the whole CC decomposition period. Preliminary analysis suggested that the climatic data during the first 60 d after CC termination were better related to the k-

values than any other summary periods. Therefore, we only presented the climatic data during the first 60 d after CC termination in this study. Finally, summarized data on intrinsic (latitude, soil, and climate) and extrinsic or management factors (CC quantity and quality) along with site information were merged together into a single data table for further analysis.

We used nonlinear mixed effect models to model CC residue decomposition as a function of the proportion of initial ash-free CC dry weight remaining on litter bags over time. A single-pool first-order exponential decay model proposed by Olson (1963) was fitted separately for each site-year using the R *nlme* package (Figure 5.1e; Pinheiro et al., 2019).

$$P_t = exp^{-k \cdot t} \qquad (1)$$

where P_t is the proportion of initial ash-free CC biomass remaining at a given time t, k is the exponential decay rate constant (day^{-1}), and t is the time since CC termination in days. A CC subsample within each subplot was included as a nested random structure in the model. A single-pool exponential decay model was selected instead of an asymptotic or double-pool exponential decay model because it has only one parameter, i.e. k-value, and the estimated k-value is independent of the pool size.

Simple linear regressions were fitted between k-values and individual controlling factors to show their independent effect on CC residue decomposition. To account for non-normality and heteroscedasticity of the residuals, the k-values were naturally log-transformed before performing regression analysis (Eq. 2). This is

equivalent to an exponential relationship between k-values and the controlling factors (Eq. 3).

$$ln(k) = \beta_1 \cdot X + \beta_0 + \varepsilon \quad (2)$$

$$k = exp^{\beta_0} \cdot exp^{\beta_1 \cdot X} \cdot \varepsilon \quad (3)$$

where X is one of the controlling factors, β_1 and β_0 are the slopes and intercepts of the regression line between $ln(k)$ and X, and ε is the residual effect. Logarithmic regression provided the better fit between k-values and CC biomass or lignin:N (Eq. 4).

$$k = \beta_1 \cdot ln(X) + \beta_0 + \varepsilon \quad (4)$$

We performed correlation analysis to assess collinearity among factors controlling k-values. Correlation analysis revealed that some of these factors were highly correlated (Figure 5.2). Therefore, partial least squares (pls) regression analysis was conducted using the R *pls* package to test the interaction effect of intrinsic and extrinsic factors on $ln(k)$ (Mevik et al., 2019). The pls regression is a dimensionality reduction technique in which the predictors are reduced into a smaller set of uncorrelated components. The pls component analysis was performed for intrinsic and extrinsic factors independently and the number of components were selected based on cross-validation technique, i.e. the lowest root mean standard error of prediction (Table A1). The pls scores representing intrinsic and extrinsic factors were calculated using loading coefficients. A full multiple linear regression model was performed considering both main and interaction effects of the pls scores. Results

suggest that there was no significant interaction effect of intrinsic and extrinsic factors on $ln(k)$ (Table A2). Moreover, due to the complexity in interpreting results from pls regression, we performed a simple additive multiple linear regression based on stepwise procedure using the *step* function in R. Three stepwise multiple linear regression models were fitted to best predict $ln(k)$: model I containing only intrinsic factors [latitude, soil (sand and clay content), and climate (cumulative rainfall, number of rainy days, mean daily air temperature, and mean daily RHair)]; model II containing only extrinsic or management factors [CC quantity (biomass) and quality (C:N, residue carbohydrate, holo-cellulose, and lignin concentrations, and lignin:N)]; and model III containing both intrinsic and extrinsic factors. The best subset of predictors among intrinsic and extrinsic factors in predicting $ln(k)$ were identified using Bayesian Information Criterion (BIC) penalty for each added predictor in the model. Models with the lowest BIC value were selected and presented here. The general form of the fitted multiple linear regression model is provided below:

$$ln(k) = \beta_1 \cdot X_1 + \beta_2 \cdot X_2 + \cdots\cdots\cdots\cdots + \beta_i \cdot X_i + \beta_0 + \varepsilon \quad (5)$$

where $X_1, X_2, \cdots, X_i$ are the independent variables (either intrinsic or extrinsic or both factors), $\beta_1, \beta_2, \cdots, \beta_i$ are the beta coefficients and represents the contribution that each of the predictor variables have in the equation predicting $ln(k)$, β_0 is the overall intercept, and ε is the residual effect. Finally, commonality analysis was performed to assess the relative contribution of the factors selected via stepwise multiple linear regression procedure in explaining the model total variance, i.e. R^2. In commonality analysis, the contribution of each regressor was assessed in terms of

unique effects and in the presence of other independent variables, i.e. common effects. The *yhat* package in R was used for commonality analysis (Nimon et al., 2020).

Results

Relationship among intrinsic and extrinsic factors

Table 5.1 provides the summary statistics of intrinsic (latitude, soil, and climate) and extrinsic or management (CC quantity and quality) factors. These factors were highly variable across site-years, suggesting that our inter-site litter bag decomposition studies captured a broad range of soil, climate, and management variables. In general, soils at lower latitude research sites (GA and NC) had more sand and less clay content as compared to sites at higher latitudes (MD and PA). Latitude was positively related to number of rainy days (r=0.70, p<0.0001), mean daily RHair (r=0.63, p<0.0001), and cumulative rainfall (r=0.35, p<0.0001) (Figure 5.2a). However, there was no significant association between latitude and mean daily air temperature (r=0.08, p=0.42). We also found that latitude was negatively related to C:N of the initial CC residue (r=-0.27, p<0.01). Among the climatic variables, cumulative rainfall, number of rainy days, and mean daily RHair were all significantly and positively related to one another (Figure 5.2a). Although not significant, the mean daily RHair was negatively related to mean daily air temperature (r=-0.10, p=0.30).

Cover crop quantity and quality variables were also highly correlated (Figure 5.2b). The CC biomass was positively related to C:N (r=0.38, p<0.0001), residue holo-cellulose concentrations (r=0.37, p<0.0001), and lignin:N (r=0.26, p<0.01), but

negatively related to residue carbohydrate concentrations (r=-0.30, p<0.01). Among CC quality variables, we found a strong positive association of C:N with residue holo-cellulose concentrations (r=0.57, p<0.0001) and lignin:N (r=0.77, p<0.0001). However, C:N ratio and residue carbohydrate concentrations were negatively correlated (r=-0.43, p<0.0001). The residue carbohydrate concentrations were negatively related to residue holo-cellulose (r=-0.94, p<0.0001) and lignin (r=-0.65, p<0.0001) concentrations and lignin:N (r=-0.65, p<0.0001).

Residue decomposition rates: Effect of intrinsic (latitude, soil, and climate) factors

Cover crop residue decomposition rates, i.e. k-values, in the mid-Atlantic and Southeastern US states ranged from 0.005 to 0.033 day^{-1} and averaged 0.015 day^{-1} across all site-years (Table 5.1). Results showed that the k-values increased with latitude (Adj. R^2=0.23, p<0.0001; Figure 5.3a). Although not expected, we found that the k-values decreased significantly with the increase in sand content at the experimental site (Adj. R^2=0.12, p<0.001; Figure 5.3c). Among climatic variables, mean daily RHair exerted greater control in k-values followed by the number of rainy days and then by cumulative rainfall (Figure 5.4). The mean daily RHair during the first 60 days since CC termination explained 26% of the variations in k-values (Figure 5.4b). Whereas, the total number of rainy days and cumulative rainfall explained only 17% and 7% of the variations in k-values (Figure 5.4c, d). The mean daily air temperature, on the other hand, had no significant effect on k-values (Figure 5.4a).

Stepwise multiple linear regression analysis was performed to subset the best predictors among intrinsic factors and determined their combined ability in predicting *k*-values. Model statistics and parameter estimates of the best model were presented in Table 5.2 and 5.3, respectively. The explanatory power of the best model I was 35% ($p<0.0001$; Table 5.2). Based on the size of parameter estimates and commonality coefficients, mean daily RHair contributed the most to the predictive ability of the model as compared to the number of rainy days (Table 5.3). The mean daily RHair and the number of rainy days uniquely explained 49 and 24% of the total variance, i.e. R^2, for model I, respectively. The squared structure coefficients for mean daily RHair and the number of rainy days in model I were 0.758 and 0.512, respectively. This suggests that, when both unique and common variance components were considered together, mean daily RHair and the number of rainy days during the first 60 d since CC termination explained 76 and 51% of the model total variance, respectively.

Residue decomposition rates: Effect of extrinsic or management (CC quantity and quality) factors

The *k*-values decreased logarithmically with increasing CC biomass (Adj. $R^2=0.31$, $p<0.0001$; Figure 5.5a). Among CC quality variables, C:N appeared to be the best predictor of *k*-values (Adj. $R^2=0.47$, $p<0.0001$; Figure 5.5b). The *k*-values decreased exponentially with increasing C:N. Results further showed that the *k*-values decreased with increasing residue holo-cellulose concentrations (Adj. $R^2=0.29$, $p<0.0001$; Figure 5.5d) and lignin:N (Adj. $R^2=0.29$, $p<0.0001$; Figure 5.5f), but increased with increasing residue carbohydrate concentrations (Adj. $R^2=0.20$,

p<0.0001; Figure 5.5c). We found no significant relationship between k-values and residue lignin concentrations (p=0.12; Figure 5.5e).

Results from stepwise multiple linear regressions, considering only extrinsic factors, suggested that the best model II contained only C:N and residue carbohydrate concentrations and explained 50% of the variations in k-values (p<0.0001; Table 5.2). Based on the size of parameter estimates and commonality coefficients, C:N contributed the most to the predictive ability of the model II than residue carbohydrate concentrations (Table 5.3). We found that C:N uniquely explained 59% of the total variance for model II, whereas it was only 6% for residue carbohydrate concentrations. Moreover, we found that a large amount of model variance explained by residue carbohydrate concentrations was also described by C:N and was probably due to correlation between these variables. When both unique and common effects variance components were considered, C:N explained 94% of the total variance for model II. These results suggest that C:N, most commonly used indicator for CC residue quality, was the single-best predictor for CC residue decomposability.

Residue decomposition rates: Combined effect of intrinsic and extrinsic factors

We found no interaction effect of intrinsic and extrinsic factors on k-values (Table A2). When both intrinsic and extrinsic factors were considered together, the explanatory power of the overall best model III increased to 70% (p<0.0001; Table 5.2). The best model III contained four predictor variables: C:N, residue holo-cellulose concentrations, mean daily RHair, and number of rainy days (Table 5.2 and 5.3). These variables uniquely explained 7-13% of the explained variance in k-values,

suggesting that the common effects among these independent variables explained a large amount of the regression effect. The common effect (i.e., variance components shared in each possible combination of the independent variables) values for C:N, residue holo-cellulose concentrations, mean daily RHair, and number of rainy days were 0.410, 0.227, 0.246, and 0.090, respectively. Based on squared structure coefficients, in total, the C:N, residue holo-cellulose concentrations, mean daily RHair, and number of rainy days explained 68, 43, 42, and 26% of the total variance for model III, respectively.

Discussion

Cover crop residue decomposition is a complex biological process that influences provisioning of agroecosystem services. Hence, it is critical to understand how *k*-values were impacted by intrinsic (latitude, soil, and climate) and extrinsic or management (CC quantity and quality) factors to maximize targeted agroecosystem services from CC. By conducting inter-site litter bag studies across the mid-Atlantic and Southeastern US states, our study provides new insights into how these multiple controlling factors impact CC residue decomposition in no-till cropping systems.

Residue decomposition rates: Effect of intrinsic (latitude, soil, and climate) factors

Quite surprisingly, we found that the *k*-values increased with increasing latitude (Figure 5.3a). This is in sharp contrast to our general understanding on how *k*-values change along latitudinal gradients. In forest ecosystems where litter decomposition was assessed for several years, it is well-established that the decrease in mean annual temperature with increasing latitudes led to decrease in *k*-values for

both leaf and root litter samples (Silver and Miya, 2001; Zhang and Wang, 2015; Zhang et al., 2008). In our study, however, there was no significant relationship between latitude and mean daily air temperature due to differences in dates over which the climatic data were summarized among site-years (Figure 5.2a). Therefore, the increase in *k*-values with latitude was likely caused by the strong positive relationship between latitude and other climatic variables, such as mean daily RHair (r=0.63, p<0.0001), number of rainy days (r=0.70, p<0.0001), and cumulative rainfall (r=0.35, p<0.0001; Figure 5.2a). Although CC biomass and residue C chemistry variables were quite similar along latitudinal gradient, latitude had a weak but significantly negative association with C:N (r=-0.27, p<0.01; Figure 5.2b). The overall decrease in C:N of CC residues at high latitudes may also explain the increase in *k*-values as latitude increases. In addition, we observed substantial variations in *k*-values among site-years within the same latitude zone due to differences in CC residue quantity and quality (Figure 5.3a). Based on these results, latitude had an indirect effect on *k*-values via influencing climatic variables such as mean daily RHair, number of rainy days, and cumulative rainfall as well as due to latitudinal variations in residue quality.

In this study, soil texture differed along latitudinal gradient (Figure 5.2a). The coarseness of the soil (i.e. sand content) decreased from low latitude (GA, NC) to high latitude (MD, PA) sites. Since *k*-values increased with latitude and the sand content decreased with latitude, the observed negative relationship between *k*-values and sand content was probably a reflection of the latitudinal effect on residue decomposition (Figure 5.3c). Soil texture could also influence *k*-values via a

moistening effect on the CC residue layer that is in contact with the underlying soil. For example, in a simulated rain experiment, Iqbal et al. (2015) observed that the water contents were higher in crop residues left on the surface of loamy soil than that on sandy soil. Higher drainage in coarser soils depleted soil moisture quickly and decreased its capacity to moisten adjacent CC residue layers. This, in turn, may have led to decrease in k-values as the underlying soils become more and more sandier.

Although models of litter decomposition in forest ecosystems suggest that mean annual temperatures have a stronger influence on k-values than mean annual precipitation (Silver and Miya, 2001; Zhang and Wang, 2015a, b; Zhang et al., 2008), we found no significant effect of temperature on k-values (Figure 5.4a). Moreover, our results do not agree with several laboratory incubation studies in which CC residue decomposition has been observed to accelerate with increasing temperature (Quemada and Cabrera, 1997; Stott et al., 1986; See Chapter 3). This was probably because CC residue decomposition in our inter-site litter bag studies were assessed only during hot summer months. Thus, temperature effects on k-values were masked by residue moisture effects. Moreover, the k-values tended to decline with increasing temperature at mean daily air temperature greater than 20 °C (Figure 5.4a). In a series of diurnal experiments, Thapa et al. (See Chapter 2) also observed that the rate of CC residue decomposition in no-till cropping systems decreased due to moisture limitations at elevated temperatures. Therefore, temperature had a nil or negative effect on CC residue decomposition in no-till systems.

Another important climatic variable that is commonly used to describe decomposition kinetics across site-years is rainfall. We found that the k-values

increased with increase in cumulative rainfall (Figure 5.4c). However, the predictive ability of rainfall on *k*-values were very low (Adj. R^2=0.07, p<0.01) as compared to mean daily RHair (Adj. R^2=0.26, p<0.0001) and total number of rainy days (Adj. R^2=0.17, p<0.0001). The overall best model containing only intrinsic factors, based on BIC penalty, further confirmed that the mean daily RHair and number of rainy days were important intrinsic determinants of CC residue decomposition in no-till systems (Table 5.2). As mean daily RHair and number of rainy days increased, *k*-values also increased indicating enhanced decomposition of CC residues in humid environments as well as in site-years with more frequent rain events (Figure 5.4b, d). This was because the water content or water potential of CC residues on soil surfaces was strongly driven by RHair and wetting cycles (See Chapter 2,4). Based on these results, we conclude that the decomposition of CC residues in no-till systems was strongly moisture-limited; environmental conditions that keep CC residues moist for a longer duration will enhance its decomposition in no-till systems.

Residue decomposition rates: Effect of extrinsic or management (CC quantity and quality) factors

The *k*-values decreased logarithmically with increasing CC biomass (Adj. R^2=0.31, p<0.0001; Figure 5.5a). This was probably associated with the inverse relationship between CC quantity and quality in this study. With increasing CC biomass, C:N (r=0.38, p<0.0001), lignin:N (r=0.26, p<0.01), and residue holo-cellulose concentrations (r=0.37, p<0.0001) also increased (Figure 5.2b). However, easily decomposable residue carbohydrate concentrations decreased as biomass increased (r=-0.30, p<0.01; Figure 5.2b). These results indicate that CC residue

quality overrides quantity effects on k-values. Previous work using the same species of crop residue have also observed decrease in k-values with increase in residue quantity and have linked it to decreasing soil-residue contact (i.e. the proportion of biomass that is in direct contact with the underlying soil; Steiner et al., 1999; Stott et al., 1990; Thorburn et al., 2001). This is based on the hypothesis that surface residue decomposition is a spatially differentiated process; CC residue layer that is in contact with the soil undergoes rapid decomposition due to spatial proximity to soil microorganisms compared to the upper residue layer, which remain relatively undecomposed, but which gradually feeds the lower layer as it decomposes and becomes incorporated into soil organic matter (Findeling et al., 2007).

Our results further indicated that CC biomass could moderate the effect of climate on k-values (Figure 5.5a). Below 4000 kg ha^{-1}, the CC residue layer was probably not thick enough to substantially influence water content or water potential of the most actively decomposing residue layers at the soil-residue interface. Thus, we saw a clear effect of climate on k-values such that MD and PA (site-years with relatively higher RHair, number of rainy days, and cumulative rainfall) had higher k-values compared to low latitude site-years from NC (Figure 5.5a). However, at CC biomass > 4000 kg ha^{-1}, k-values remained relatively constant with no obvious inter-site differences. This was probably because the most actively decomposing lower residue layers were physically protected by the top residue layers and were less impacted by climate. In support to our findings, Williams et al. (2018) observed similar k-values while examining the decomposition of cereal rye residues ranging between 5000 to 15,000 kg ha^{-1}. Dietrich et al. (2019) also found no significant

differences in *k*-values of sugarcane residues ranging between 4000 to 12,000 kg ha^{-1}. Increasing CC residue quantity above 4000 kg ha^{-1} probably increased residue thickness in such a manner that the residue water content or water potential remained optimal for decomposition for prolonged periods at the soil-residue interface. Therefore, CC residue quantity has an antagonistic effect on *k*-values, that is the decrease in *k*-values due to decrease in soil-residue contact at higher biomass may have been compensated by the increase in *k*-values due to more conducive environmental conditions for decomposition at the soil-residue interface.

k-values decreased exponentially with increasing C:N (Adj. R^2=0.47, p<0.0001; Figure 5.5b). Although C:N is simply a representation of the proportion of C and N in crop residues and does not tell how these elements were distributed among different C fractions, the importance of C:N in crop residue decomposition has been historically documented (Jensen, 1929). Our results confirm prior CC decomposition studies showing that CC residues with high C:N decomposed slowly due to limited N availability to decomposing communities (Poffenbarger et al., 2015a). Among the variables considered, C:N showed the tightest relation with *k*-values and explained 47% of the variations in *k*-values, much higher than any other individual variables (Figures 5.3, 5.4, and 5.5). Similarly, C:N explained 94% of the total variance of the overall best model II considering only extrinsic factors (Table 5.3). Likewise, in the best model III containing both intrinsic and extrinsic factors, C:N explained 68% of the total model variance which was also higher than any other predictor variables in the model (Table 5.3). These results indicate that C:N has a dominant control on *k*-values in the mid-Atlantic and Southeastern US states.

Besides C:N, CC residue C chemistry also influenced *k*-values (Figure 5.5c, d). For example, the *k*-values increased with increasing non-structural carbohydrate concentrations in the initial CC residues (Adj. R^2=0.20, p<0.0001; Figure 5.5c), but decreased with increasing structural holo-cellulose concentrations (Adj. R^2=0.29, p<0.0001; Figure 5.5d). Holo-celluloses are complex C compounds present in the cell wall of crop residues that must undergo enzymatic breakdown before they can be degraded by microorganisms. Hence, they require more energy and are more resistant to decomposition than labile carbohydrates. Although lignin is a highly recalcitrant C constituent in CC tissues, we found no significant effect of residue lignin concentrations on *k*-values (Figure 5.5e). This was probably due to low range of lignin concentrations in the initial CC residues (Table 5.1). Since residue lignin concentrations increased as residue decomposes, it is likely that lignin control on decomposition will appear at later stages during which residue carbohydrate and holo-cellulose fractions were mostly decomposed. In our study, both N-related quality traits (C:N and lignin:N) significantly decreased *k*-values (Figure 5.5b, f). This implies that CC residue decomposition in no-till systems was limited by N availability; CC residues with high N concentrations decomposed faster compared to those with poor N concentrations.

Residue decomposition rates: Combined effect of intrinsic and extrinsic factors

Among three models considered, the combination of CC residue quality (C:N and residue holo-cellulose concentrations) and climatic (mean daily RHair and number of rainy days) variables provided the best empirical model for predicting *k*-

values for CC residue decomposition in no-till corn systems (Table 5.2 and 5.3). The overall best model III explained in total 70% of the variations in k-values. Results from commonality analysis further suggest that the majority of the explained variance by model III were commonly explained by CC residue quality and climatic variables (Table 5.3). The unique contribution of each predictor variable to model total variance was less than 13%. Based on beta and structure coefficients, CC residue quality and climatic variables had an inverse regression effect on k-values, i.e. k-values were negatively impacted by C:N and residue holo-cellulose concentrations, but were positively impacted by mean daily RHair and number of rainy days. Moreover, our study suggests that the relative importance of these variables in predicting k-values decreased in the order: C:N > residue holo-cellulose concentrations = mean daily RHair > number of rainy days. Therefore, we conclude that CC residue quality has a dominant effect on k-values than does climate in the mid-Atlantic and Southeastern US states.

Conclusions

Our inter-site litter bag studies provided new insights on the factors controlling CC residue decomposition in no-till corn systems in the mid-Atlantic and Southeastern US states. The k-values increased along the latitudinal gradient. As latitude increases, climatic variables that keep CC surface residues moist for prolonged periods also increase. Among climatic variables, the mean daily RHair and number of rainy days had stronger influence on k-values than cumulative rainfall. These results indicate faster decomposition of CC surface residues in humid environments and in site-years with more frequent rain events. Mean daily air

temperature, on the other hand, had no significant effect on *k*-values. A clear separation of *k*-values between low and high latitude sites were observed at CC biomass < 4000 kg ha^{-1}, above which the inter-site differences on *k*-values caused by climate were less obvious. Above 4000 kg ha^{-1}, as CC residue thickness increased, the top residue layers likely maintained the optimal water content for decomposition at the soil-residue interface for a longer duration, thereby compensating for the decrease in *k*-values due to decrease in the proportion of biomass that is in contact with the soil. We further demonstrated that the *k*-values decreased with C:N, residue holo-cellulose concentrations, and lignin:N, but increased with residue carbohydrate concentrations. All these results suggest that CC surface residue decomposition in no-till corn systems was limited by moisture and N availability to decomposing microorganisms. The overall best model that has CC C:N and residue holo-cellulose concentrations as quality variables and mean daily RHair and number of rainy days as climatic variables provided the best predictive model for *k*-values (70% variance explained). This empirical model can be used to predict longevity of CC residues in no-till corn systems and assist farmers and land managers with CC residue management decisions to better achieve targeted agroecosystem services under present and future climate change scenarios. Results further suggest that CC residue quality has greater control over *k*-values than does climate in the mid-Atlantic and Southeastern US states. Based on our findings, we conclude that residue C chemistry (residue holo-cellulose concentrations) and climatic (RHair and rainy days) variables, not commonly considered in CC residue decomposition models, controlled *k*-values.

Thus, currently available proceed-based or mechanistic models predicting CC surface residue decomposition in no-till systems need updating.

Acknowledgements

This research is part of a regional collaborative project supported by the USDA Natural Resources Conservation Services (Conservation Innovation Grant # 8042-21660-004-36-R) and the USDA National Institute of Food and Agriculture (Award # 2018- 68011-28372). The first author (Resham Thapa) is also grateful to the Northeast Sustainable Agriculture Research and Education (SARE) graduate student grant (Award # GNE17-160-31064). Special thanks to Ethan Sweep, Alondra Thompson, Esleythor Henriquez Inoa, many other research technicians, research interns, and extension personnel involved in this multi-state on-farm cover crop decomposition studies. Our sincere thanks to all participating farmers who voluntarily participated in this research. We also thank Dr. Matthew H. Kramer (Statistician, USDA-ARS, Beltsville) for his statistical advice.

Tables and Figures

Table 5.1 Summary statistics of the intrinsic (latitude, soil, and climate) and extrinsic or management (cover crop quantity and quality) factors controlling cover crop (CC) residue decomposition rates in the mid-Atlantic and Southeast US states.

Factors or variables of interest		Measured variables	Units	n	Mean	SD	Median	Min	Max
A. Intrinsic factors	Geographic	Latitude	°	105	37.4	2.3	38.8	32.6	40.7
	Soil	Sand	%	105	47.3	23.7	48.2	6.6	88.4
		Clay	%	105	16.5	7.4	16.0	4.2	38.2
	Climate†	Mean daily air temperature	°C	105	19.6	3.0	19.9	14.0	25.5
		Cumulative rainfall	mm	105	231.7	67.8	228.4	104.1	366.3
		Mean daily RHair	%	105	76.2	3.0	76.5	69.4	81.2
		Number of rainy days	-	105	27.9	5.87	28	16	41
B. Extrinsic factors	Cover crop quantity	Biomass	kg ha^{-1}	105	2,942	2,037	2,561	171	10,595
	Cover crop quality	C:N	-	105	22.5	9.5	21.8	6.6	60.9
		Carbohydrate	%	103	43.0	10.2	44.0	22.7	63.0
		Holo-cellulose	%	103	47.7	9.6	48.2	28.6	67.5
		Lignin	%	103	4.6	1.8	4.9	1.1	8.6
		Lignin:N	-	103	2.5	1.7	2.1	0.4	9.3
C. Dependent variable	Decay rate constant	k-value‡	day^{-1}	105	0.015	0.006	0.014	0.005	0.033

† Climate variables were summarized for the first 0-60 days since cover crop (CC) termination. RHair represents relative humidity of the air.

‡ The *k*-value represents the single-pool first-order decay rate constants.

Table 5.2 Model statistics of the best model predicting cover crop (CC) residue decomposition rates, i.e. k-value based on stepwise regression procedure. See Table 5.3 for parameter estimates and commonality coefficients for the predictor variables.

Model	Predictors (X_i)	F-value	P_r(>F)	R^2	Adj. R^2	BIC[†]
I. Intrinsic factors only (Latitude, Soil, and Climate)	Mean daily RHair; Number of rainy days	27.7	<0.0001	0.352	0.339	-212.0
II. Extrinsic or management factors only (Cover crop quantity and quality)	C:N; % Carbohydrate	50.8	<0.0001	0.504	0.494	-233.4
III. Both Intrinsic and Extrinsic factors	C:N; % Holo-cellulose; Mean daily RHair; Number of rainy days	56.7	<0.0001	0.698	0.686	-275.3

[†] BIC represents Bayesian Information Criterion. Model with the lowest BIC value were selected and presented here.

Table 5.3 Parameter estimates and commonality coefficients for the best regression model predicting cover crop (CC) residue decomposition rates, i.e. *k*-value, as presented in Table 5.2.

Model	Predictors (X_i)	Parameter estimates[†]					Commonality analysis[‡]					
		β	SE	Std. β	t-value	Pr(>|t|)	r_s	r_s^2	Unique	Common	Simple r^2	Unique as % of total variance
I. Intrinsic factors only (Latitude, Soil, and Climate)	Intercept	-9.561	0.866		-11.04	<0.0001						
	Mean daily RHair	6.115	1.177	0.431	5.193	<0.0001	0.871	0.758	0.171	0.095	0.267	48.76
	No. of rainy days	0.022	0.006	0.304	3.656	<0.001	0.716	0.512	0.085	0.095	0.180	24.17
II. Extrinsic or management factors only (Cover crop quantity and quality)	Intercept	-4.042	0.191		-21.22	<0.0001						
	C:N	-0.027	0.004	-0.602	-7.720	<0.0001	-0.967	0.936	0.296	0.176	0.472	58.68
	% Carbohydrate	0.008	0.003	0.199	2.554	<0.05	0.643	0.413	0.032	0.176	0.208	6.43
III. Both Intrinsic and Extrinsic factors	Intercept	-6.605	0.709		-9.314	<0.0001						
	Mean daily RHair	3.537	0.905	0.241	3.907	<0.0001	0.648	0.420	0.047	0.246	0.293	6.73
	No. of rainy days	0.025	0.005	0.348	5.431	<0.0001	0.509	0.259	0.091	0.090	0.181	13.01
	C:N	-0.015	0.003	-0.330	-4.469	<0.0001	-0.822	0.675	0.062	0.410	0.472	8.81

	% Holo-cellulose	-0.016	0.003	-0.354	-4.757	<0.0001	-0.652	0.425	0.070	0.227	0.296	9.98

† β and Std. β represents beta-coefficients and standardized beta-coefficients for the predictor variables, respectively. SE represents standard error for the beta-coefficients.

‡ r_s represents structure coefficients. The squared structure coefficients (r_s^2) denotes the total effect of each predictor on the dependent variable and is equivalent to the ratio of simple r^2 to model total variance, i.e. R^2. Commonality analysis partitions the model R^2 into variance that is unique to each predictor and variance that is commonly shared by all possible subsets of predictors.

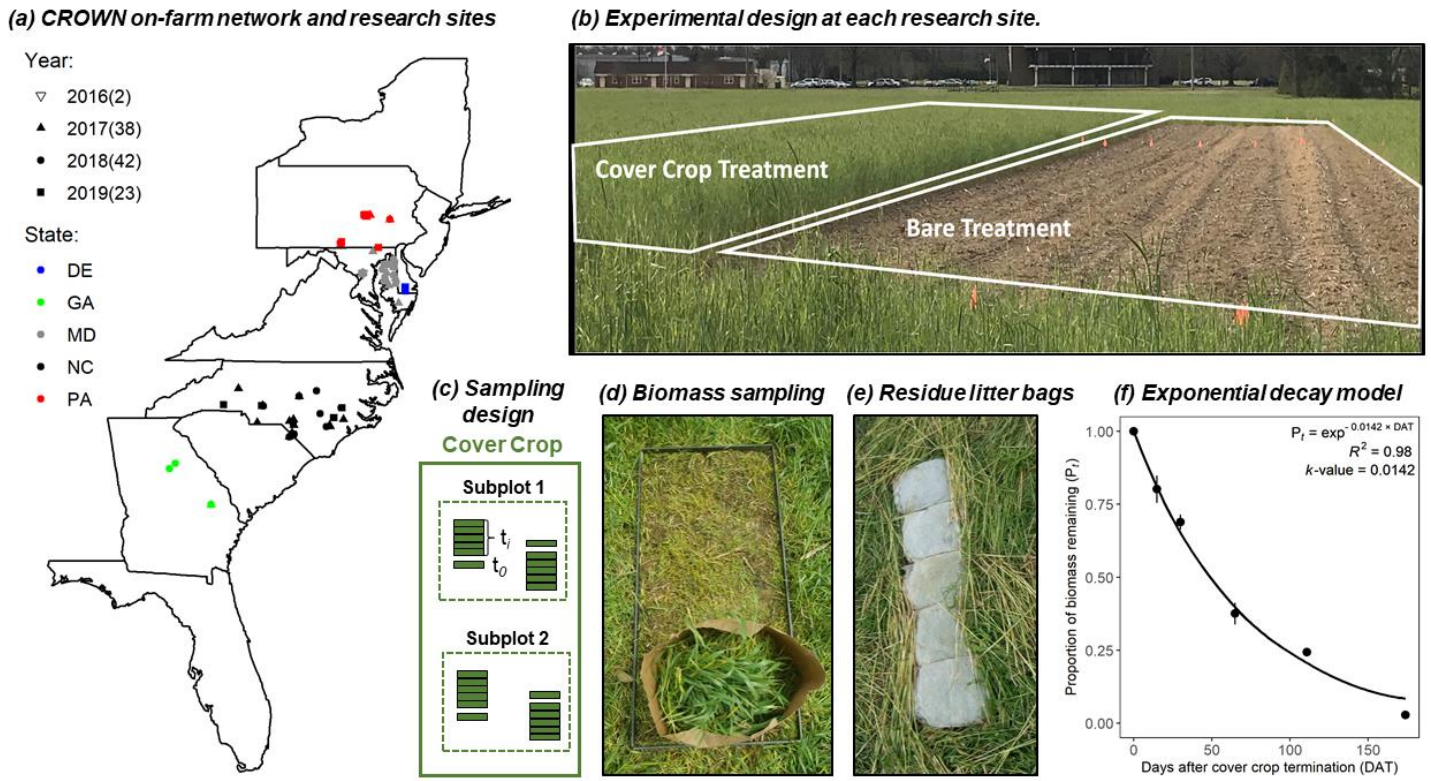

Figure 5.1 Illustrations of on-farm network of cover crop (CC) adopters and experimental methodology for the inter-site litter bag decomposition studies. (a) Spatial map of the experimental sites, enrolled in Cover Crops: Real time Observation of Water and Nutrients (CROWN) project, with corn as subsequent cash crop. Number in parenthesis represents the number of experimental sites in each year. Methods: (b) Field site with CC and bare soil as adjacent strip plots, (c) Sampling design showing two subplots and two sets of six litter bags in each subplot, (d) Cover crop biomass sampling using quadrants, (e) Deployment of remaining five litter bags on the soil surface, and (f) Example of single-pool first-order exponential decay model to determine decay rate constants (k-value) for each site-year.

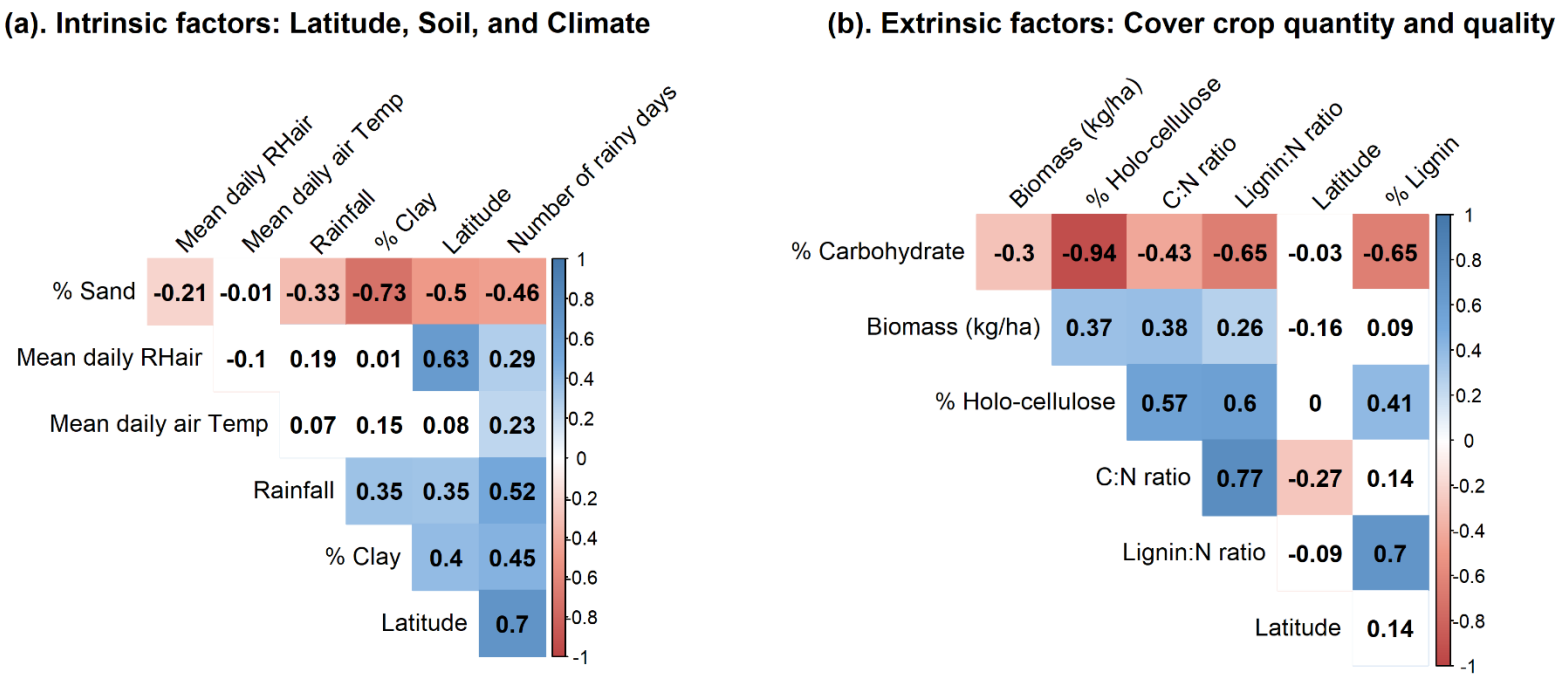

Figure 5.2 Correlation matrix showing the association among (a) intrinsic and (b) extrinsic or management factors. Numbers represent the correlation coefficients. Note: correlation coefficients that showed significant association between variables ($p<0.05$) were shaded with colors.

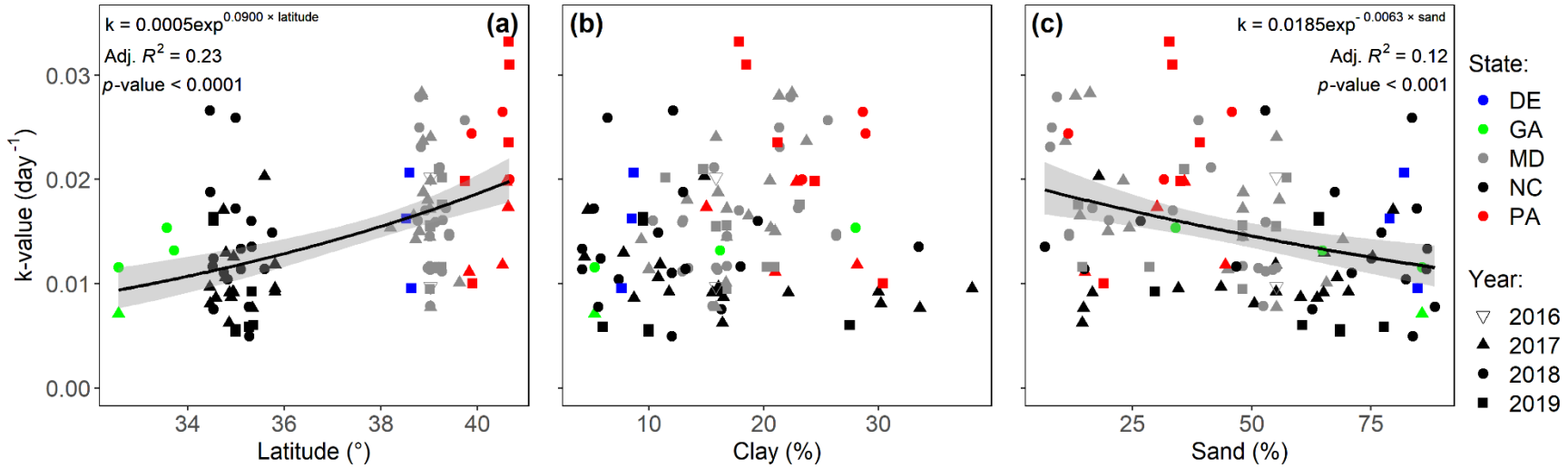

Figure 5.3 The cover crop (CC) decomposition rates, i.e. *k*-values in relation to geographic and soil factors: (a) Latitude, (b) Clay, and (c) Sand content at the experimental site. The solid line represents a significant relationship, and the grey band represents the 95% confidence interval. Different colors and shapes represents different state and experimental year, respectively.

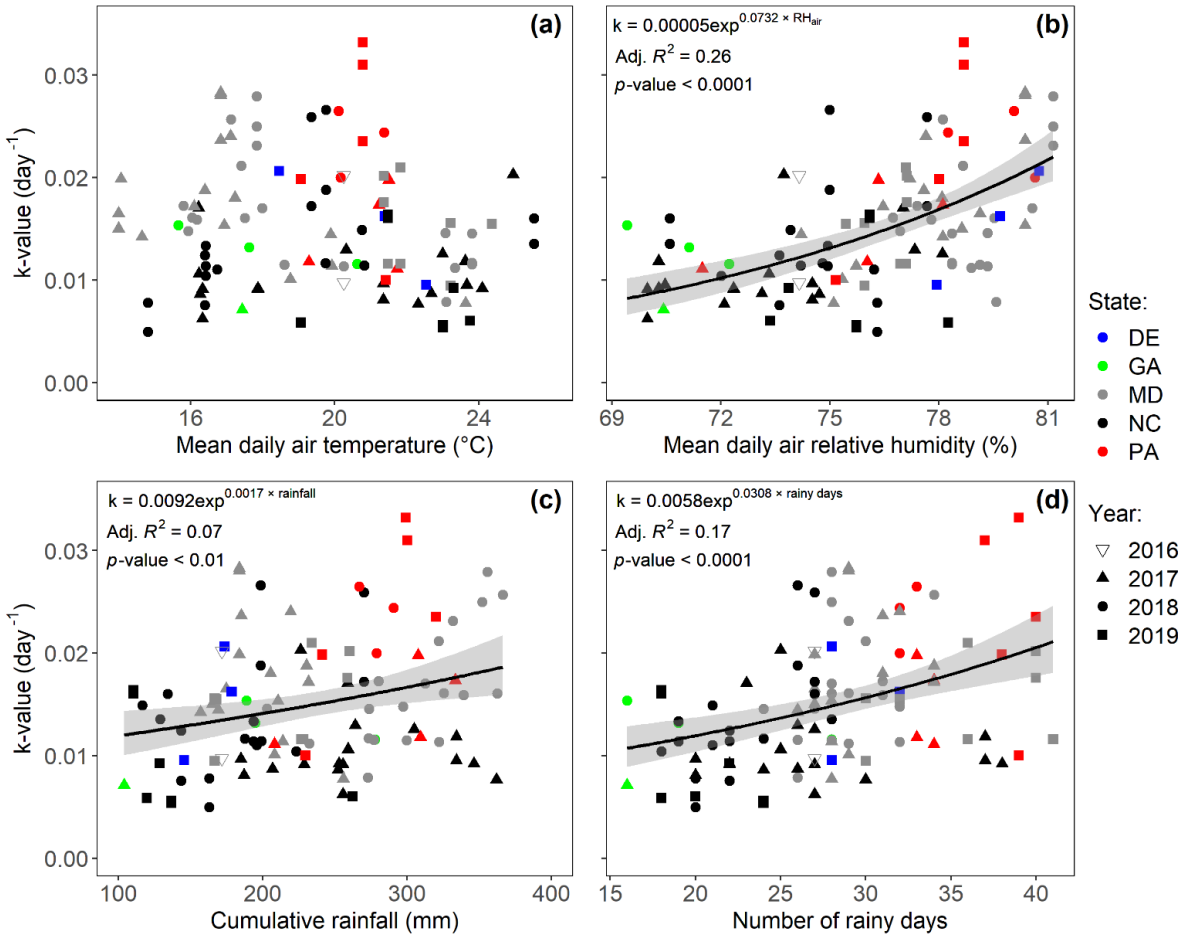

Figure 5.4 The cover crop (CC) decomposition rates, i.e. *k*-values in relation to climatic factors: (a) Mean daily air temperature, (b) Mean daily relative humidity of the air (RHair), (c) Cumulative rainfall, and (d) Number of rainy days. Climatic variables were summarized for the first 60 days since CC termination. The solid line represents a significant relationship, and the grey band represents the 95% confidence interval. Different colors and shapes represents different state and experimental year, respectively.

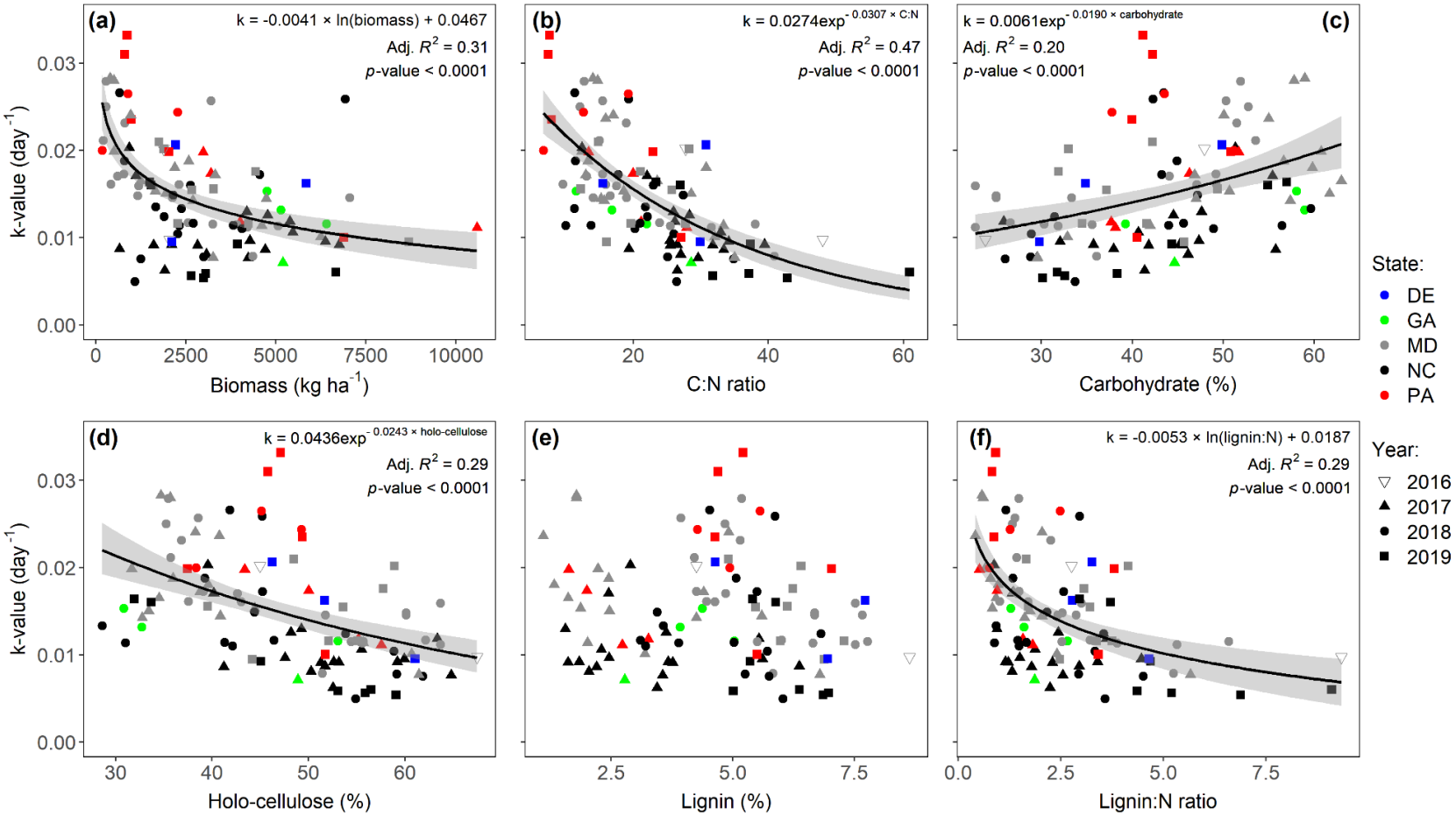

Figure 5.5 The cover crop (CC) decomposition rates, i.e. *k*-values in relation to extrinsic or management factors: (a) CC quantity or biomass, (b) C/N, (c) residue carbohydrate concentrations, (d) residue holo-cellulose concentrations, (e) residue lignin concentrations, and (f) lignin/N. The solid line represents a significant relationship, and the grey band represents the 95% confidence interval. Different colors and shapes represents different state and experimental year, respectively.

Chapter 6: Conclusion

The overall goal of this study was to tighten N cycling within soil-crop systems by improving our understanding on the decomposition and N mineralization kinetics from cover crop (CC) residues left on the soil surface in conservation tillage-based corn (*Zea mays* L.) production systems in the mid-Atlantic and Southeastern US states. To do so, experiments at varying temporal (diurnal to seasonal) and spatial (laboratory to regional) scales were performed to elucidate the relative impact of various factors controlling surface CC residue decomposition in conservation tillage systems.

Cover crop residue layers left on the soil surface are directly exposed to solar radiation, wind, dew, and rainfall in conservation tillage systems. In a series of diurnal experiments, I found that the moisture (θ_g) or water potential ($\psi_{residue}$) of the residue layer fluctuate more dramatically and dynamically at a diurnal scale in response to changes in water potential gradient between the residue and the air above it. The rate of residue decomposition also showed distinct diurnal patterns that were closely linked to diurnal fluctuations in residue θ_g or $\psi_{residue}$. However, moisture becomes limited at elevated temperatures reducing residue decomposition rates in conservation tillage fields. As decomposition progressed, the water retention properties of CC residues decreased due to increase in residue lignin concentrations. Therefore, less and less rainwater will be intercepted by surface CC residues as they decompose in the fields. Based on these results, the existing residue decomposition models (i.e., CERES-N) should consider both diurnal variations in $\psi_{residue}$ and changes in residue water retention properties as residues decomposes. Researchers

should develop a simplistic model that can simulate $\psi_{residue}$ using easily available weather variables such as the air relative humidity, air temperature, and rainfall.

Improving the capability of CERES-N sub-model to accurately predict decomposition and N mineralization from surface CC residues will also require adjustments of first-order decay rate constants based on residue environment ($\psi_{residue}$ and temperature). In a controlled microcosm experiment, I found that the temporal dynamics in C and N mineralized from surface-applied CC residues were adequately described by the first-order rate kinetic models. Two-dimensional response surface equations, which included $\psi_{residue}$ and temperature as variables, were developed to mathematically describe the integrative effects of these variables on C and N mineralization from surface-applied CC residues. These equations were integrated into the existing CERES-N sub-model; calibration and validation of the integrated CERES-N sub-model is on-going.

Our second controlled microcosm experiment investigating the effect of dry-wet cycles also highlighted the importance of residue water dynamics on regulating C and N mineralization from CC residues. As compared to surface-applied CC residues, incorporated residues decomposed quickly and subsequently, more N was either mineralized or immobilized depending on residue type. I found that CC residues when incorporated maintained water content for a longer duration during the drying phase and were more colonized by soil prokaryotes and saprophytic fungi. Residue management also influenced soil and residue microbiota. While soils amended with crimson clover residues (N-rich soil environments) were dominated by copiotrophs, oligotrophs dominated cereal rye-amended soils (N-poor soil environments). Residue

location may have a greater effect than residue type in determining residue microbiota. I found that fungi can effectively colonize both surface-applied and incorporated CC residues. Prokaryotes, on the other hand, colonized incorporated residues more effectively than surface-applied residues. While soil and residue microbiota were differentially affected by residue management, the effect of residue location on C and N mineralization was primarily explained by differences in residue water dynamics between surface-applied and incorporated CC residues.

In the mid-Atlantic and Southeastern US, the rate at which CC residues decomposes (i.e., k-values) in conservation tillage fields increased along the latitudinal gradient. As latitude increases from GA to PA, climatic variables that keeps surface CC residues moist for prolonged periods also increased, enhancing residue decomposition rates. I found that the surface CC residues decomposes faster in humid environments and in years with more frequent rain events. The k-values decreased with increasing biomass, C:N, residue holo-cellulose concentrations, and lignin:N (metrics of low quality), but increased with increasing residue carbohydrate concentrations (metrics of high quality). The empirical model, that has both CC quality (C:N and residue holo-cellulose concentrations) and climatic (mean daily relative humidity of the air and number of rainy days) variables, developed in this study can be used to determine k-values and hence, the longevity of surface CC residues in conservation tillage-based crop production systems.

The research presented in this dissertation indicated that the persistence of surface CC residues in conservation tillage systems depends on the rate of decomposition which in turn is influenced by residue quality (C:N, residue C

chemistry), climate (residue θ_g or $\psi_{residue}$ and temperature), and the activity of decomposer communities. Various insights were made that will be key to improving the performance of existing decision support tool (i.e. *Cover Crop N Availability Calculator* which is based on the CERES-N sub-model) in accurately predicting the decomposition and N mineralization from surface CC residues in conservation tillage-based crop production systems. Once such tools are well-calibrated and well-validated, they can be used to make evidence-based management recommendations to farmers. Thus, this work will help to optimize provisioning of agroecosystem services with CCs in conservation tillage-based crop production systems.

Appendices

Table A1. Loading values for the minimum number of components obtained by partial least squares (pls) regression analysis based on cross-validation technique. The pls analysis was performed between naturally log-transformed k-values, i.e. $ln(k)$ and intrinsic or extrinsic factors independently.

(a) Intrinsic factors			(b) Extrinsic factors		
Predictors (x)	Loadings from (pls1)		Predictors (x)	Loadings from (pls2)	
	Comp 1	Comp 2		Comp 1	Comp 2
Latitude (°)	0.539		Biomass (kg ha^{-1})	-0.294	-0.341
% Sand	-0.412	0.308	C:N ratio	-0.451	-0.426
% Clay	0.324	-0.563	% Carbohydrate	0.462	-0.385
Rainfall (mm)	0.348	-0.209	% Holo-cellulose	-0.480	0.116
Number of rainy days	0.470	-0.244	% Lignin	-0.298	0.733
Mean daily air temp (°C)		-0.559	Lignin:N ratio	-0.481	0.154
Mean daily RHair (%)	0.415	0.474			
SS loadings	1.079	1.053	SS loadings	1.055	1.020
Proportion variance	0.154	0.150	Proportion variance	0.176	0.170
Cumulative variance	0.154	0.305	Cumulative variance	0.176	0.346

Table A2. Results of multiple linear regression analysis that considered both main and interaction effects of intrinsic and extrinsic or management factors on naturally log-transformed k-values, i.e. $ln(k)$. The effects of intrinsic and extrinsic factors were represented by scores calculated based on loading values for each partial least square (pls) components retained in Table A1.

Coefficients†	Estimate	Std. Error	t-value	Pr(>|t|)	Significance
(Intercept)	-4.282	0.031	-137.76	< 2e-16	***
scores(pls1)[, 1]	0.109	0.019	5.851	7.42e-08	***
scores(pls1)[, 2]	0.012	0.029	0.414	0.6801	
scores(pls2)[, 1]	0.127	0.018	7.123	2.29e-10	***
scores(pls2)[, 2]	0.066	0.028	2.369	0.0199	*
scores(pls1)[, 1]:scores(pls1)[, 2]	0.016	0.020	0.817	0.4162	
scores(pls1)[, 1]:scores(pls2)[, 1]	-0.008	0.011	-0.684	0.4955	
scores(pls1)[, 1]:scores(pls2)[, 2]	-0.003	0.017	-0.145	0.8851	
scores(pls1)[, 2]:scores(pls2)[, 1]	0.000	0.013	-0.019	0.9851	
scores(pls1)[, 2]:scores(pls2)[, 2]	-0.013	0.027	-0.464	0.6436	
scores(pls2)[, 1]:scores(pls2)[, 2]	0.015	0.019	0.768	0.4442	

Signif. codes: 0 ‘***’ 0.001 ‘**’ 0.01 ‘*’ 0.05 ‘.’ 0.1 ‘ ’ 1

Residual standard error: 0.2606 on 92 degrees of freedom

Multiple R-squared: 0.6678, Adjusted R-squared: 0.631

F-statistic: 8.49 on 10 and 92 DF, p-value: 2.20e-16

†pls1 and pls2 represents the intrinsic and extrinsic factors, respectively. Numbers within the big brackets followed by commas represents the pls components 1 or 2. There were two pls components each representing intrinsic (pls1) and extrinsic (pls2) factors, respectively.

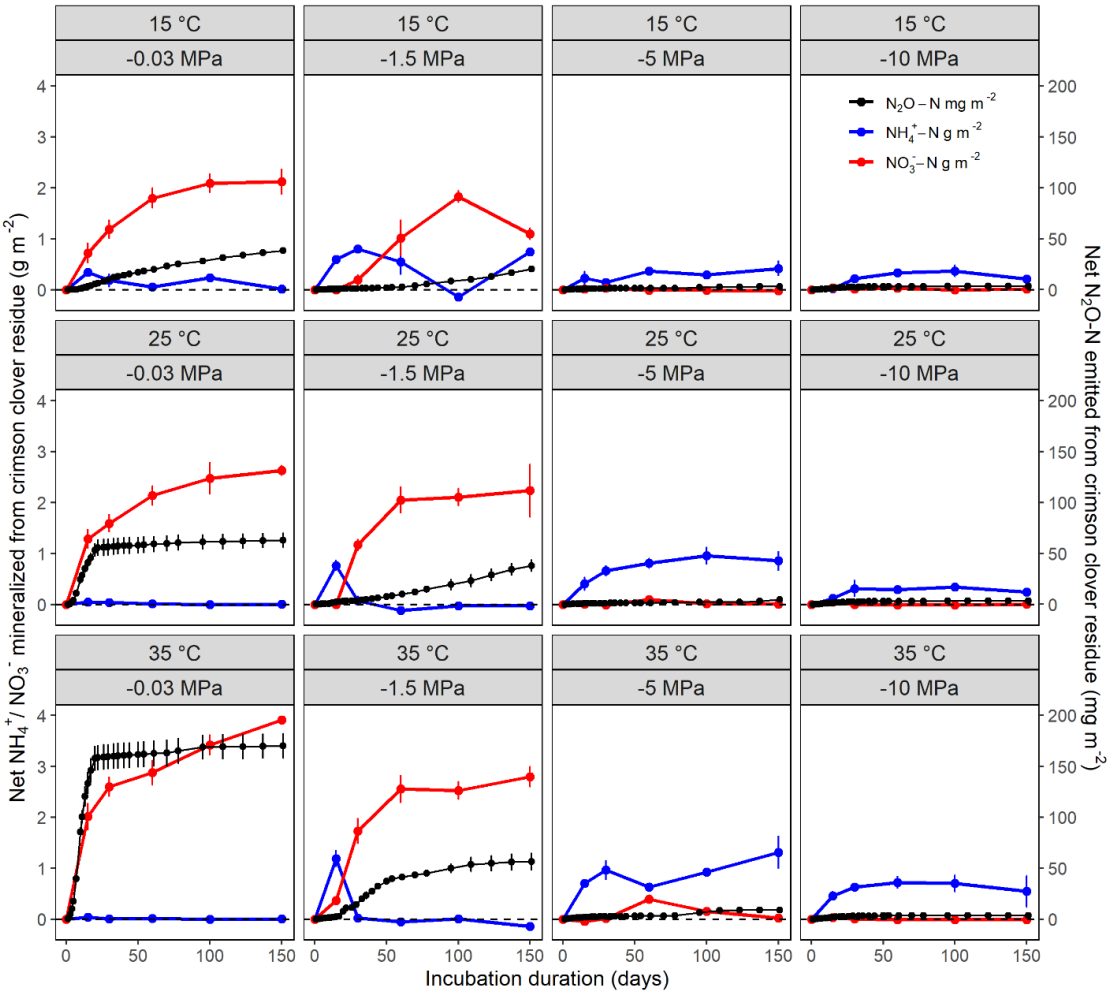

Figure A1 Temporal dynamics of soil inorganic N (NH_4^+-N and NO_3^--N) and nitrous oxide (N_2O) emitted from surface-applied crimson clover residues during a 150-d incubation experiment at different residue water potential ψ (MPa) and temperature T (°C).

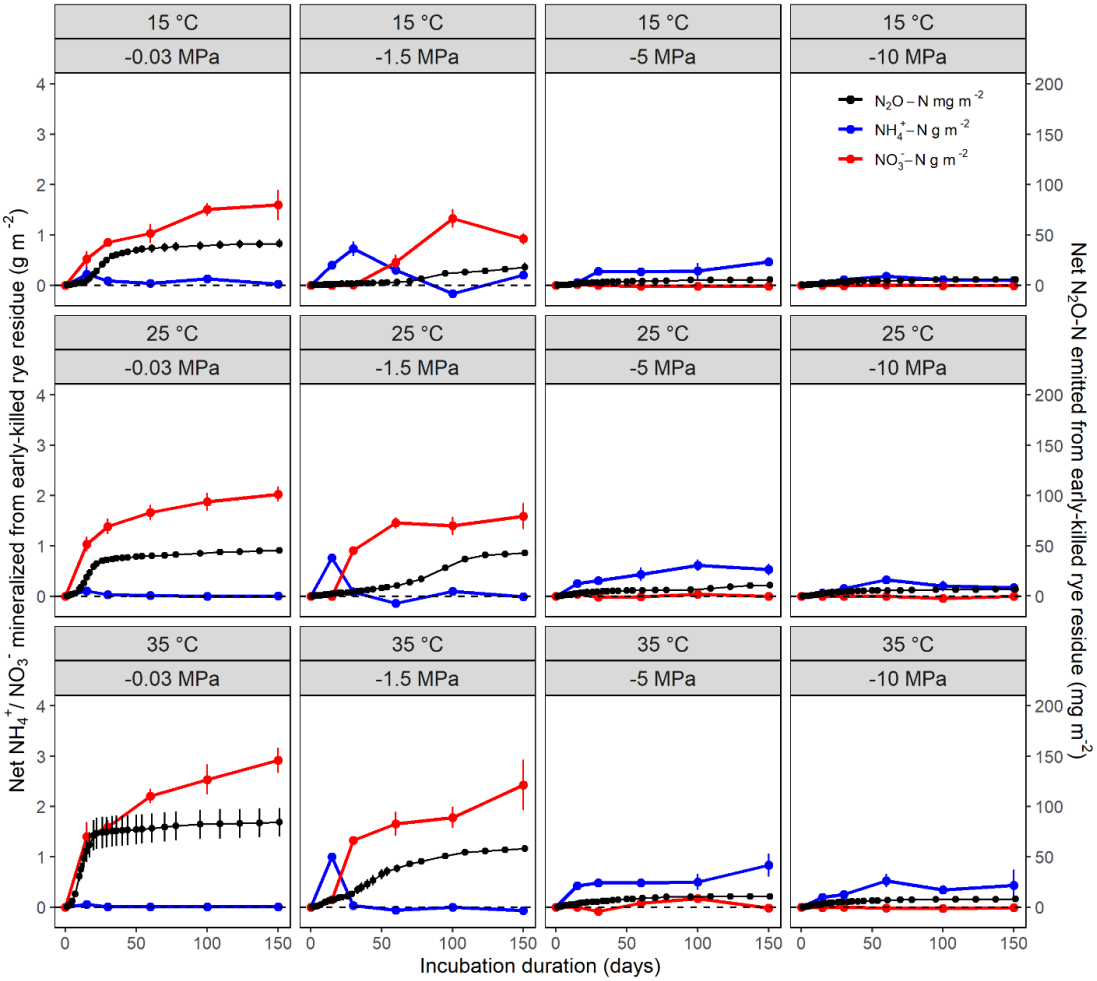

Figure A2 Temporal dynamics of soil inorganic N (NH_4^+-N and NO_3^--N) and nitrous oxide (N_2O) emitted from surface-applied early-killed cereal rye residues during a 150-d incubation experiment at different residue water potential ψ (MPa) and temperature T (°C).

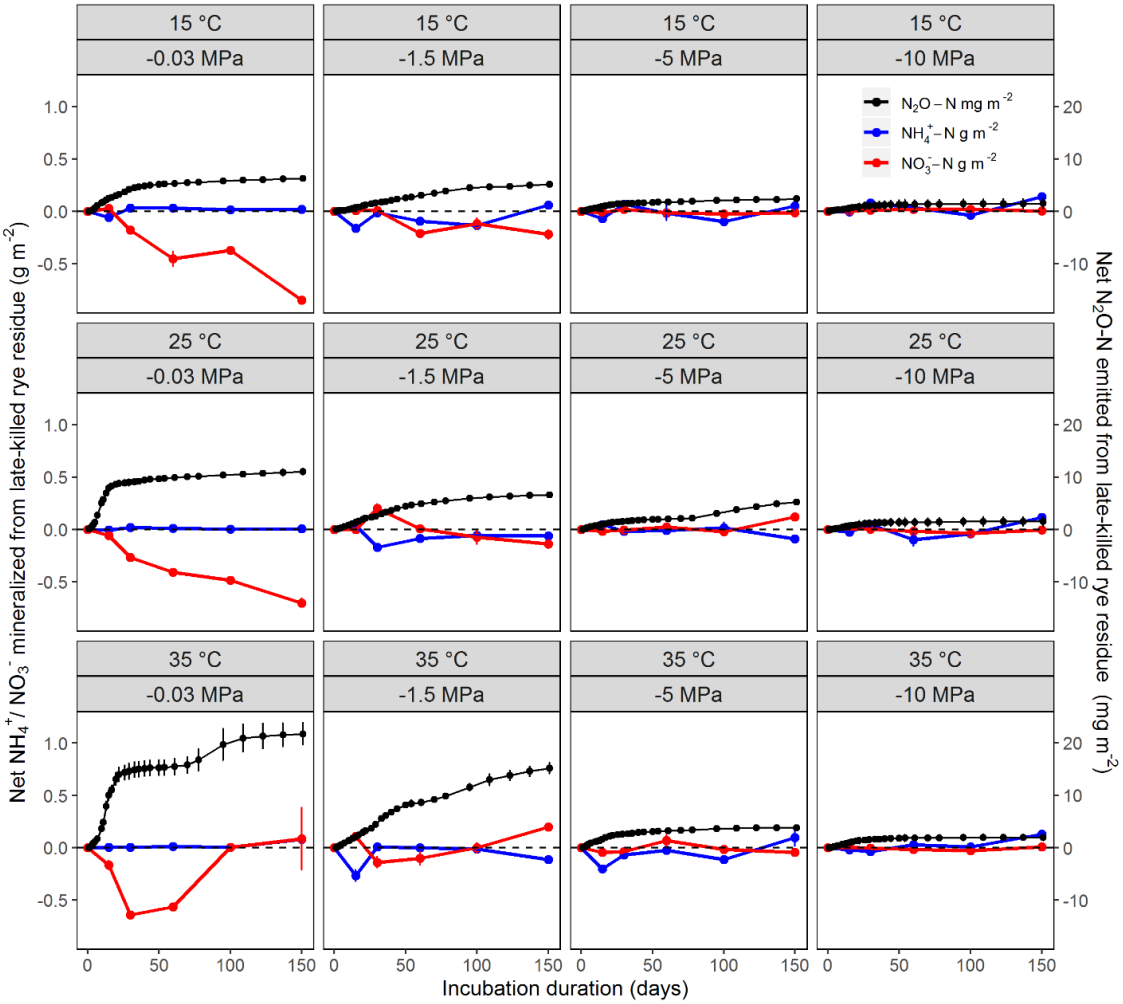

Figure A3 Temporal dynamics of soil inorganic N (NH_4^+-N and NO_3^--N) and nitrous oxide (N_2O) emitted from surface-applied late-killed cereal rye residues during a 150-d incubation experiment at different residue water potential ψ (MPa) and temperature T (°C).

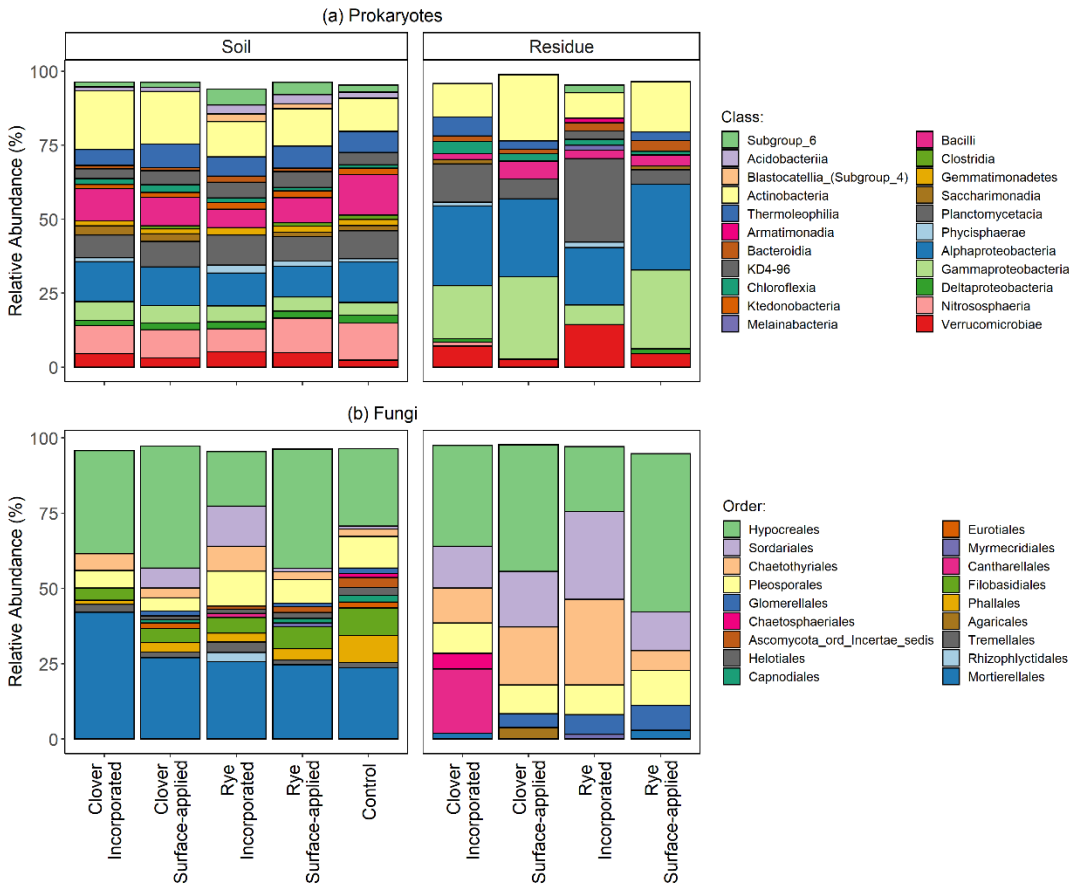

Figure A4 Relative abundances of (a) prokaryotic community at the class rank and (b) fungal community at the order rank for the soil and residue samples, respectively. Rare taxa with abundance less than 1% were excluded.

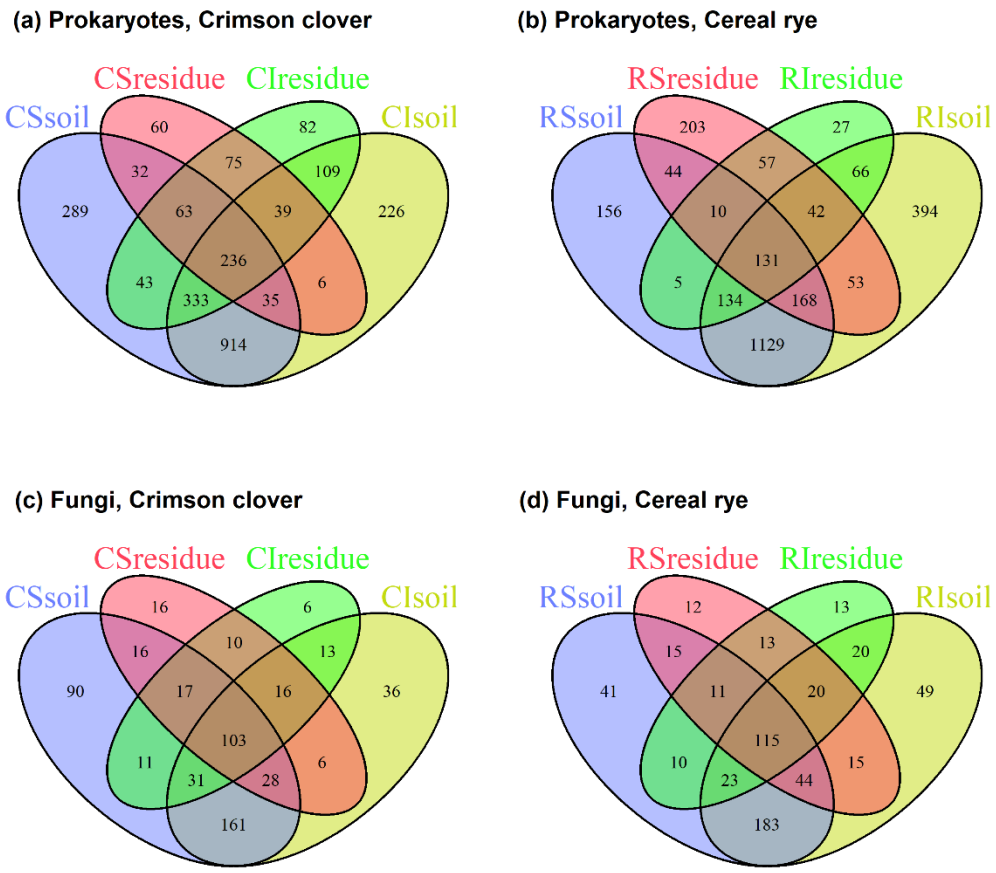

Figure A5 Venn diagram showing the number of shared and unique amplicon sequence variants (ASV) between soil and residue samples for each cover crop residue treatments: (a) Prokaryotes, Crimson clover; (b) Prokaryotes, Cereal rye; (c) Fungi, Crimson clover; and (d) Fungi, Cereal rye. Treatments were abbreviated for clear representation in the plots: C- Clover, R- Rye, S- Surface-applied, I- Incorporated.

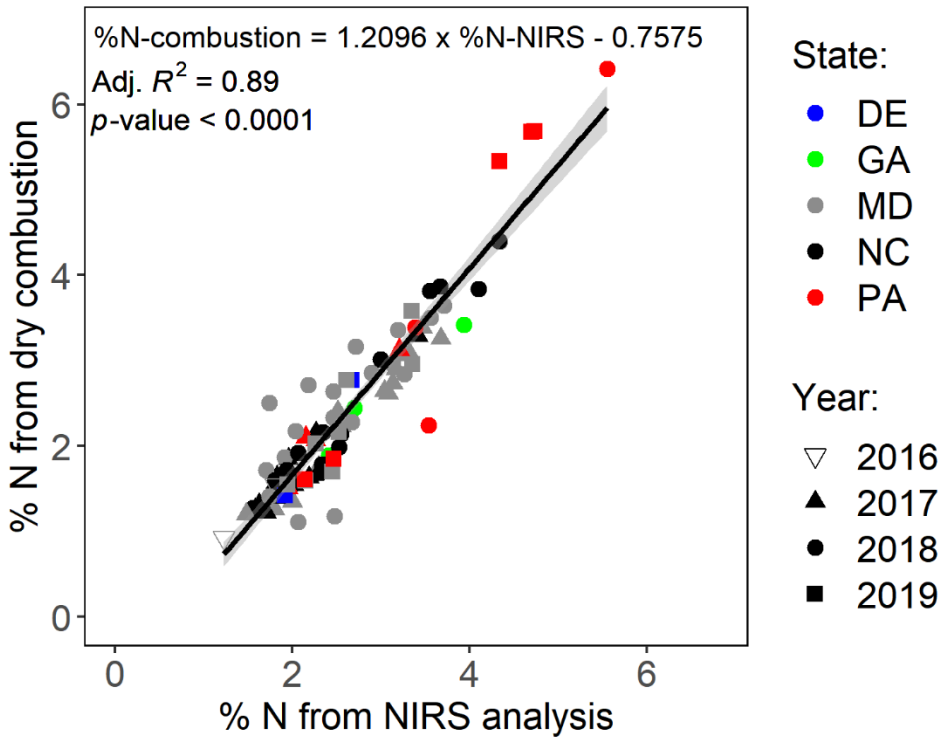

Figure A6 Relationship between cover crop (CC) residue N concentrations determined via dry combustion analysis with that estimated via near infra-red reflectance spectroscopy (NIRS) technique. The solid line represents a significant linear relationship, and the grey band represents the 95% confidence interval. Different colors and shapes represents different state and experimental year, respectively.

Bibliogrpahy

Aerts, R. 1997. Climate, leaf litter chemistry and leaf litter decomposition in terrestrial ecosystems: a triangular relationship. Oikos 79:439-449.

Alonso-Ayuso, M., J.L. Gabriel, and M. Quemada. 2014. The kill date as a management tool for cover cropping success. PLoS One 9(10):e109587–e12. doi:10.1371/journal.pone.0109587

Banerjee, S., C.A. Kirkby, D. Schmutter, A. Bissett, J.A. Kirkegaard, and A.E. Richardson. 2016. Network analysis reveals functional redundancy and keystone taxa amongst bacterial and fungal communities during organic matter decomposition in an arable soil. Soil Biology and Biochemistry 97: 188-198.

Bastian, F., L. Bouziri, B. Nicolardot, and L. Ranjard. 2009. Impact of wheat straw decomposition on successional patterns of soil microbial community structure. Soil Biology and Biochemistry 41 (2): 262-275.

Birch, H.F. 1958. The effect of soil drying on humus decomposition and nitrogen. Plant and Soil 10: 9-31.

Birch, H.F. 1964. Mineralization of plant nitrogen following alternate wet and dry conditions. Plant and Soil 20: 43-49.

Borken, W., E.A. Davidson, K. Savage, J. Gaudinski, and S.E. Trumbore. 2003. Drying and wetting effects on carbon dioxide release from organic horizons. Soil Science Society of America Journal 67(6): 1888-1896.

Bristow, K.L. 1988. The role of mulch and its architecture in modifying soil temperature. Aust. Journal of Soil Research 26, 269-80.

Bristow, K.L., and G.G. Campbell. 1986. Simulation of heat and moisture transfer through a surface residue-soil system. Agricultural and Forest Meteorology 36, 193-214.

Cabrera, M.L., D.E. Kissel, and M.F. Vigil. 2005. Nitrogen mineralization from organic residues: research opportunities. Journal of Environmental Quality 34:75-79.

Calcium chloride handbook. 2003. A guide to properties, forms, storage and handling. The Dow Chemical Company. 2003.

Callahan, B.J., P.J. McMurdie, M.J. Rosen, A.W. Han, A.J.A. Johnson, and S.P. Holmes. 2016. DADA2: High-resolution sample inference from Illumina

amplicon data. Nature Methods 13: 581-583. (URL:https://doi.org/10.1038/nmeth.3869).

Caporaso, J.G., C.L. Lauber, W.A. Walters, D. Berg-Lyons, C.A. Lozupone, P.J. Turnbaugh, N. Fierer, and R. Knight. 2011. Global patterns of 16S rRNA diversity at a depth of millions of sequences per sample. Proceedings of the National Academy of Sciences USA. 108: 4516-4522.

Chen, H. 2018. VennDiagram: Generate High-Resolution Venn and Euler Plots. R package version 1.6.20. https://CRAN.R-project.org/package=VennDiagram

Cheneby, D., D. Bru, N. Pascault, P.A. Maron, L. Ranjard, and L. Philippot. 2010. Role of plant residues in determining temporal patterns of the activity, size, and structure of nitrate reducer communities in soil. Applied Environmental Microbiology 76 (21): 7136-7143.

Clocchiatti, A., S.E. Hannula, M. van den Berg, G. Korthals, and W. de Boer. 2020. The hidden potential of saprotrophic fungi in arable soil: Patterns of short-term stimulation by organic amendments. Applied Soil Ecology 147: 103434.

Coppens, F., P. Garnier, A. Findeling, R. Merckx, and S. Recous. 2007. Decomposition of mulched vs. incorporated crop residues: Modelling with PASTIS clarifies interactions between residue quality and location. Soil Biology and Biochemistry 39: 2339-2350. doi:10.1016/j.soilbio.2007.04.005.

Coppens, F., P. Garnier, S. De Gryze, R. Merckx, and S. Recous. 2006. Soil moisture, carbon and nitrogen dynamics following incorporation and surface application of labelled crop residues in soil columns. European Journal of Soil Science 57(6): 894-905.

Corbeels, M., A.M. O'Connell, T.S. Grove, D.S. Mendham, and S.J. Rance. 2003. Nitrogen release from eucalypt leaves and legume residues as influenced by their biochemical quality and degree of contact with soil. Plant and Soil 250(1): 15-28.

Curtin, D., F. Selles, H. Wang, C.A. Campbell, and V.O. Biederbeck. 1998. Carbon dioxide emissions and transformation of soil carbon and nitrogen during wheat straw decomposition. Soil Science Society of America Journal 62(4): 1035-1041.

Dabney, S.M. 1998. Cover crop impacts on watershed hydrology. Journal of Soil and Water Conservation 53: 207-13.

Dabney, S.M., J.A. Delgado, and D.W. Reeves. 2001. Using winter cover crops to improve soil and water quality. Communication in Soil Science and Plant Analysis 37: 1221-1250.

Davis, A.S., and G.B. Frisvold. 2017. Are herbicides a once in a century method of weed control? Pest Management Sciences 73(11): 2209-20.

Detheridge, A.P., G. Brand, R. Fychan, F.V. Crotty, R. Sanderson, G.W. Griffith, and C.L. Marley. 2016. The legacy effect of cover crops on soil fungal populations in a cereal rotation. Agriculture, Ecosystems and Environment 228: 49-61.

Dietrich, G., S. Recous, P.L. Pinheiro, D.A. Weiler, A.L. Schu, M.R.L. Rambo, and S.J. Giacomini. 2019. Gradient of decomposition in sugarcane mulches of various thickness. Soil and Tillage Research 192:66-75.

Erisman, J.W., M.A. Sutton, J. Galloway, Z. Klimont, and W. Winiwarter. 2008. How a century of ammonia synthesis changed the world. Nature Geosciences 1: 636-639.

Fierer, N. and J.P. Schimel. 2003. A proposed mechanism for the pulse in carbon dioxide production commonly observed following the rapid rewetting of a dry soil. Soil Science Society of America Journal 67(3): 798-805.

Fierer, N., M.A. Bradford, and R.B. Jackson. 2007. Toward an ecological classification of soil bacteria. Ecology 88(6): 1354-1364.

Findeling, A., P. Garnier, F. Coppens, F. Lafolie, and S. Recous. 2007. Modelling water, carbon and nitrogen dynamics in soil covered with decomposing mulch. European Journal of Soil Science 58:196-206.

Finney, D.M., C.M. White, and J.P. Kaye. 2016. Biomass production and carbon/nitrogen ratio influence ecosystem services from cover crop mixtures. Agronomy Journal 108: 39-52.

Foley, J.A., N. Ramankutty, K.A. Brauman, E.S. Cassidy, J.S. Gerber, M. Johnston, N.D. Mueller, C. O'Connell, D.K. Ray, P.C. West, C. Balzer, E.M. Bennett, S.R. Carpenter, J. Hill, C. Monfreda, S. Polasky, R. Rockström, J. Sheehan, S. Siebert, D. Tilman, and D.P.M. Zaks. 2011. Solutions for a cultivated planet. Nature 478: 337-342.

Frankenberger, W.T, and H.M. Abdelmagid. 1985. Kinetic parameters of nitrogen mineralization rates of leguminous crops incorporated into soil. Plant Soil 87:257-271.

Franzluebbers, K., R.W. Weaver, A.S.R. Juo, and A.J. Franzluebbers. 1994. Carbon and nitrogen mineralization from cowpea plants part decomposing in moist and in repeatedly dried and wetted soil. Soil Biology Biochemistry 26(10): 1379-1387.

Frey, S.D., E.T. Elliott, K. Paustian, and G.A. Peterson. 2000. Fungal translocation as a mechanism for soil nitrogen inputs to surface residue decomposition in no-tillage agroecosystem. Soil Biology and Biochemistry 32:689-698.

Gao, H., X. Chen, J. Wei, Y. Zhang, L. Zhang, J. Chang, and M.L. Thompson. 2016. Decomposition dynamics and changes in chemical composition of wheat straw residue under anaerobic and aerobic conditions. PLoS ONE 11(7): e0158172. doi:10.1371/journal. Pone.0158172

Gaskin, J.W., M.L. Cabrera, D.E. Kissel, and R. Hitchcock. 2019. Using the cover crop N calculator for adaptive nitrogen fertilizer management: a proof of concept. Renewable Agriculture and Food Systems 1-11.

Gee, G.W., and J.W. Bauder. 1986. Particle-size analysis. In "Methods of soil analysis. Part 1. Physical and mineralogical methods." (Ed. A Klute) pp. 383-411. Soil Science Society of America: Madison.

Grandy, A.S., and G.P. Robertson. 2007. Land-use intensity effects on soil organic carbon accumulation rates and mechanisms. Ecosystems 10(1): 59-74.

Grant, R.F., N.G. Juma, and W.B. McGill. 1993. Simulation of carbon and nitrogen transformations in soil: Mineralization. Soil Biology and Biochemistry 25:1317-1329.

Griffin, D.M. 1977. Water potential and wood-decay fungi. Annual Review of Phytopathology 15:319-329.

Griffin, D.M. 1981. Water and microbial stress. Advances in Microbial Ecology 5:91-136.

Gunnarsson, S. and H. Marstorp. 2002. Carbohydrate composition of plant materials determines N mineralisation. Nutrient Cycling in Agroecosystems 62: 175-183. DOI 10.1023/A:1015512106336

Gunnarsson, S., H. Marstorp, A.S. Dahlin, and E. Witter. 2008. Influence of non-cellulose structural carbohydrate composition on plant material decomposition in soil. Biology and Fertility of Soils 45: 27-36 DOI 10.1007/s00374-008-0303-5

Harman, J., D. Moorhead, and B. Berg. 2008. The relationship between rates of lignin and cellulose decay in aboveground forest litter. Soil Biology and Biochemistry 40(10): 2620-2626.

Harreither, W., C. Sygmund, M. Augustin, M. Narciso, M.L. Rabinovich, L. Gorton, D. Haltrich, and R. Ludwig. 2011. Catalytic properties and classification of cellobiose dehydrogenases from ascomycetes. Applied Environmental Microbiology 77(5): 1804-1815.

Hiscox, J., J. O'Leary, and L. Boddy. 2018. Fungus wars: basidiomycete battles in wood decay. Stud. Mycology 89: 117-124.

Holland, E.A. and D.C. Coleman. 1987. Litter placement effects on microbial and organic-matter dynamics in an agroecosystem. Ecology 68(2): 425-433.

Iqbal, A., S. Aslam, G. Alavoine, P. Benoit, P. Garnier, and S. Recous. 2015. Rain regime and soil type affect the C and N dynamics in soil columns that are covered with mixed-species mulches. Plant and Soil 393:319-334.

Iqbal. A., J. Beaugrand, P. Garnier, and S. Recous. 2013. Tissue density determines the water storage characteristics of crop residues. Plant and Soil 367: 285-299. https://doi.org/10.1007/s11104-012-1460-8

Jahanzad, E., A.V. Barker, M. Hashemi, T. Eaton, A. Sadeghpour, and S.A. Weis. 2016. Nitrogen Release Dynamics and Decomposition of Buried and Surface Cover Crop Residues. Agronomy Journal 108(4): 1735-1741. doi:10.2134/agronj2016.01.0001

Jensen, H.L. 1929. On the influence of carbon:nitrogen ratios of organic material on the mineralisation of nitrogen. The Journal of Agricultural Science 19:71–82.

Jian, J., B.J. Lester, X. Du, M.S. Reiter, and R.D. Stewart. 2020. A calculator to quantify cover crop effects on soil health and productivity. Soil and Tillage Research 199: 104575.

Jiang. Y., M. Lawrence, A. Hussain, M. Ansell, and P. Walker. 2019. Comparative moisture and heat sorption properties of fibre and shiv derived from hemp and flax. Cellulose 26, 823-843. https://doi.org/10.1007/s10570-018-2145-0

Jomura, M., Y. Kominami, and M. Ataka. 2012. Differences between coarse woody debris and leaf litter in the response of heterotrophic respiration to rainfall events. Journal of Forest Research 17(3): 305-311.

Joshi, D.R., D.E. Clay, S.A. Clay, and A.J. Smart. 2019. Seasonal losses of surface litter in northern great plains mixed-grass prairies. Rangeland Ecology and Management 73(2): 259-264. doi:https://doi.org/10.1016/j.rama.2019.11.003

Kassambara, A. 2020. rstatix: Pipe-Friendly Framework for Basic Statistical Tests. R package version 0.4.0. https://CRAN.R-project.org/package=rstatix

Kerdraon, L., M.H. Balesdent, M. Barret, V. Laval, and F. Suffert. 2019. Crop residues in wheat-oilseed rape rotation system: a pivotal, shifting platform for microbial meetings. Microbial Ecology 77: 931-945.

Kern, J.S., and M.G. Johnson. 1993. Conservation tillage impacts on national soil and atmospheric carbon levels. Soil Science Society of America Journal 57(1): 200.

Kozak, J.A., L.R. Ahuja, T.R. Green, and L. Ma. 2007. Modelling crop canopy and residue rainfall interception effects on soil hydrological components for semi-arid agriculture. Hydrological Processes 21: 229-241.

Kriauciuniene, Z., R. Velicka, S. Raudonius, and M. Rimkeviciene. 2008. Changes of lignin concentration and C: N in oilseed rape, wheat and clover residues during their decomposition in the soil. Agronomy Research 6(2): 489-498.

Kruse, J.S., D.E. Kissel, and M.L. Cabrera. 2004. Effects of drying and rewetting on carbon and nitrogen mineralization in soils and incorporated residues. Nutrient Cycling in Agroecosystems 69(3): 247-256.

Kuo, S., and U.M. Sainju. 1998. Nitrogen mineralization and availability of mixed leguminous and non-leguminous cover crop residues in soil. Biology and Fertility of Soils 26:346-353.

Kuo, S., U.M. Sainju, and E.J. Jellum. 1997. Winter cover cropping influence on nitrogen in soil. Soil Science Society of America Journal 61: 1392-1399.

Kutlu, T., A.K. Guber, M.L. Rivers, and A.N. Kravchenko. 2018. Moisture absorption by plant residue in soil. Geoderma. 316: 47-55. https://doi.org/10.1016/j.geoderma.2017.11.043

Lawson, A., A.M. Fortuna, C. Cogger, A. Bary, and T. Stubbs. 2013. Nitrogen contribution of rye–hairy vetch cover crop mixtures to organically grown sweet corn. Renewable Agriculture and Food Systems 28(01):59-69. doi:10.1017/S1742170512000014.

Lee, H., J. Fitzgerald, D.B. Hewins, R.L. McCulley, S.R. Archer, T. Rahn, and H.L. Throop. 2014. Soil moisture and soil-litter mixing effects on surface litter decomposition: A controlled environment assessment. Soil Biology and Biochemistry 72: 123-132.

Lenth, R. 2019. emmeans: Estimated Marginal Means, aka Least-Squares Means. R package version 1.4.2. https://CRAN.R-project.org/package=emmeans

Ligges, U., and M. Mächler. 2003. Scatterplot3d - an R Package for Visualizing Multivariate Data. Journal of Statistical Software 8(11):1-20.

Liu, Q., Edwards, N.T., Post, W.M., Gu, L., Ledford, J., Lenhart, S., 2006. Temperature-independent diel variation in soil respiration observed from a temperate deciduous forest. Global Change Biology 12, 2163-2145.

Lüneberg, K., D. Schneider, C. Siebe, and R. Daniel. 2018. Drylands soil bacterial community is affected by land use change and different irrigation practices in the Mezquital Valley, México. Scientific Reports 8: 1413.

Makita, N., Y. Kosugi, A. Sakabe, A. Kanazawa, S. Ohkubo, and M. Tani. 2018. Seasonal and diurnal patterns of soil respiration in an evergreen coniferous forest: Evidence from six years of observation with automatic chambers. PLoS ONE 13(2), E0192622.

Maloney, T.C. and H. Paulapuro. 1999. The formation of pores in the cell wall. Journal of Pulp Paper Science 25, 430-436.

Manstretta, V. and V. Rossi. 2015. Modelling the effect of weather on moisture fluctuations in maize stalk residues, an important inoculum source for plant diseases. Agricultural and Forest Meteorology 207: 83-93.

Manzoni, S., J.P. Schimel, and A. Porporato. 2012. Responses of soil microbial communities to water stress: results from a meta-analysis. Ecology 93:930e938.

Martin, M. 2011. Cutadapt removes adapter sequences from high throughput sequencing reads. EMBnet J 17:10 –12. https://doi.org/10 .14806/ej.17.1.200.

Martinez Arbizu, P. 2019. pairwiseAdonis: Pairwise multilevel comparison using adonis. R package version 0.3

Maul, J.E., J.S. Buyer, R.M. Lehman, S. Culman, C.B. Blackwood, D.P. Roberts, I.A. Zasada, and J.R. Teasdale. 2014. Microbial community structure and abundance in the rhizosphere and bulk soil of a tomato cropping system that includes cover crops. Applied Soil Ecology 77: 42-50.

McGill, W.B., H.W. Hunt, R.G. Woodmansee, and J.O. Reuss. 1981. Phoenix- A model of the dynamics of carbon and nitrogen in grassland soils. In: Clark FE, Rosswall T (Eds.), Terrestrial Nitrogen Cycles, Ecol Bull (Stockholm) 33:49-115.

Meisinger, J.J., W.L. Hargrove, R.L. Mikkelsen, J.R. Williams, and V.W. Benson. 1991. Effects of cover crops on groundwater quality. In: W.L. Hargrove, editor, *Cover crops for clean water. Proceedings of an international conference*, Jackson, TN. 9-11 Apr. 1991. Soil Water Conservation Society, Ankeny, IA. p. 57-68.

Melkonian, J., H.J. Poffenbarger, S.B. Mirsky, M.R. Ryan, and B.N. MoebiusClune. 2017. Estimating nitrogen mineralization from cover crop mixtures using the precision nitrogen management model. Agronomy Journal 109:1944-1959.

Mendiburu, F.D. 2019. Agricolae: Statistical Procedures for Agricultural Research. R Package Version 1.3-1. http://CRAN.R-project.org/package=agricolae

Merten, G.H., A.G. Araújo, R.C.M. Biscaia, G.M.C. Barbosa, and O. Conte. 2015. No-till surface runoff and soil losses in southern Brazil. Soil and Tillage Research 152: 85-93.

Mevik, B.H., R. Wehrens, and K.H. Liland. 2019. pls: Partial Least Squares and Principal Component Regression. R package version 2.7-2. https://CRAN.R-project.org/package=pls

Miller, A.E., J.P. Schimel, T. Meixner, J.O. Sickman, and J.M. Melack. 2005. Episodic rewetting enhances carbon and nitrogen release from chaparral soils. Soil Biology and Biochemistry 37(12): 2195-2204.

Mirsky, S.B., J.T. Spargo, W.S. Curran, S.C. Reberg-Horton, M.R. Ryan, H.H. Schomberg, and V.J. Ackroyd. 2017. Characterizing cereal rye biomass and allometric relationships across a range of fall available nitrogen rates in the Eastern United States. Agronomy Journal 109:1520-1531.

Mirsky, S.B., M.R. Ryan, W.S. Curran, J.R. Teasdale, J. Maul, J.T. Spargo, J. Moyer, A.M. Grantham, D. Weber, T.R. Way, and G.G. Camargo. 2012. Conservation tillage issues: Cover crop-based organic rotational no-till grain production in the mid-Atlantic region, USA. Renewable Agriculture and Food Systems 27(1): 31-40.

Mirsky, S.B., V.J. Ackroyd, S. Cordeau, W.S. Curran, M. Hashemi, S. Chris Reberg-Horton, M.R. Ryan, and J.T. Spargo. 2017. Hairy vetch biomass across the Eastern United States: Effects of latitude, seeding rate and date, and termination timing. Agronomy Journal 109(4): 1510-1519.

Mirsky, S.B., W.S. Curran, D.M. Mortenseny, M.R. Ryan, and D.L. Shumway. 2011. Timing of cover crop management effects on weed suppression in no-till planted soybean using a roller-crimper. Weed Science 59(3): 380-389.

Molina, J.E., C.E. Clapp, M.J. Schaeffer, F.W. Chichester, and W. Larson. 1983. NCSOIL, a model of nitrogen and carbon transformation in soil: description, calibration and behaviour. Soil Science Society of America Journal 47: 85-91.

Moore, A.M. 1986. Temperature and moisture dependence of decomposition rates of hardwood and coniferous leaf litter. Soil Biology and Biochemistry 18: 427-435.

Morrison, E.W., A. Pringle, L.T.A. van Diepen, and S.D. Frey. 2018. Simulated nitrogen deposition favors stress-tolerant fungi with low potential for decomposition. Soil Biology and Biochemistry 125: 75-85.

Moyano, F.E., S. Manzoni, and C. Chenu. 2013. Responses of soil heterotrophic respiration to moisture availability: an exploration of processes and models. Soil Biology and Biochemistry 59: 72-85.

National Research Council. *Achieving Nutrient and Sediment Reduction Goals in the Chesapeake Bay: An Evaluation of Program Strategies and Implementation*; The National Academies Press: Washington, DC, USA, 2011.

Nevins, C.J., C. Nakatsu, and S. Armstrong. 2018. Characterization of microbial community response to cover crop residue decomposition. Soil Biology and Biochemistry 127: 39-49.

Nguyen, N.H., Z.W. Song, S.T. Bates, S. Branco, L. Tedersoo, J. Menke, J.S. Schilling, and P.G. Kennedy. 2016. FUNGuild: An open annotation tool for parsing fungal community datasets by ecological guild. Fungal Ecology 20: 241-248.

Nicolardot, B., L. Bouziri, F. Bastian, and L. Ranjard. 2007. A microcosm experiment to evaluate the influence of location and quality of plant residues on residue decomposition and genetic structure of soil microbial communities. Soil Biology and Biochemistry 39: 1631-1644.

Nilsson, R.H., K.H. Larsson, A.F.S. Taylor, J. Bengtsson-Palme, T.S. Jeppesen, D. Schigel, P. Kennedy, K. Picard, F.O. Glöckner, L. Tedersoo, I. Saar, U. Kõljalg, and K. Abarenkov. 2019. The UNITE database for molecular identification of fungi: handling dark taxa and parallel taxonomic classifications. Nucleic Acids Research 47: D259 –D264.

Nimon, K., F. Oswald, and J.K. Roberts. 2020. yhat: Interpreting Regression Effects. R package version 2.0-2. https://CRAN.R-project.org/package=yhat

Oksanen, J., F.G. Blanchet, M. Friendly, R. Kindt, P. Legendre, D. McGlinn, P.R. Minchin, R.B. O'Hara, G.L. Simpson, P. Solymos, M. Henry, H. Stevens, E. Szoecs, and H. Wagner. 2019. vegan: Community Ecology Package. R package version 2.5-6. https://CRAN.R-project.org/package=vegan

Olson, J.S. 1963. Energy storage and the balance of producers and decomposers in ecological systems. Ecology 44: 322-331.

Osipitan, O.A., J.A. Dille, Y. Assefa, and S.Z. Knezevic. 2018. Cover crop for early season weed suppression in crops: systemic review and meta-analysis. Agronomy Journal 110: 2211-2221.

Osipitan, O.A., J.A. Dille, Y. Assefa, E. Radicetti, A. Ayeni, and S.Z. Knezevic. 2019. Impact of cover crop management on level of weed suppression: a meta-analysis. Crop Science 59: 833-842.

Otte, B., S.B. Mirsky, H.H. Schomberg, B.W. Davis, and K.L. Tully. 2019. Effect of cover crop termination timing on pools and fluxes of inorganic nitrogen in no-till corn. Agronomy Journal 0: 0–11.

Parkin, T.B. and T.C. Kaspar. 2003. Temperature controls on diurnal carbon dioxide flux: Implications for estimating soil carbon loss. Agronomy Journal 67: 1763-1772.

Pascault, N., L. Cecillon, O. Mathieu, C. Henault, A. Sarr, J. Leveque, P. Farcy, L. Ranjard, and P.A. Maron. 2010. In situ dynamics of microbial communities during decomposition of wheat, rape, and alfalfa residues. Microbial Ecology 60(4): 816-828.

Paudel, E., G.G.O. Dossa, M. de Blécourt, P. Beckschäfer, J. Xu, and R.D. Harrison. 2015. Quantifying the factors affecting leaf litter decomposition across a tropical forest disturbance gradient. Ecosphere 6(12):267.

Paustian, K. and T.A. Bonde. 1987. Interpreting incubation data on nitrogen mineralization from soil organic matter. In: Cooley JH (Ed.) Soil organic matter dynamics and soil productivity. Proceedings of INTECOL workshop, Athens, GA, pp 101-112.

Pianka, E. 1970. On r- and K-selection. The American Naturalist 104: 592-597.

Pinheiro, J., D. Bates, S. DebRoy, and D. Sarkar. 2020. nlme: Linear and Nonlinear Mixed Effects Models_. R package version 3.1-145, <URL: https://CRAN.R-project.org/package=nlme>.

Poeplau, C. and A. Don. 2015. Carbon sequestration in agricultural soils via cultivation of cover crops – A meta-analysis. Agriculture, Ecosystems and Environment. 200: 33-41.

Poffenbarger, H.J., S.B. Mirsky, R.R. Weil, M. Kramer, J.T. Spargo, and M.A. Cavigelli. 2015b. Legume proportion, poultry litter, and tillage effects on cover crop decomposition. Agronomy Journal 107(6): 2083-2096. doi:10.2134/agronj15.0065

Poffenbarger, H.J., S.B. Mirsky, R.R. Weil, J.E. Maul, M. Kramer, J.T. Spargo, and M.A. Cavigelli. 2015a. Biomass and nitrogen content of hairy vetch-cereal rye cover crop mixtures as influenced by species proportions. Agronomy Journal 107(6): 2069-2082.

Quast, C., E. Pruesse, P. Yilmaz, J. Gerken, T. Schweer, P. Yarza, J. Peplies, and F.O. Glöckner. 2013. The SILVA ribosomal RNA gene database project: improved data processing and Web-based tools. Nucleic Acids Research 41: D590 – D596.

Quemada, M. and M.L. Cabrera. 1995. CERES-N model predictions of nitrogen mineralized from cover crop residues. Soil Science Society of America Journal 59: 1059-1065. doi:10.2136/sssaj1995.03615995005900040015x

Quemada, M. and M.L. Cabrera. 1997. Temperature and moisture effects on C and N mineralization from surface applied clover residue. Plant and Soil 189: 127-137.

Quemada, M. and M.L. Cabrera. 2002. Characteristic moisture curves and maximum water content of two crop residues. Plant and Soil 238: 295-299.

Quemada, M., M.L. Cabrera, and D.V. McCracken. 1997. Nitrogen release from surface-applied cover crop residues: Evaluating the CERES-N submodel. Agronomy Journal 89: 723-729.

Ranells, N.N. and M.G. Wagger. 1992. Nitrogen release from crimson clover in relation to plant growth stage and composition. Agronomy Journal 84:424-430.

Ranells, N.N. and M.G. Wagger. 1996. Nitrogen release from grass and legume cover crop monocultures and bicultures. Agronomy Journal. 88: 777-782.

Reardon, C.L. and S.B. Wuest. 2016. Soil amendments yield persisting effects on the microbial communities-a 7-year study. Applied Soil Ecology 101: 107-116.

Reberg-Horton, S.C., J.M. Grossman, T.S. Kornecki, and A.D. Meijer. 2012. Utilizing cover crop mulches to reduce tillage in organic systems in the southeastern USA. Renewable Agriculture and Food Systems 27: 41-48. https://doi.org/10.1017/S1742170511000469.

Roper, M.M. 1985. Straw decomposition and nitrogenase activity (C2H2 reduction): Effects of soil moisture and temperature. Soil Biology and Biochemistry 17(1): 65-71.

Savabi, M.R. and D.E. Stott. 1994. Plant residue impact on rainfall interception. ASAE Paper No. 92-2634.

Schjonning, P., I.K. Thomsen, P. Moldrup, and B.T. Christensen. 2003. Linking soil microbial activity to water- and air-phase contents and diffusivities. Soil Science Society of America Journal l 67: 156-165.

Schomberg HH, Ford PB, Hargrove WL (1994) Influence of crop residues on nutrient cycling and soil chemical properties. In: Unger PW (Ed.), Managing Agricultural Residues, Lewis Publishers, Boca Raton, FL, USA, pp. 99-121.

Schomberg, H.H., and M.L. Cabrera. 2001. Modeling in situ N mineralization in conservation tillage fields: Comparison of two versions of the CERES nitrogen submodel. Ecological Modelling 145: 1-15.

Schomberg, H.H., J.L. Steiner, and P.W. Unger. 1994. Decomposition and nitrogen dynamics of crop residues - residue quality and water effects. Soil Science Society America Journal 58(2): 372-381.

Scopel, E., F.A.M. Da Silva, M. Corbeels, F. Affholder, and F. Maraux. 2004. Modelling crop residue mulching effects on water use and production of

maize under semi-arid and humid tropical conditions. Agronomie 24: 383-395. DOI: 10.1051/agro:2004029.

Shaver, T.M., G.A. Peterson, L.R. Ahuja, D.G. Westfall, L.A. Sherrod, and G. Dunn. 2002. Surface soil physical properties after twelve years of dryland no-till management. Soil Science Society of America Journal 66(4): 1296.

Silver, W.L. and R.K. Miya. 2001. Global patterns in root decomposition: comparisons of climate and litter quality effects. Oecologia 129: 407-19.

Six, J., C. Feller, K. Denef, S. Ogle, J.C. de M. Sa, and A. Albrecht. 2002. Soil organic matter, biota and aggregation in temperate and tropical soils- Effects of no-tillage. Agronomie 22(7-8): 755-75.

Skopp, J., M.D. Jawson, and J.W. Doran. 1990. Steady-state aerobic microbial activity as a function of soil-water content. Soil Science Society of America Journal 54: 1619-1625.

Soil Survey Staff. 2020. Natural Resources Conservation Service, United States Department of Agriculture. Web Soil Survey. Available online at the following link: https://websoilsurvey.sc.egov.usda.gov/. Accessed [1/2/2020].

Stark, J. and M. Firestone. 1995. Mechanisms for soil moisture effects on activity of nitrifying bacteria. Applied Environmental Microbiology 61: 218-221.

Steiner, J.L., H.H. Schomberg, P.W. Unger, and J. Cresap. 1999. Crop residue decomposition in no-tillage small-grain fields. Soil Science Society of America Journal 63: 1817-1824.

Stott, D.E., H.F. Stroo, L.F. Elliott, R.I. Papendick, and P.W. Unger. 1990. Wheat residue loss from fields under no-tillage management. Soil Science Society of America Journal 54: 92-98.

Stott, D.E., L.F. Elliott, R.I. Papendick, and G.S. Campbell. 1986. Low temperature or low water effects on microbial decomposition of wheat residue. Soil Biology and Biochemistry 18(6): 577-582.

Teasdale, J.R. and C.L. Mohler. 1993. Light transmittance, soil temperature, and soil moisture under residue of hairy vetch and rye. Agronomy Journal 85: 673-680.

Thapa, R., A. Chatterjee, J.M.F. Johnson, and R. Awale. 2015. Stabilized nitrogen fertilizers and application rate influence nitrogen losses under rainfed spring wheat. Agronomy Journal 107: 1885-1894. doi:10.2134/agronj15.0081

Thapa, R., H. Poffenbarger, K.L. Tully, V. Ackroyd, M. Kramer, and S.B, Mirsky. 2018b. Biomass production and nitrogen accumulation by hairy vetch–cereal

rye mixtures: a meta-analysis. Agronomy Journal 110: 1197-1208. https://doi.org/10.2134/agronj2017.09.054

Thapa, R., S.B. Mirsky, and K.L. Tully. 2018a. Cover crops reduce nitrate leaching in agroecosystems: A global meta-analysis. Journal of Environmental Quality 47(6): 1400-11. https://doi.org/10.2134/jeq2018.03.0107

Thapa, V.R., R. Ghimire, V. Acosta-Martinez, M.A. Marsalis, and M.E. Schipanski. 2021. Cover crop biomass and species composition affect soil microbial community structure and enzyme activities in semiarid cropping systems. Applied Soil Ecology 157: 103735.

Thorburn, P.J., M.E. Probert, and F.A. Robertson. 2001. Modelling decomposition of sugarcane surface residues with APSIM-Residue. Field Crops Research 70: 223-232.

Tilman, D., K.G. Cassman, P.A. Matson, R. Naylor, and S. Polasky. 2002. Agricultural sustainability and intensive production practices. Nature 418: 671-677.

Trenberth, K.E., A. Dai, G. Van Der Schrier, P.D. Jones, J. Barichivich, K.R. Briffa, and J. Sheffield. 2014. Global warming and changes in drought. Nature Climate Change 4: 17-22.

Tully, K.L. and C. McAskill. 2020. Promoting soil health in organically managed systems: a review. Organic Agriculture 1-20.

Verberne, E.L.J., J. Hassink, P. De Willigen, J.J.R. Groot, and J.R. van Veen. 1990. Modelling organic matter dynamics in different soils. Netherlands Journal of Agricultural Science 38: 221-238.

Vigil, M.F. and D.E. Kissel. 1991. Equations for estimating the amount of nitrogen mineralized from crop residues. Soil Science Society of America Journal 55: 757-761.

Voriskova, J. and P. Baldrian. 2013. Fungal community on decomposing leaf litter undergoes rapid successional changes. The ISME Journal 7(3): 477-486.

Wagger, M.G. 1989. Time of desiccation effects on plant composition and subsequent Nitrogen release from several winter annual cover crops. Agronomy Journal 81: 236-241.

Wagger, M.G., M.L. Cabrera, and N.N. Ranells. 1998. Nitrogen and carbon cycling in relation to cover crop residue quality. Journal of Soil and Water Conservation 53: 214-218.

Wallace, J.M., A. Williams, J.A. Liebert, V.J. Ackroyd, R.A. Vann, W.S. Curran, C.L. Keene, M.J. VanGessel, M.R. Ryan, and S.B. Mirsky. 2017. Cover Crop-

Based, Organic Rotational No-Till Corn and Soybean Production Systems in the Mid-Atlantic United States. Agriculture 7(4): 34.

Wang, W.J., C.J. Smith, and D. Chen. 2003. Towards a standardized procedure for determining the potentially mineralisable nitrogen of soil. Biology and Fertility of Soils 37: 362-374.

Wells MS, S.C. Reberg-Horton, S.B. Mirsky, J.E. Maul, and S. Hu. 2017. In situ validation of fungal N translocation to cereal rye mulches under no-till soybean production. Plant and Soil. 410: 153-165.

White, T.J., T.D. Bruns, S. Lee, and J. Taylor. 1990. Amplification and direct sequencing of fungal ribosomal RNA genes for phylogenetics, p 315–322. In Innis, M.A., Gelfand, D.H., Sninsky, J.J., White, T.J. (ed), PCR protocols, a guide to methods and applications. Academic Press, San Diego, CA.

Wickham, H. and E. Ruiz. 2020. dbplyr: A 'dplyr' Back End for Databases. R package version 1.4.3. https://CRAN.R-project.org/package=dbplyr

Wickham, H., J. Ooms, and K. Müller. 2019. RPostgres: 'Rcpp' Interface to 'PostgreSQL'. R package version 1.2.0. https://CRAN.R-project.org/package=RPostgres

Wickham, H., R. François, L. Henry, and K. Müller. 2020. dplyr: A Grammar of Data Manipulation. R package version 0.8.5. https://CRAN.R-project.org/package=dplyr

Williams, A., M.S. Wells, D.A. Dickey, S.J. Hu, J. Maul, D.T. Raskin, S.C. Reberg-Horton, and S.B. Mirsky. 2018. Establishing the relationship of soil nitrogen immobilization to cereal rye residues in a mulched system. Plant and Soil 426(1-2): 95-107.

Witcamp, M. 1969. Cycles of temperature and carbon dioxide evolution from litter and soil. Ecology 50(5): 922-924.

Woloszynek, S., J.C. Mell, G. Simpson, and G.L. Rosen. 2017. Exploring thematic structure in 16S rRNA marker gene surveys. bioRxiv 146126. doi: https://doi.org/10.1101/146126.

Woodruff, L.K., D.E. Kissel, M.L. Cabrera, R. Hitchcock, J. Gaskin, M. Vigil, L. Sonon, U. Saha, M.Y. Habteselassie, and J. Rema. 2018. A web-based model of N mineralization from cover crop residue decomposition. Soil Science Society of America Journal 82: 983-993.

Xia, Y., K. MItchell, M. Ek, J. Sheffield, B. Cosgrove, E. Wood, L. Luo, C. Alonge, H. Wei, J. Meng, B. Livneh, D. Lettenmaier, V. Koren, Q. Duan, K. Mo, Y. Fan, and D. Mocko. 2012. Continental-scale water and energy flux analysis and validation for the North American Land Data Assimilation System project

phase 2 (NLDAS-2): 1. Intercomparison and application of model products. Journal of Geophysical Research 117: D03109. doi:10.1029/2011JD016048

Yanni, S.F., Diochon A, Helgason BL, Ellert BH, Gregorich EG (2018) Temperature response of plant residue and soil organic matter decomposition in soil from different depths. European Journal of Soil Science 69: 325-335. doi:10.1111/ejss.12508.

Zadoks, J.C., T.T. Chang, and C.F. Konzak. 1974. A decimal code for the growth stages of cereals. Weed Research 14: 415-421. doi:10.1111/j.1365-3180.1974.tb01084.x

Zhang, D., D. Hui, Y. Luo, and G. Zhou. 2008. Rates of litter decomposition in terrestrial ecosystems: global patterns and controlling factors. Journal of Plant Ecology 1(2): 85-93.

Zhang, J., K. Howard, C. Langston, B. Knaey, Y. Qi, L. Tang, H. Grams, Y. Wang, S. Cocks, S.M.A. Arthur, K. Cooper, J. Brogden, and D. Kitzmiller. 2016. Multi-Radar Multi-Sensor (MRMS) quantitative precipitation estimation: Initial operating capabilities. The Bulletin of the American Meteorological Society 97(4): 621-638. doi:https://doi.org/10.1175/BAMS-D-14-00174.1.

Zhang, X. and W. Wang. 2015. The decomposition of fine and coarse roots: their global patterns and controlling factors. Scientific Reports 5: 09940.

Zhong, Y.Q.W., J. Liu, X.Y. Jia, Z.P. Shangguan, R.W. Wang, and W.M. Yan. 2020. Microbial community assembly and metabolic function during wheat straw decomposition under different nitrogen fertilization treatments. Biology and Fertility of Soils 10.1007/s00374-020-01438-z

Zhong, Y.Q.W., W.M. Yan, R.W. Wang, W. Wang, and Z.P. Shangguan. 2018. Decreased occurrence of carbon cycle functions in microbial communities along with long-term secondary succession. Soil Biology and Biochemistry 123: 207-217.

Zhou, G., L. Guan, X. Wei, X. Tang, S. Liu, j. Liu, D. Zhang, and J. Yan. 2008. Factors influencing leaf litter decomposition: an intersite decomposition experiment across China. Plant and Soil 311: 61-72.

Zibilske, L.M. and J.M. Bradford. 2007. Soil aggregation, aggregate carbon and nitrogen, and moisture retention induced by conservation tillage. Soil Science Society of America Journal 71(3): 793-802.

Zimmermann, M., Meir, P., Bird, M., Malhi, Y., Ccahuana, A., 2009. Litter contribution to diurnal and annual soil respiration in a tropical montane cloud forest. Soil Biology and Biochemistry 41: 1338-1340.

Zulauf, C. and B. Brown. 2019. "Cover Crops, 2017 US Census of Agriculture." farmdoc daily (9):135, Department of Agricultural and Consumer Economics, University of Illinois at Urbana-Champaign, July 24, 2019.